PREPARATION AND CHARACTERIZATION OF MODIFIED TiO_2 THIN FILMS FOR PHOTOCATALYTIC APPLICATIONS

A THESIS SUBMITTED TO THE

UNIVERSITY OF PUNE

FOR THE DEGREE OF

DOCTOR OF PHILOSOPHY

(IN CHEMISTRY)

By

RAVINDRA SHRAWAN SONAWANE

CATALYSIS DIVISION
NATIONAL CHEMICAL LABORATORY
PUNE- 411 008 INDIA

MARCH 2006

CERTIFICATE

This is to certify that, the work incorporated in the thesis "**Preparation and characterization of modified TiO_2 thin films for photocatalytic applications"** submitted by **Mr. Ravindra Shrawan Sonawane,** for the Degree of **Doctor of Philosophy,** was carried out by the candidate under my supervision in the Catalysis Division, National Chemical Laboratory, Pune, INDIA

Dr. M. K. Dongare
Research Guide

ACKNOWLEDGEMENTS

I express my profound gratitude to my research guide Dr. M. K. Dongare, Scientist, National Chemical Laboratory, Pune for his invaluable guidance, discussions and constructive suggestions throughout the course of the thesis work.

I am grateful to Dr. B. B. Kale, our group leader, C-MET, Pune and Dr. A. V. Ramaswamy Ex. Head, Catalysis Division, NCL, for providing me all facilities required for my work.

I am also deeply indebted to Dr. S. G. Hegde for his invaluable suggestions and personal help rendered throughout this investigation.

I also wish to express special thanks to my collegues, Mr. S. K. Apte, Mrs. Sonali Naik, Mrs. Lalita, Mrs Aarti , Mrs. Nilakshi, Mr. Shrikant Takle, Mr. Rahul Babhale and Mr. Sandeep Bodhale for their help, cooperation and support during this work.

I wish to express my thanks to Dr. Amalnerkar, Dr. Mulik, Mr. Sadanandan, Dr. Khanna, Dr. Phatak, Dr. Tanay Seth, Dr. Gurunathan, Dr. Kulkarni, Dr. A. V. Murugan, Dr. Varsha Raut, Dr. V. B. Rane, Mr. R. Marimuthu Mrs. Shubhangi Damakale, Mr. Goyal, Mrs Shany Joseph, Mrs. Vijaya Giramkar, Mrs. Rina Gorte, other staff from C–MET, Pune and Dr. Shubhangi Umbarkar, Dr. C. V. V. Satyanarayana, Sachin Malwadkar, Sharada, Pratap Patil, Miss Kusum, Ankush from NCL, for their help and cooperation extended to me in completing my research work.

I take the opportunity to thank my friends, Mr. S. R. Ballal, Mr. B. S. Jadhav, Mr. R. M. Damkale, Mr. P. V. Bhoite, Mr. V. N Shete Mr. Sandeep Parsankar, Mr. J. D. Ambekar, Mr. C. N. Chavan, Mr. Y. S. Madake Mr. A. Y. Kanap and numerous other friends from whom I received individual help and moral support.

It gives me pleasure to thank my father & mother, brothers, sister, nephew, nice, my wife Sharmila and son Amol for their love, unfailing support, tremendous patience, trust on me and encouragement that they have shown to me.

Finally, my thanks to Dr. B. K. Das Ex- Executive Director C-MET and Dr. P. Ratnasamy, Ex-Director, NCL for permitting me to carry out my research work at NCL.

Ravindra S. Sonawane

DECLARATION OF CANDIDATE

No part of this thesis has been submitted for a degree or diploma or other academic award. The literature concerning the problem investigated has been surveyed and all the necessary references are given in the thesis. The experimental work has been carried out entirely by me. In accordance with the usual practice, due acknowledgement has been made whenever the work presented is based on the results of other workers.

Ravindra Shrawan Sonawane
Candidate

Dr. M. K. Dongare
Research guide

LIST OF SYMBOLS

AOP	Advanced Oxidation Processes
AOS	Average Oxidation State
BOD	Biological Oxygen Demand
c	Light speed
C_{eq}	Equilibrium concentration
C_i	Initial concentration
CB	Conduction Band
COD	Chemical Oxygen Demand
CR	Concentration Ratio
DOC	Dissolved Organic Carbon
E_{bg}	Semiconductor band-gap energy
E_{HOMO}	Energy of the Highest Occupied Molecular Orbital
E_{LUMO}	Energy of the Lowest Unoccupied Molecular Orbital
HPLC	High Performance Liquid Chromatography
I	Photon flux density
k	First-order rate constant
K	Adsorption constant
l	Litre
L-H	Langmuir Hinshelwood model
MW	Molecular Weight
NHE	Normal Hydrogen Electrode
pKa	Acid dissociation constant

PZC	Point of Zero Charge
tr	Residence time
V	Volume
vo	Initial degradation rate
V_{TOT}	Total volume
UV_D	Direct ultraviolet light
UV_G	Global ultraviolet light
VB	Valence Band

TABLE OF CONTENTS

ACKNOWLEDGMENTS i

LIST OF SYMBOLS ii

CHAPTER I
INTRODUCTION 1

1.1 Introduction 1

1.2 Background 2

1.3 Homogeneous photocatalysis 4

1.4. Heterogeneous photocatalysis 4

1.4.1 Mechanism of TiO2 mediated photocatalysis 8

1.5 Thin Film Deposition Techniques 12

1.5.1 Sol-Gel Dip Coating 15

1.5.2 Sol-gel Film Formation 17

1.5.3 Influence of precursor structure and reactivity 18

1.5.4 Effect of substrate speed 19

1.6 Kinetics of TiO2 photo-catalysis 20

1.6.1 Catalyst concentration 20

1.6.2 Initial reactant concentration 21

1.6.3 Temperature 21

1.6.4 pH of the solution 22

1.6.5 Inorganic ions 22

1.6.6 Light intensity 23

1.6.7 Oxygen 23

1.6.8 Wavelength 24

1.6.9 Temperature 24

1.7 Application of heterogeneous photo-catalysis in pollution abatement 25

References 26

CHAPTER II

PREPARATION, CHARACTERIZATION AND PHOTOCATALYTIC ACTIVITY OF TiO_2 THIN FILMS

2.1 Introduction 32

2.2 Preparation Methods 36

2.3. Experimental 44

2.3.1 Materials 44

2.3.2 Preparation of TiO_2 precursor sol 45

2.3.3 Deposition of thin films of TiO_2 on glass plates 48

2.3.4 Deposition of thin films of TiO_2 on glass helix and silica rashig rings 49

2.4 Photocatalytic reactions using thin film photocatalyst 50

2.5 Characterization of thin films and powders 52

2.5.1 Measurement of viscosity of the sol 52

2.5.2 Measurement of film thickness 53

2.5.3 UV-visible spectroscopic characterization 53

2.5.4 X-ray diffraction studies 54

2.5.5 Thermo-gravimetric analysis 55

2.5.6 Surface morphology 56

2.5.7 Surface area analysis 56

2.5.8 Fourier transform infrared spectroscopy 57

2.5.9 Chemical analysis of the photocatalyst 58

2.6 Results and Discussion 58

2.6.1 Variation of viscosity of the sol with time 58

2.6.2 Variation of film thickness with viscosity 60

2.6.3 UV-visible spectroscopic characterization 62

2.6.4 X-Ray diffraction studies of TiO_2 photocatalyst 64
2.6.5 Thermo-gravimetric analysis 66
2.6.6 Surface Morphology 67
2.6.7 Surface Area of TiO_2 powder 69
2.6.8 Fourier transform infrared spectroscopic analysis 70
2.6.9 Photo-catalytic study of thin film photo-catalyst 71
2.7 Conclusions 81
References 82

CHAPTER III

PREPARATION, CHARACTERIZATION AND PHOTOCATALYTIC ACTIVITY OF Fe/TiO_2 THIN FILMS

3.1 Introduction 87
3.2. Iron doped TiO_2 (Fe/TiO_2) 88
3.3 Experimental 92
3.3.1 Materials 92
3.3.2 Preparation of Fe doped TiO_2 sol 93
3.3.3 Deposition Fe/TiO_2 thin films on glass plates 94
3.3.4 Deposition Fe/TiO_2 thin films on glass helix/silica rings 95
3.3.5 Photo-catalytic reactions using Fe/TiO_2 thin film photocatalyst 95
3.4 Results and Discussion 97
3.4.1 Effect of Fe addition on sol –gel behavior 97
3.4.2 Film thickness measurement 99
3.4.3 Addition Polyethylene glycol (PEG) in Fe/TiO_2 sol 100
3.4.4 Chemical composition of Fe/TiO_2 102
3.4.5 UV-visible spectroscopic characterization 102
3.4.6 XRD studies of Fe/TiO_2 photocatalyst 104
3.4.7 Thermo-gravimetric analysis 106
3.4.8 Surface morphology of Fe/TiO_2 films 107
3.4.9 Fourier transform infrared spectrometric analysis 110

3.4.10 Photo-catalytic activity of thin film Fe/TiO_2 photocatalyst 112

3.5 Conclusions 123

References 124

CHAPTER IV

PREPARATION, CHARACTERIZATION AND PHOTOCATALYTIC ACTIVITY OF Au/TiO_2 THIN FILMS.

4.1 Introduction 129

4.2 Experimental 133

4.2.1 Materials 133

4.2.2 Preparation colloidal Au solution 134

4.2.4 Preparation Au/TiO_2 sol 134

4.2.5 Deposition Au/TiO_2 thin films on glass plates 136

4.3 Results and Discussion

4.3.1 Effect of Fe addition on sol-gel behavior 137

4.3.2 UV-visible spectroscopic characterization 138

4.3.3 XRD characterization of Au/TiO_2 photocatalyst 141

4.3.4 Thermo-gravimetric analysis 144

4.3.5 Surface morphology of Au/TiO_2 films 145

4.3.6 Photo-catalytic reactions using Au/TiO_2 thin films 147

4.4 Conclusions 161

References 162

CHAPTER IV

SUMMARY AND CONCLUSIONS

SUMMARY 166

CHAPTER-I

INTRODUCTION

1.1 Introduction

As the life style and the living environment of the society is changing rapidly, the concern about the regional and global environment is also growing changing the total outlook of the industrial world. With the change in the production technologies in the modern industries the environmental impact is taken up very seriously. The pollution control measures are becoming more and more stringent and the polluting industries have to be either closed down or the necessary technologies have to be developed and implemented for the degradation of the environmentally harmful waste products. The end of pipe treatment approach by the early chemical engineers while designing the new chemical plant has changed. The minimization of the byproduct formation and its treatment or adopting a new process with totally zero waste has become the major requirement while designing the new chemical plant or any other production unit.

Environmental pollution and destruction of pollutants on a global scale has drawn attention to the vital need for totally new, safe and clean chemical technologies and processes, the most important challenge faced by the scientists of the 21st century. As the environmental concern about global and regional problems grows, environmental

catalysts have become more and more important. The world “Environmental catalysis” has gained wide acceptance and significant progress has been made with respect to the fundamental research and applications of environmental catalysts. Photocatalysts which can operate at room temperature in a clean and safe manner are being widely studied as the promising catalysts. The applications of such photocatalytic systems are urgently desired for the purification of polluted water, the decomposition of offensive odors and toxins, the fixation of CO_2 and decomposition of NO_x and chlorofluorocarbons on a global scale. To address such a enormous task, photocatalytic systems which are effective and efficient not only in UV but also in sunlight, the most environmentally ideal energy source must be established.

1.2 Background

Recently the advanced oxidation processes (AOP) such as homogeneous and heterogeneous photo-catalysis are being considered an attractive alternative for the conventional water treatment methods [1-6]. The conventional methods such as adsorption, precipitation, air stripping, flocculation, reverse osmosis, combustion and aerobic biological oxidation may convert the pollutants from one phase or form to other phase or form whereas the advanced methods lead to complete degradation of organic pollutants into harmless carbon dioxide and water. The new methods based on the chemical treatments or photo-catalytic treatments have been introduced named as “Advanced Oxidation Process” (AOP). In these methods, the strong oxidizing hydroxyl

radicals ($^{\bullet}OH$) and peroxy radicals are generated by using O_3/H_2O_2, H_2O_2/UV , $O_3/H_2O_2/UV$[2, 6-8], UV/TiO_2 [5, 9-12] and Fe^{2+}/H_2O_2 [13-16] systems. The radicals are responsible for the complete mineralization of organic substances to water and carbon dioxide.

$$^{\bullet}OH + RH \longrightarrow R^{\bullet} + H_2O \qquad (1.1)$$

$$R^{\bullet} + O_2 \longrightarrow RO_2^{\bullet} \longrightarrow \text{Products} + CO_2 \qquad (1.2)$$

The above mechanism responsible for the formation of radicals has been reported for the degradation of various kind of impurities as well as conversion to less toxic materials. [17-19] All these AOP are very efficient and effective in degradation of toxic materials. Most of these reactions occur in UV radiation (wavelength <300 nm) which is the main drawback increasing the operational cost of the process compared to the biodegradation process. The process effective under the solar energy will be an attractive alternative. In one of the known examples in homogeneous catalysis, both H_2O_2 and O_3 do not absorb the solar radiation, but the combination of Fe^{2+} with H_2O_2 i.e Fe^{2+}/ H_2O_2, (Fenton's reagent) shows very encouraging results in solar light and it has been utilized for the degradation of several organic compounds[13-16]. The same principle can be used for increasing the photo-catalytic activity of TiO_2. TiO_2 absorbs only 3-5% of the solar radiation reaching to the earth, this restricts its applicability. Therefore for widespread applications, the TiO_2 active in visible light or solar light[20-23] should be developed as future generation of heterogeneous photocatalysts.

1.3 Homogeneous photo-catalysis

This process is defined as ' photo-catalysis taking place in a homogeneous phase' where the combination of oxidizing species and UV radiation has been utilized for degradation of impurities. Use of oxidizing species such as O_3 or H_2O_2 alone may not be able to completely dissociate the organic impurities. The coupling of these two with UV radiation i.e O_3/UV and H_2O_2/UV results in complete destruction of organic impurities in waste water. In this , the photo-degradation occurs by two ways (i) Direct photo-degradation, where UV light excites the organic pollutants (ii) Photo-oxidation, in which irradiation light produces hydroxyl radicals ($^{\bullet}OH$) responsible for photo-oxidation. The oxidants used in this process are O_3, H_2O_2 and fenton's reagent. As stated earlier, the use of UV/H_2O_2 as well as O_3/UV system need a UV radiation of $\lambda < 300$ nm . This irradiation generates •OH radicals by cleavage of H_2O_2 as per the equation given below.

$$H_2O_2 \xrightarrow{h\nu} 2\ ^{\bullet}OH \qquad (1.3)$$

$$H_2O_2 + 2HO^-_2 \longrightarrow O_2 + H_2O_2 + 2\ ^{\bullet}OH \qquad (1.4)$$

1.4 Heterogeneous photocatalysis

It is the technology which is becoming more popular in the area of pollution abatement, in which a semiconductor photocatalyst is irradiated with the light of energy greater than or equal to the band gap of that semiconductor. This irradiation creates a electron-hole pair(charge carriers) at the surface of semiconductor by excitation of one electron from

valence band (VB) to conduction band (CB), as illustrated in fig.1.1. The charge carriers formed are either diffuses rapidly into the semiconductor surface or recombines radiatively and or nonradiatively. The process of diffusion of charge carriers results in nonequilibrium distribution of electrons and holes to the surface. Among these, electrons are very strong reducing sites whereas holes are strong oxidants, which are responsible for reduction or oxidation of adsorbed pollutants on the surface of semiconductor. The efficiency of these redox processes at the surface of semiconductor depend on the following factors.

1. Efficient absorption of light for excitation of electrons
2. Separation of charge carriers after light absorption
3. Product separation to prevent the reverse reactions.
4. Adjustment of redox potentials as per the redox reactions.
5. Stability of the photo-catalyst for long term use

Fig.1.1 illustrates the process of general heterogeneous photo-catalysis on any semiconductor surface. The reduction occurs, if the redox level of 'A' lies below the conduction band of semiconductor and oxidation occurs when redox level of 'D' is positioned above valence band of semiconductor. A class of metal oxides and sulfides can be useful as a semiconductor material which can be used in photo-catalysis. The list of these semiconductors, their VB and CB potentials, band gap energy and wavelength of absorption is given in table.1.1.

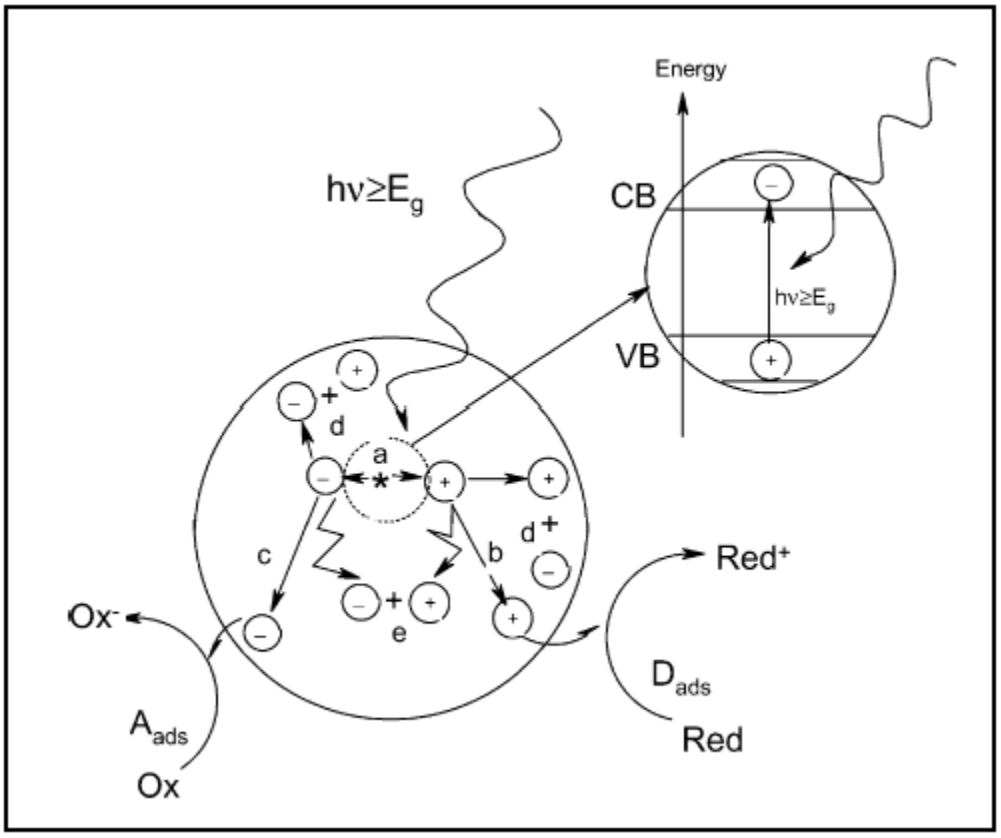

Fig. 1.1 : Process of illumination of a semiconductor with light and subsequent promotion of an electron from the VB to the CB, the resulting formation of electrons and holes and subsequent reduction of electron acceptors 'A' and oxidation of electron donors 'D'.

To get the electron-hole pair, the radiation used for excitation must have wavelength(λ) equal to or lower than calculated by using planks equation (Eqn.1.5) or equation 1.6 given below.

$$\lambda = \frac{hc}{E_{bg}} \qquad (1.5)$$

where λ is the wavelength of radiation, E_{bg} is the band gap energy, h is the plank's constant and c is the velocity of light in vacuum.

$$\lambda = \frac{1240}{E_{bg}} \qquad (1.6)$$

Table. 1.1

Common photo-catalysts used along with their band edge positions, band gap and wavelength in aqueous solution at pH-1

Semiconductor	Valence Band (eV)	Conduction Band (eV)	Band gap (eV)	Wavelength (nm)
GaAs	+ 1.0	- 0.4	1.4	886
CdSe	+ 1.6	- 0.1	1.7	729
GaP	+ 1.3	-1.0	2.3	539
CdS	+ 2.1	- 0.4	2.5	496
WO_3	+3.0	+ 0.2	2.8	443
ZnO	+3.0	- 0.2	3.2	387
TiO_2	+3.1	- 0.1	3.2	387
ZnS	+ 1.4	- 2.3	3.7	335
SnO_2	+4.1	+0.3	3.9	318

From the table, it is seen that, semiconductors such as CdS, CdSe and GaP has band gap energy at lower side and are absorbing visible light as well but during the photoreaction they themselves are photo-corroded making them unsuitable for this application. ZnO and TiO_2 have the same band gap energy (3.2 eV), but TiO_2 is the preferred photo-catalyst because of its favourable properties. TiO_2 is stable in aqueous medium under UV light, chemically and biologically inert, comparatively cheaper and commercially

manufactured on large scale. On the other hand, ZnO is not stable in acidic medium, it starts dissolving and hence cannot be used as a photo-catalyst. There is no other material superior to TiO_2 for photo-catalytic applications hence it is becoming an important and integral part of the photo-catalysis.

TiO_2 exists in three crystallographic forms namely, Anatase, Brookite and Rutile[4]. Among these, rutile is the most stable form and it is used as pigment, as a sunscreen in cosmetics and in medicine as a builder. Anatase is less stable as compared to rutile and it is mostly used in photo-catalytic applications. Anatase is thermodynamically less stable but its formation is kinetically favored at lower temperature and at lower particle dimensions. At low temperature, the hydroxyl content of TiO_2 is more, the particle size will be on lower side, the surface area as well as number of active sites will be more resulting in the higher activity of such a catalyst.

1.4.1 Mechanism of TiO_2 mediated heterogeneous photo-catalysis

In 1972 Fujishima and Honda[24] have reported first time the photo-catalytic splitting of water on TiO_2 electrodes. This study marks the beginning of new era in heterogeneous photo-catalysis. Since then the continued efforts have been made to understand the fundamentals of the process by various research groups.[25-27] Through this extensive research a mechanism of this process has been proposed which suggests that, the hydroxyl radical formation is the main step which is responsible for the photo-oxidation of organic compounds.[28-30] The semiconductors have a band structure where partially or completely filled valence band (VB) and empty conduction bands(CB) are

separated, this separation is known as band gap. In TiO_2 this band gap is 3.2 eV and in order to promote an electron from VB to CB it should be irradiated with light of energy greater than or equal to the band gap energy of TiO_2 . This process leads to the formation of charge carriers (electron-hole pair) in VB and CB as per the equation.

$$TiO_2 + h\nu \longrightarrow TiO_2 (e^- , h^+) \qquad (1.7)$$

The detailed process of this charge carrier formation is as shown in fig.1.2,

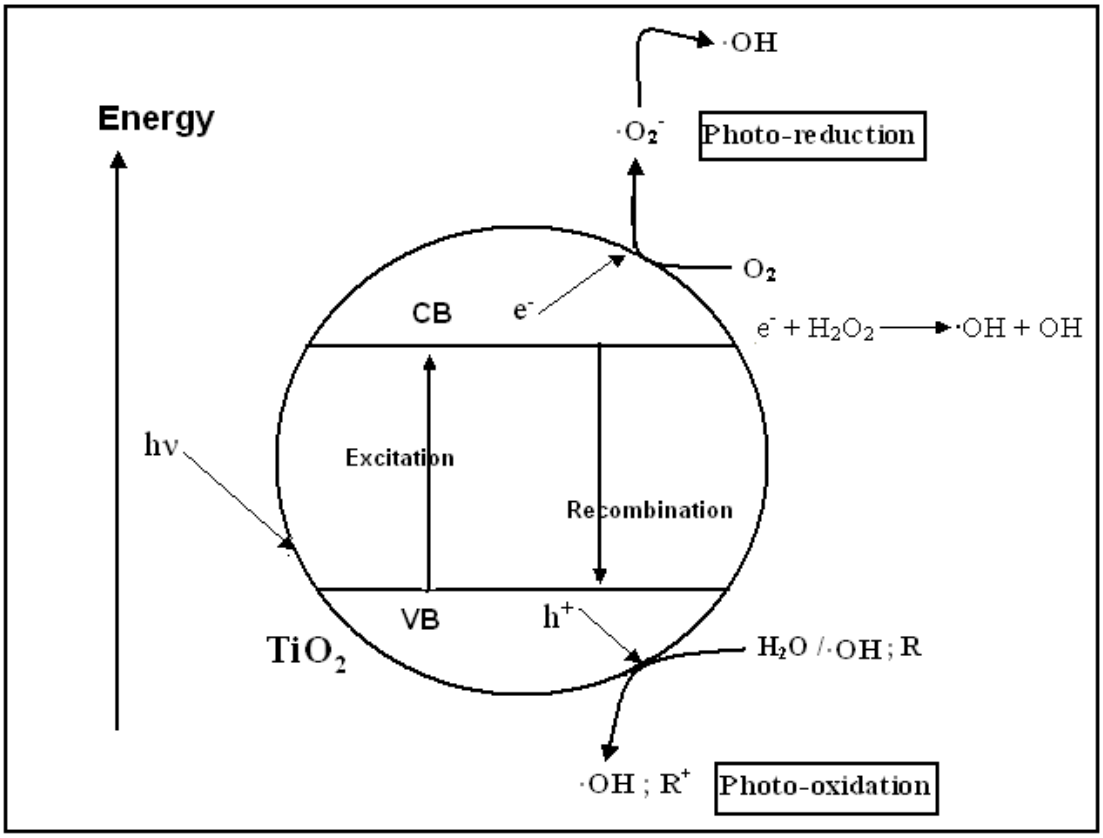

$$\bullet OH + R \longrightarrow \text{intermediates} \longrightarrow CO_2 + H_2O$$

Fig. 1.2: Scheme of TiO_2 mediated photo-catalysis process showing the photo-physical and photo-chemical processes occurring on the surface of photo-catalyst.

From the figure it can be seen that, the h^+ produced in 1st step combines with $H_2O_{(ad)}$ as well as on the surface of photo-catalyst resulting in the formation of OH radicals (Eq. 1.8 and 1.9).

$$TiO_2 (h^+) + H_2O_{(ad)} \longrightarrow TiO_2 + {}^{\bullet}OH_{ad} + H^+ \quad (1.8)$$

$$TiO_2 (h^+) + OH_{ad} \longrightarrow TiO_2 + {}^{\bullet}OH_{ad} \quad (1.9)$$

As stated previously , these OH radicals are strong oxidants which combine with the organic species landed on the surface of TiO_2 results in complete degradation of the organic species to minerals via various intermediates. The various reactions involved in this process are as given in equations below (Eq.1.10-1.13)

The oxygen supplied during the photo-oxidation process accepts or captures electron promoted in C.B, the super oxide anion and its protonated form subsequently dissociate to yield hydrogen peroxide or peroxide anion as per following equation.

$$TiO_2 (e^-) + O_2 \longrightarrow TiO_2 + {}^{\bullet}O_2^- \quad (1.10)$$

$${}^{\bullet}O_2^- + H^+ \longrightarrow HO_2^{\bullet} \quad (1.11)$$

$${}^{\bullet}O_2^- + HO_2^{\bullet} \longrightarrow {}^{\bullet}OH + O_2 + H_2O_2 \quad (1.12)$$

$$2\,HO_2^{\bullet} \longrightarrow O_2 + H_2O_2 \quad (1.13)$$

The Major processes and their characteristic times for TiO_2 mediated photo-oxidative mineralization of organic compounds by dissolved oxygen in aqueous solutions is shown in fig1.3. The figure suggests that, all the processes are very fast and time required to these processes is few micro to few nanoseconds.

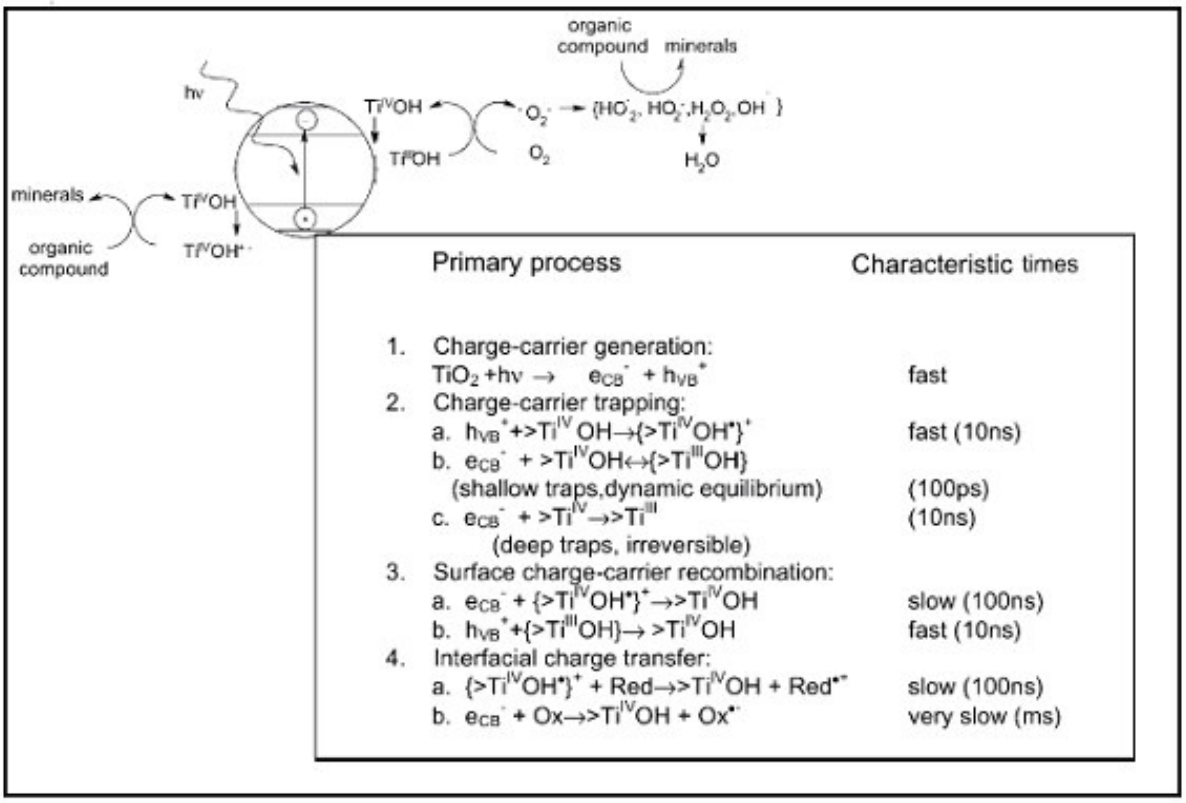

Fig. 1.3 : Major processes and their characteristic times for TiO_2 mediated photo-oxidative mineralization of organic compounds by dissolved oxygen in aqueous solutions.

Generally TiO_2 Degussa P-25 (Degussa make) a mixed phase material containing anatase and rutile in the proportion of 70:30 has been taken as a standard material for TiO_2 mediated photo-catalysis and well studied for photo-catalytic applications.[4,31,32] However some workers have reported the preparation of TiO_2 by different methods and used it for destruction of various organic pollutants. In previous studies[31-33], TiO_2 particles suspended in various types of photo reactor such as slurry type reactor, annular reactor, immersion type reactor and distribution type reactor has been successfully used for destruction of organic contaminants. But the disadvantages such as

need of stirring during photo-catalytic experiments, separation of catalyst powder were essential steps, ultimately the time required for photo-reaction and cost of the process was more.[34,35] In order to overcome these problems some authors have tried to use thin films of TiO_2 on various support materials and found as an attractive alternative to this conventional suspended type of photo-reactors[33-35]. The results obtained by using the immobilized type of photo-catalyst suggests that, the thin film photo-catalyst has not only solved the problem of stirring and separation of catalyst but there is an enhancement in photo-activity has also been observed. The enhanced photo-activity observed in immobilized type photo-catalyst is attributed to the more surface to volume ratio, efficient diffusion of charge carriers on the surface of catalyst due to the short diffusion distance and quantum size effect as the particles are less than 10 nm in diameter. Since the film is very thin, there is more surface to volume ratio, as a result, there is increase in number of active sites on the surface and as number of active sites are more which ultimately improves photo-activity of the catalyst. Thin films are of few nanaometer to few micron thickness so the diffusion of charge carriers, an important step in photo catalytic experiments is easy. As a result there is an enhancement in photo activity in films than powder catalyst.

1.5 Thin film deposition techniques

There are various techniques[36-39] which can be used for deposition of TiO_2 on different substrates depending on the application, some of them are,

1. Physical vapor deposition

2. Chemical vapor deposition
3. Electrodeposition
4. Chemical spray pyrolysis
5. Spin coating
6. Evaporation or sputtering
7. Sol-gel dip coating

Each technique has its own advantages and disadvantages. Compared to the conventional thin film deposition techniques such as electrodeposition, chemical vapor deposition, evaporation or sputtering and spray pyrolysis, sol-gel dip coating technique requires considerably less equipments and hence is potentially less expensive. However the most important advantage of sol-gel dip coating method is its ability to tailor the microstructure of the deposited films. The sol gets easily anchored on the substrates and films are deposited on large as well as complex surfaces. These advantages and its simplicity for large area deposition required for photocatalytic applications prompted us to take up this study for our present work.

The sol-gel dip coating consists of making a suitable sol of the solids to be deposited in the form of thin films, dipping the substrate into the sol and the withdrawal of the substrate from the sol, gravitational draining, solvent evaporation and condensation reaction which result in the formation of uniform solid film on the substrate.

In sol-gel process the inorganic or metal organic compounds (metal alkoxides) are used as precursor material. These precursors in aqueous or organic solvent are hydrolyzed and

allowed to form inorganic polymer having M-O-M network via condensation process as follows.

$$M(OR)_x + x\,H_2O \longrightarrow M(OH)_x + x\,ROH \quad \text{(Hydrolysis)} \quad (1.14)$$

$$M(OH)_x \longrightarrow M\text{-}O\text{-}M + H_2O \quad \text{(Polycondensation)} \quad (1.15)$$

In conventional sol-gel processes, the metal alkoxides are dissolved in alcohol and hydrolyzed by addition of required amount of water under acidic, basic, or neutral conditions. The sol formed in this process contains alcohol or other organic solvents. The sol is adhered to the substrate by dipping the substrate into the sol, the substrate is pulled out slowly and the sol adhered to the substrate is allowed to dry in open atmosphere. A very critical control of process parameters is required to obtain a transparent gel otherwise it leads to the formation of precipitate which is not useful for the deposition of thin films by dip coating. The resulting gel from metal hydroxide sol precursor is stable only for short period of time and it gets solidified making it unsuitable for dip coating.

To overcome these drawbacks titanium peroxide sol could be an attractive alternative for thin film deposition and has been investigated in the present study. To the best of our knowledge, similar study has not been reported earlier. In this process the titanium precursor (Mainly alkoxide) was hydrolyzed by using double distilled water resulting in the formation of titanium oxyhydroxide. The titanium oxyhydroxide is reacted with hydrogen peroxide which is further diluted with water to adjust the required viscosity of the final gel.

1.5.1 Sol-gel Dip Coating

In dip coating, the substrate is withdrawn vertically from the liquid at a specific speed U_0. The viscous sol in the bath adheres to the substrate, upon drying the gel forms a solid film of finite thickness h(x).

Since the solvent is draining and evaporating, the fluid film terminates at a well defined drying line ($X = 0$, in fig.1.4). When the receding drying line velocity equals U_0, the process is steady state with respect to the liquid bath surface. A. non constant evaporation rate in the vicinity of the drying line (due to geometrical factors affecting the diffusing of solvent vapor from the liquid surface) results in a parabolic thickness profile,[40]

$$h(x) \propto x^{1/2} \qquad (1.16)$$

where, h(x) is the film thickness as a function of position x below the drying line.

In an excellent review of dip coating[41] it is stated that the thickness $h(x)$ of the deposited film is related to the position of the streamline dividing the upward and downward moving layers. A competition between as many as six forces in the film deposition region governs the film thickness and position of the streamline. When the liquid viscosity η and substrate speed U_0, are high enough to lower the curvature of the meniscus, the deposited film thickness h is that which balances the viscous drag proportional to $\eta \cdot U_0 / h$ and gravity force $(\rho . g . h)$[41,42]

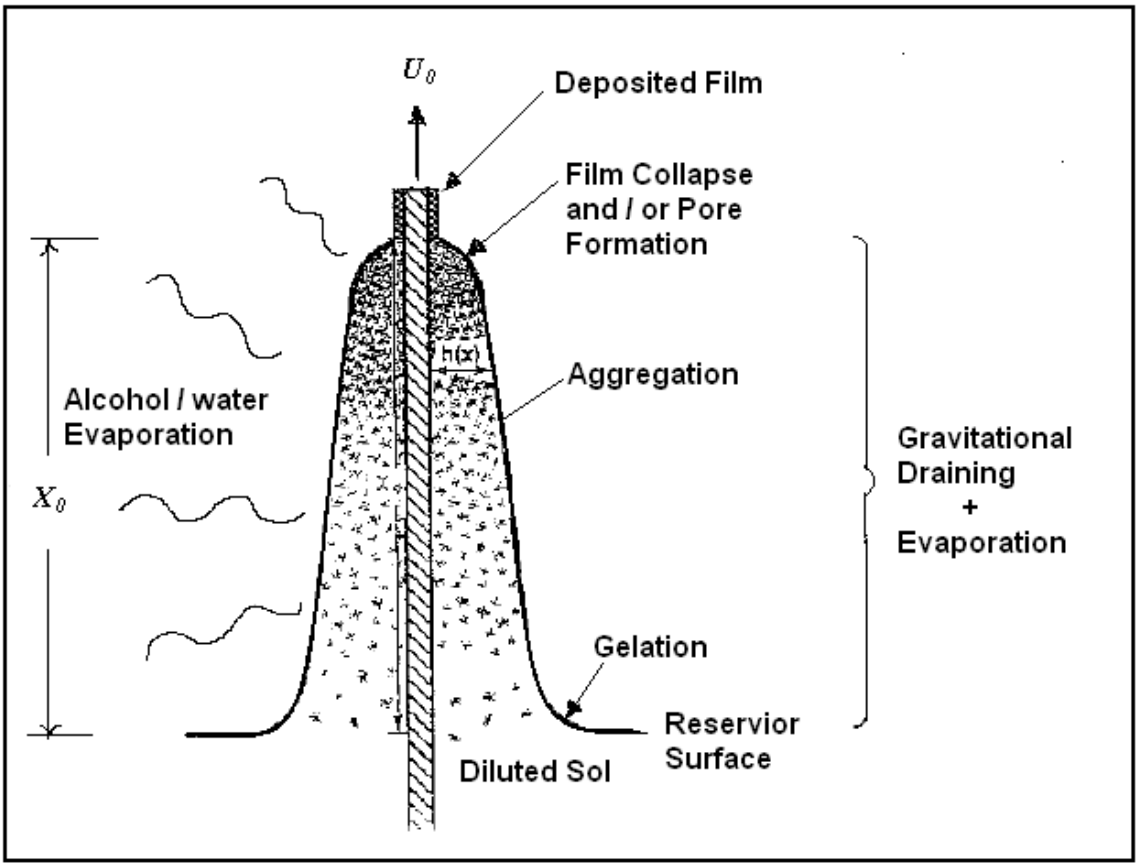

Fig. 1.4 : Schematic diagram of the dip coating and subsequent film formation process showing the sequential stages of structure development after gravitational draining, accompanied by solvent evaporation and continued condensation reactions.

$$h = c_1(\eta U_0 / (\rho g)^{1/2} \qquad (1.17)$$

where the constant c_1 is about 0.8 for Newtonian liquids. When the substrate speed and viscosity are low (often the case for sol-gel film deposition), this balance is modulated by the ratio of viscous drag to liquid-vapor surface tension γ_{LV} according to the relationship derived by Landau and Levich [43]

$$h = 0.94(\eta U_0)^{2/3} / \gamma_{LV}^{1/6} (\rho g)^{1/2} \qquad (1.18)$$

1.5.2 Sol-gel film formation

Deposition of the inorganic film occurs as the entrained inorganic precursor (polymers or particles) are rapidly concentrated on the substrate surface by gravitational draining and evaporation often accompanied by continued condensation reactions. The increasing concentration forces the precursors into close proximity, causing reactive species to aggregate and gel while repulsive particles appear to assemble into liquid or crystal like structures depending on the withdrawal rate. For reactive precursors a competition is established between solvent evaporation which compacts the structure and continuing condensation reactions which stiffen the structure, increasing its resistance to compaction. Unlike conventional bulk gel formation, the drying step overlaps the aggregation-gelation stages, establishing only a brief time span for condensation reactions to occur. A common result is rather compliant structures that are collapsed at the final stage of drying by the capillary pressure P created by the liquid-vapor menisci as they recede into the film interior

$$P = 2\gamma_{LV}\cos(\theta)/r \qquad (1.19)$$

where θ is the wetting angle and r is the hydraulic radius of the pore at the moment the meniscus recedes into the gel interior[43]. Because r may be very small (less than1.0 nm), P may exceed 60 Mpa even for liquids with low surface tension.

The draining and evaporation which accompany dipping cause the thickness h and volume fraction ϕ of solids of the depositing film to change continuously with distance above the liquid bath surface. Above the stagnation point where all fluid elements are

moving upward, steady state conditions require that the solids mass in any horizontal slice must be constant

$$h(x)\,\phi(x) = \text{constant} \qquad (1.20)$$

so ϕ varies inversely with h in the thinning films. For a planar substrate there is a parabolic thickness profile.[41] From the brief description of sol-gel dip coating presented above it seems obvious that the structure of the depositing film will be sensitive to variety of factors such as polymer (or particle) size, structure and reactivity, relative rates of condensation and evaporation, liquid surface tension and dipping speed.

1.5.3 Influence of precursor structure and reactivity

The possible structures of the inorganic precursors range from weakly branched polymers to high condensed particles. For fractal objects the packing efficiency (i.e the solids volume fraction) depends on the fractal dimension, size and condensation rate. The fractal dimension and size dictate steric constraints. If two structures of radius are placed independently in the same region of space, the mean number $M_{1.2}$ of intersections is expressed as

$$M_{1.2} \alpha R^{D_1 + D_2 - d} \qquad (1.21)$$

where D_1 and D_2 are the corresponding fractal dimensions and d is the dimension of space. Thus if the object has fractal dimension less then 1.5, the structures (Films) are transparent and if it exceeds 1.5 the films are opaque.

1.5.4 Effect of substrate speed

An increase in the substrate speed U_0 results in an increase in film thickness according to equations (1.17) and (1.18). Since virtually all solvent evaporation occurs at the exterior surface of the entrained sol (i.e at the sol-vapor interface), thicker films take longer to dry increasing the aging time for reactive sols and as we shall see that the time for ordering of repulsive sols. A second effect of substrate speed is the shear field induced within the depositing sol. When the shear rate experienced by the particle is high with respect to its diffusion coefficients , it is expected that mutually repulsive particles could align in close packed planes oriented parallel to the substrate surface.

By using this method, thin films of TiO_2 were prepared on various substrates such as glass slides, silica rings, silica/glass helix, quartz plates and stainless steel plates. The films deposited on glass plates were mainly used to study the effect of sol viscosity as well as substrate withdrawal speed on the film thickness and for physico-chemical characterization. The films deposited were first dried at 100 ^{0}C, calcined at various temperatures and then used to study the physical properties such as optical properties by UV-Visible spectroscopy, film thickness measurement by tally step profilometer and surface microstructure by SEM technique. However it is reported by few workers that, the substrates containing sodium such as soda lime glass shows decrease in photo-activity than silica substrates hence for study of photo-catalytic activity of these films silica rings as well as silica helix were used . These deposited TiO_2 films were used either as it is or after thermal treatment at certain temperature to induce the crystallization of TiO_2. In order to study the photo-activity of the thin film photo-catalyst

various model pollutants such as salicylic acid, methylene blue, methyl orange and phenol were used. The photo-catalytic experiments using pure TiO_2 films were performed on Rayonet type reactor having in-built facility of UV irradiation source since TiO_2 absorbs only UV radiation. However for study of doped catalysts such as Fe doped TiO_2 (Fe/TiO_2) and Au doped TiO_2 (Au/TiO_2) the natural radiation source the Sun (sunlight in open atmosphere) has been used. For this, an in-house fabricated quartz photo-reactor was installed.

1.6 Kinetics of TiO_2 photocatalysis

1.6.1 Catalyst concentration

Generally, in dynamic, static, slurry and flow type photo-reactors, the initial decomposition rates are directly proportional to the catalyst mass (*m*). This may be attributed to the higher surface area of the catalyst that is available for adsorption as well as decomposition with increase in catalyst mass. However, above a certain *m* limit value, the reaction rate levels off and becomes independent of *m*. This limit also depends on, the nature of the compound to be treated and on the geometry and working conditions of the photo-reactor corresponding to the maximum TiO2 concentration in which all the particles (i.e., all the surface exposed) are totally illuminated. At higher catalyst concentration, a screening effect of exceeding particles masks part of the photosensitive surface. In slurry type reactors, optimal catalyst concentrations lies in the range of 0.15 to 8 gm/l [44-46] whereas in immobilized TiO_2 no such optimum concentration has been reported. For TiO_2 immobilized system there is an optimum

thickness of the films deposited. Since the interfacial area is proportional to the thickness of catalyst as the films are porous, the thick films favor catalytic oxidation. However the possibility of charge carrier recombination increases with film thickness as a consequence the degradation performance is reduced.

1.6.2 Initial reactant concentration

The degradation rate of organic pollutants usually exhibit a saturation behavior hence the observed rate constant decreases with increase in initial concentration of organic pollutant. Generally, in photo-catalytic reactions, the degradation kinetics of compounds follow a Langmuir-Hinshelwood[45] mechanism where reaction rate (r) varies proportionally to the fraction of surface covered by the substrate as follows:

$$r = k\theta = k\left(\frac{KC}{1+KC}\right) \qquad (1.22)$$

where , K is the adsorption constant of the compound, k is the reaction rate constant and C is the initial concentration of pollutant. For diluted solutions, KC becomes $<<1$ and the reaction is of apparent first order, whereas for higher concentrations, $KC>>1$ the reaction rate is maximum and of zero order.[47-49]

1.6.3 Temperature

It is well known that, the photo-oxidation rate is not much sensitive to small variations in temperature. In very few cases it has shown an Arrhenius dependence during

detoxification.[50,51] This weak dependence of the degradation rate on temperature is reflected by the low activation energy compared to ordinary thermal reactions.

1.6.4 pH of the solution

The pH of the aqueous solution significantly affects the particle size, the surface charge, and the band edge positions of the TiO_2 due to its amphoteric character.[52] The Zero Point Charge (pH_{ZPC}) or pH at which the surface of an oxide is uncharged, for TiO_2 is around 7. Above and below this value, the catalyst is negatively or positively charged according to Equations 1.11 and 1.12. In consequence the photo-catalytic degradation of organic compounds is affected by the pH.

1.6.5 Inorganic ions

Some anions commonly found in natural or polluted waters (e.g., chloride, bromide, sulfate, phosphate) have an inhibiting effect on the photo-degradation process if they are bound to TiO_2 or close to its surface.[50,53,5] Consequently, the pH and pH_{PZC} should be determining properties for the ions effect, as well as the chemical affinities of the ions for TiO_2. Significant inhibition in the degradation rate of different compounds has been observed in presence of chloride at pH=3.[55] According to Equation 1.11, at acidic pH, $TiOH_2^+$ and TiOH are the main species on the catalyst surface, and the chloride ions compete with organic compounds for active sites lowering the degradation rates. At higher pH, the negatively charged catalyst surface (Equation 1.12) repulses the approach of chloride ions and no inhibiting effect is observed. Nitrate ions, with charge similar to

that of chloride, only slightly inhibit the reaction at pH=3, indicating the role of individual ions.

1.6.6 Light intensity

In most of the previous studies it is reported that, the light intensity has a key role in photo-degradation process and rate of degradation is proportional to light intensity, which confirms the photo-induced nature of the process, with the participation of photoinduced electrical charges (electrons and holes) in the reaction mechanism.[56] However, at high light intensity the degradation rate becomes proportional to the square root of this parameter.[57] The optimal light power utilization corresponds to the domain where the degradation rate is proportional to light intensity.

1.6.7 Oxygen

Oxygen was found to be very important and essential part of the semiconductor mediated photocatalytic degradation of organic compounds [58]

The rates and efficiencies of photo-assisted degradation of organic substrates are reportedto be significantly improved in the presence of oxygen or by the addition of several oxidizing species such as peroxydisulfate or peroxides.[2,59] The oxygen concentration dependence has been explained by involvement of O_2 adsorption and depletion, both in the dark and during illumination at the photocatalyst surface. Molecular oxygen acts as a conduction band electron trap, suppressing totally or partially the surface electron-hole recombination[60,61] as shown in Equation 1.10. The superoxide ($^{\bullet}O_2^-$) formed is an effective oxidizing agent. Alternatively, the sequence

shown in Equations 1.10 to 1.13 generates hydrogen peroxide to form $^{\bullet}OH$ radicals which also initiate oxidative reactions. But higher concentration leads to a downturn of the reaction rate, which may be attributed to the fact that the TiO_2 surface becomes highly hydroxylated to the extent of inhibiting the adsorption of pollutant at active sites.[62]

1.6.8 Wavelength

The variation of the reaction rate as a function of the wavelength follows the catalyst absorption spectrum, with a threshold corresponding to its band gap energy. Titanium dioxide, having a band gap energy of 3.2 eV, absorbs in the near-UV at $\lambda < 387$ nm. In addition, it must be checked that the reactants do not absorb at that wavelength to conserve the exclusive catalyst photo-activation for a true heterogeneous catalytic regime[47]

1.6.9 Adsorption

One important consideration in the TiO_2 photo-catalyzed reactions is the adsorption of the organic compounds on the surface of the semiconductor particles. The Langmuir-type relationship between degradation rates and initial organic compound concentrations, indicates that adsorption plays a role in the photo-catalytic reaction. However, this role on the photo-catalyzed degradation rate is still uncertain.

1.7 Application of heterogeneous photo-catalysis in pollution abatement

The application of semiconductor (TiO_2) mediated photo-catalysis for the remediation of waste water containing harmful impurities, removal of various toxic gasses in air and synthesis of organic compounds has been increased since last 10-15 year. The reason behind is that, this process is very simple in operation, catalyst can be regenerated and use of solar radiation which ultimately saves the energy. In figure 1.5, graphical representation of the year wise total publications of TiO_2 and the work published on TiO_2 mediated photo-catalysis has been presented. Now more and more research is undertaken by various research groups to improve photo-catalytic performance as well as possible other potential applications of TiO_2.

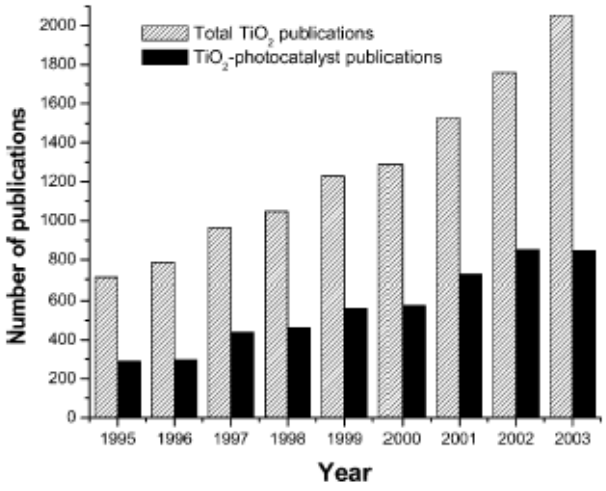

Fig. 1.5 : Year wise publications on TiO_2 and TiO_2 mediated photo-catalysis[63].

The graph suggests that, the number of TiO_2 publications and TiO_2 mediated photocatalysis has been increasing every year. This shows importance and seriousness of the environmental problem. Now there is need to increase the efficiency of TiO_2 by

modifying the structure, absorption of major part of visible radiation and increasing the reactivity . The present study is one such sincere attempt to prepare and characterize modified TiO_2 photo-catalyst.

References

1. O. Legrini, E. Oliveros, and A.M. Braun, Chem. Rev., 1993. 93(2) 671-698.
2. P.Robertson, Semiconductor photocatalysis: an environmentally acceptable alternative production technique and effluent treatment process. J. Cleaner Prod. , 1996. 4(3-4): p.203-212.
3. M. Hoffmann, *et al.*, Environmental Applications of semiconductor catalysis. Chem. Rev. 1995.95: p. 69-96.
4. F. A. Cotton, Wilkinson, G. *Advanced Inorganic Chemistry*, 4th ed. John Wiley & Sons, New York, 1980, p 695.
5. D. Bahnemann, *et al.*, Photocatalytic Treatment of Waters, in Aquatic and Surface Photochemistry, G.R. Helz, R.G. Zepp, and D.G. Crosby, Editors. 1994, Lewis Publishiers Boca Raton. p. 261-316.
6. J.R. Bolton and S.R. Cater, Homogeneous photodegradation of pollutants in contaminated water: an introduction., in Aquatic and Surface Photochemistry, G.R. Helz, R.G. Zepp, and D.G. Crosby, Editors**.** 1994, Lewis Publishiers: Boca Raton. p. 467-490.
7. F.J. Beltran, J.M. Encinar, and J. Gonzalez, F., Industrial wastewater advanced

oxidation. Ozone combined with hydrogen peroxide or UV radiation. Water research, 1997. 31(10): p. 2415-2448.

8. J. Beltran-Heredia, et al., Comparison of the degradation of p-hydroxybenzoic acid in aqueous solution by several oxidation process. Chemosphere, 2001. 42: p. 351.
9. D.F. Ollis, E. Pelizzetti, and N. Serpone, Heterogeneous Photocatalysis in the environment:Application to Water purification, in Photocatalysis: Fundamentals and applications, N. Serpone and E. Pelizzetti, Editors. 1989, Wiley: New York. 603.
10. C.Walling, Fenton's reagent revisited. Acc. Chem. Res., 1975. 8: p. 125-131.
11. Y.F. Sun, and J.J. Pignatello, Photochemical-Reactions Involved in the Total Mineralization of 2,4-D by Fe^{3+}/H_2O_2/UV Environ Sci Technol, 1993. 27(2) 304.
12. R. Bauer and H. Fallmann, The photo-Fenton oxidation -a cheap and efficient wastewater treatment method. Res. Chem. Intermed, 1997. 23(4): p. 341-354.
13. S. H.Bossmann, et al., new evidence against hydroxyl radicals as reactive intermediates in the thermal and photochemically enhanced Fenton reactions**.** J. Phys. Chem., 1998. 102, 5542.
14. P. Pichat, Partial or complete heterogeneous photocatalytic oxidatation of organic compounds in liquid organic or aqueous phase. Catalysis Today, 1994, 19, 313.
15. M.A Fox. and M.T. Dulay, Heterogeneous photo-catalysis, Chem. Rev., 1993. 93 341- 357.
16. N. Serpone, Brief introductory remarks on heterogeneous photo-catalysis, Solar energy materials and solar cells, 1995. 38: p. 369-379.
17. N. Nogishi, T. Iyoda, K. Hashimoto, A. Fujishima, Chem. Lett. 1995, 841.

18. M. R. Hoffamnn, S. T. Martin, W. Choi, D. W. Bahnemann, Chem. Rev. 95 1995 69.

19. P. V. Kamat, in Nanoparticles and Nanostructured Films, ed. J. H. Fedler, Wiley-VCH, New York 1998).

20. K.E. Karakitsou and X. E. Verykios, J. Phys. Chem. 97 (1993) 1184**.**

21. M. Graetzel and R. F. Howe, J. Phys. Chem. 94, 1990, 1566.

22. J. Soria, J. C. Conesa, V. Augugliaro, L. Palmisano, M. Schiavello and A. Sclafani, J. Phys. Chem. 1991, 95 274.

23. J. Kiwi and C. Morrison, J. Phys. Chem. 88. 1984, 6146.

24. A. Fujishima, K. Honda, Nature, 238, 1972, 37.

25. H. P. Maruska, A.K. Ghosh Solar Energy 1978, 20, 443.

26. H. Gerischer, Heller A. J. Electrochem Soc 1992, 139,113.

27. R.I Bickley, Gonzales-Carreno T, J.L.Lees, L. Palmisano, Tilley RJD**.** J. Solid State Chem. 1991, 92, 178.

28. C. Kormann, D.W. Bahnemann, Hoffmann. Environ. Sci. Technol. 1988, 22, 798.

29. A.J. Hoffmann, E.R. Carraway, M.R. Hoffmann . Environ. Sci. Technol. 1994, 28, 776.

30. Carraway E.R, Hoffmann A.J, Hoffmann M.R. Environ. Sci. Technol. 1994;28:786.

31. A.Mills, and S. Le Hunte, An overview of semiconductor photocatalysis. Journal of Photochemistry and Photobiology A: Chemistry, 1997. 108, p. 1-35.

32. M. Litter, Heterogeneous photocatalysis transition metals ions in photocatalytic systems. Applied Catalysis B: Environmental, 1999, 23, 89-114.

33. Ajay K. Ray, Catalysis Today 1998, 44 , 357-368

34 Yu-Hong Zhang, Armin Reller, J. Mater. Chem. 2001,11, 2537.

35. Misook Kang, J. Mol. Catal. A: Chemical, 2003, 197, 173.

36. L. Kavan, M. Gratzel, Electrochim. Acta, 1995, 40, 643.

37. L. Kavan, B. O'Regan, A. Ray, M. Gratzel, Electroanal. Chem., 1993, 346, 291.

38. C. Natarajan, G. Nogami, J. Electrochem. Soc. 1996, 146, 1547.

39. Y. Hamasaki, S. Ohkubo, K. Murakami, H. Sei, G. Nogami, J. Electrochem. Soc. 1994, 141, 660.

40. L. E. Scriven, C. J. Brinker, D. E. Clark and D. R. Ulrich (eds.), Better ceramics through chemistry III Materials Research Society, Pittsburgh, PA, 1988, 717-1025.

41. R. P. Spires, C. V. Subaram and W. L. Wilkinson, Chem. Eng. Sci. 1974. 29, 389.

42. L. D. Landau and B. G. Levich, Acta physiochim. U. S. S. R, 1942, 17, 42- 54.

43. Yu Y, Leu RM, Lee KC. Water Res 1996,30,1169.

44. Okamoto K, Yamamoto Y, Tanaka H, Itaya A. Bull. Chem. Soc. Jpn.1985, 58, 2023.

45. D. Chen, A.K. Ray Appl Catal B: Environ 1999, 23,143.

46. J.C.Crittenden, J. Liu, D.W. Hand, D.L. Perran Water Res 1997, 31, 429.

47. J.M. Herrmann, Heterogeneous photocatalysis: fundamentals and applications to the removal of various types of aqueous pollutants. Catalysis Today, 1999. 53, 115-129.

48. Y. Inel, and A.N. Okte, J. of Photochemistry and Photobiology A: Chemistry, 1996 96 175-180.

49. I. Arslan, I.A. Balcioglu, and D.W. Banheman, Applied Catalysis B: Environmental, 2000, 26, 193-206.

50. Herrmann, J.M., C. Guillard, and P. Pichat, Catalysis Today, 1993, 17, 7-20.

51. T. Zhang, *et al.* Journal of Photochemistry and Photobiology A: Chemistry, 2001. 140: p.163-172.

52. Fernandez-Ibanez, P., F.J. de las Nieves, and S. Malato, Journal of Colloid and Interface Science, 2000, 227, 510-516.

53. E. Pelizzetti, 1995, 38, 453-457.

54. Wang, K.H., *et al.*, The pH and anion effects on the heterogeneous photocatalytic degradation of o-methylbenzoic acid in TiO2 aqueous suspension. Chemosphere, 2000, 40, 389-394.

55. Wang, K.H., *et al.*, Photocatalytic degradation of 2-chloro and 2-nitrophenol by titanium dioxide suspensions in aqueous solution. Applied Catalysis B: Environmental, 1999, 21, 1-8.

56. Ollis, D.F Solar-assisted photocatalysis for water purification: issues data, questions, in Photochemical conversion and storage of solar energy. 1991, Kluwer Academic Publishers, 593-622.

57. Al-Sayyed, G., J.C. D'Oliveira, and P. Pichat, Journal of Photochemistry and Photobiology A: Chemistry, 1991, 58, 99-114.

58. Al-Ekabi H, Safarzadeh-Amiri A, Sifton W, Story J. Int J Environ Pollut 1991;1:125.

59. Wang, y. and C.S. Hong, Water research, 2000, 34(10), 2791-2797.

60. Ollis D.F, Pelizzetti E, Serpone N. Environ. Sci. Technol. 1991,25,1522.

61. Murov S.L, Carmichael I, Huy G.L.Handbook of photochemistry. New York: Marcel Dekker, 1993.

62. Braun A.M, Oliveros E. Water Sci. Technol. 1997, 35, 17.

CHAPTER-II

PREPARATION, CHARACTERIZATION AND PHOTOCATALYTIC ACTIVITY OF TiO_2 THIN FILMS

2.1 Introduction

Titanium dioxide (TiO_2) belongs to the family of transition metal oxides.[1-3] In the beginning of 20th century, the industrial production of TiO_2 started where toxic lead oxides were replaced by TiO_2 as pigment for white paint. At present, the annual production of TiO_2 has been raised up to 4 million tons.[4-6] It is the most stable oxide of titanium and can be obtained from either natural or synthetic sources. The material exists naturally in three crystal modifications known as rutile, anatase, and brookite.[7] Naturally occurring titanium dioxide may appear red or reddish brown to black. The color is normally due to the presence of iron, chromium, or vanadium contamination, which may amount up to 10 % of the total titanium content. Synthetically purified titanium dioxide exists as a white,[8] odorless, tasteless powder. It reacts only with hot, concentrated mineral acid solutions, stable with respect to light, oxidation, change in pH of suspensions and microbiological attack. It has been found to be stable at all temperatures up to its melting point of 1850ºC.[9] In addition, TiO_2 itself does not have any toxic effect whatsoever and is biocompatible. The most important use of TiO_2 is as a white pigment(85-90% of the total production) , owing to its very high reflectance at visible and

ultraviolet wavelengths. Among all semiconductors, the refractive index (~ 2) of this material is so high that fine particles scatter light with almost total efficiency. Anatase was the first commercial titanium dioxide pigment. In coatings and plastics, anatase has now been replaced by rutile because the latter has a scattering advantage over the former of about 20%. These two are used in a wide variety of applications, for example, formulation of surface coating, printing inks, coloring of plastics, rubber, linoleum, paper, cement, and concrete etc. The application of pigment in minor end use sectors such as textiles, food (it is approved in food contact application and food coloring)[10], leather, pharmaceuticals, toothpaste and UV absorber in sunscreen cream with high protection factors has been increased day by day.[11-13]

Titanium dioxide is now becoming more popular in the area of photo-catalysis, a well-known semiconductor that possesses a high photo-activity. It participates in many photo-catalytic reactions including oxidative degradation of organics,[14-23] reduction of metal ions,[24] evolution of dihydrogen from water,[25] photo conversion(oxidation or reduction) of inorganic compounds. Due to its low cost, ease of handling, and high resistance to photoinduced corrosion TiO_2 is gaining more importance in all types of photo-reactions. In particular, TiO_2 has been proven to be a very efficient photo-catalyst for the degradation of biorefractory contaminants. The effectiveness of titania as a photo-catalyst depends on its crystal phase, particle size, and crystallinity. The crystal structure of anatase and rutile is as shown in Fig. 2.1and 2.2. The figure shows the crystal structure showing unit cell, cation polyhedra of anatase and rutile type of TiO_2.

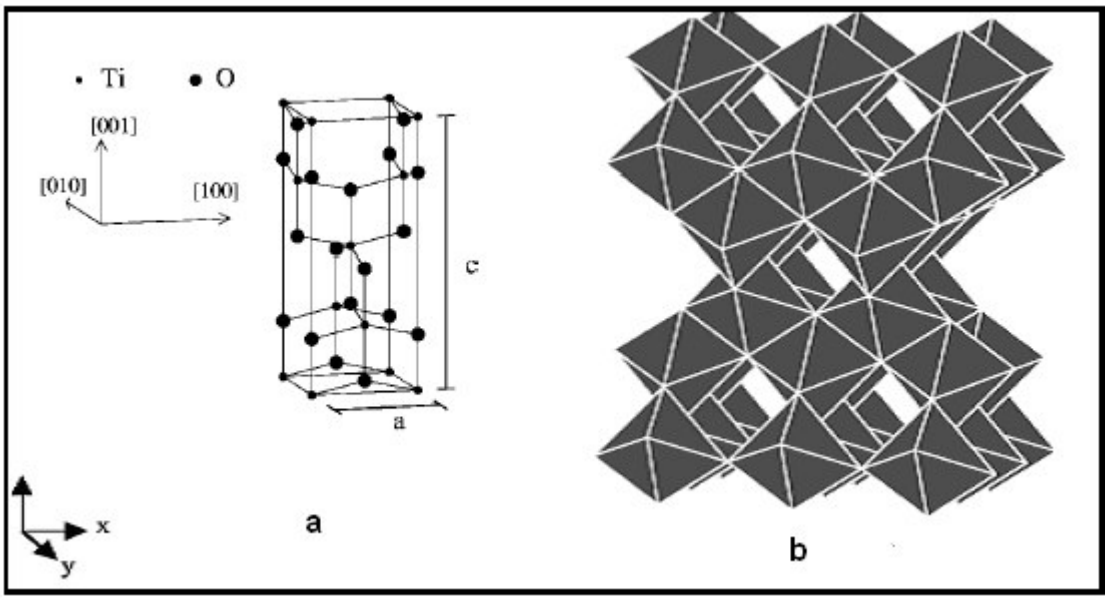

Fig. 2.1 : **Crystal structure of anatase TiO_2 (a) Unit cell. (b) Cation Polyhedra.**

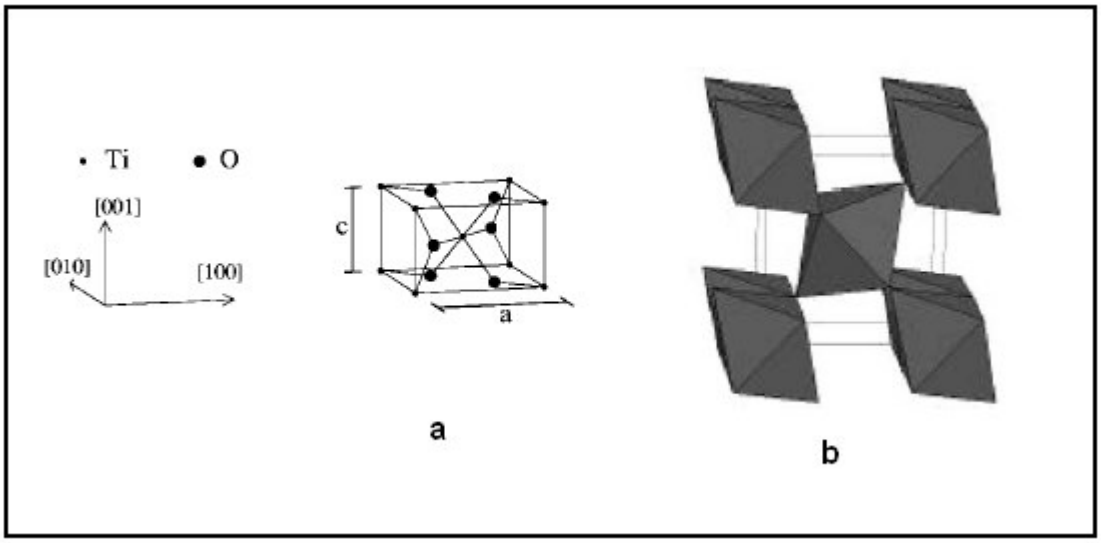

Fig. 2.2 : **Crystal structure of rutile TiO_2 (a) Unit cell. (b) Cation Polyhedra.**

Both the crystals are formed by chains of distorted TiO_6 octahedra and their tetragonal structure can be described in terms of three parameters: two cell edges *a* and *c* and one internal parameter *d*. In rutile , the unit cell contains two TiO_2 units, each Ti atom is coordinated to six neighboring oxygen via two apical (long) and four equatorial (short) bonds. Each O atom is coordinated to three Ti atoms via one long bond and two short bonds, lying in the same plane. The anatase phase is ~ 9% less dense than rutile and has a tetragonal unit cell containing four TiO_2 units. The coordination of Ti and O atoms is same as in rutile, however the octahedra are significantly more distorted[25d].

Among the common crystalline forms of TiO_2, anatase is generally recognized to be the most active phase. The more activity of anatase as compared to rutile is ascribed to difference of fermi level and the extent of surface hydroxylation of solid. Apart from this, anatase is more stable at lower particle dimensions/particle size, smaller particles are usually better photo-catalysts due to their high surface area to volume ratio. However, the band gap is a strong function of titania particle size for diameters less than 10 nm, which can be attributed to the well-known quantum size effect.[26a-29] Particles in this size range have extremely high surface area, but the blue shift in usable photon energy with decreasing size limits their usefulness. Clearly, an optimum particle size balancing the appropriate band gap with the high surface area is needed for adsorption of molecules and photocatalysis. It is agreed that a good degree of crystallinity is essential in order to have photoactive titania.[30-32] However, the influence of degree of crystallinity on photo-activity has not been well understood.

2.2 Preparation methods

TiO_2 can be prepared in the form of powder, crystals, or thin films. The powder and films of TiO_2 can be built up from crystallites ranging from a few nanometers to several micrometers. Titanium dioxide powder required for various applications can be manufactured on large scale by two main processes, the sulfate and the chloride proces[33]. In the sulfate process, ilmenite is transformed into iron- and titanium sulfates by reaction with sulfuric acid. Titanium hydroxide is precipitated by hydrolysis, filtered, and calcinated at 900 ^{0}C. Straight hydrolysis yields only anatase on calcination. To obtain rutile, seed crystals, generated by alkaline hydrolysis of titanyl sulfate or titanium tetrachloride are added during the hydrolysis step. The sulfate process yields a substantial amount of waste iron sulfide and poor quality TiO_2. The chloride process has now become the dominant and popular for the production of TiO_2. In this process crude rutile TiO_2 produced from ilmenite using the Becher process has been used. The Becher process reduces the iron oxide in the ilmenite to metallic iron and then re-oxidizes it to iron oxide separating out the titanium dioxide as synthetic rutile of about 91–93% purity. In this process, the ilmenite ore is heated in high temperature furnace along with coal and sulfur. The slurry of reduced ilmenite (which consists of a mixture of iron and titanium dioxide in water) is oxidized with air and can be separated in settling ponds. The iron oxide (that represented at least 40% of the ilmenite) is returned to the mine site as waste and for land filling process. The TiO_2 produced by above two methods has been mainly used for paint and pigment applications where particle size, shape and purity are not much important. However for certain applications such as solar cells, antireflection

coating, photo-catalysis and many other applications where particle size, purity are important factors, the fine TiO_2 powder as well as films prepared by other methods have been used. Depending on the application and crystal phase requirement the following methods are used to prepare films as well as fine powder.

1. Co-precipitation method
2. Hydrothermal or solvothermal method,
3. Microemulsion method,
4. Spray pyrrolysis
5. Sol-gel method.
6. Combustion method.

It should be noted that nanosized crystallites tend to agglomerate and for isolation of nanosized particles without agglomerates, a deagglomeration step was necessary in many preparation methods. However by using some novel methods nanoparticles without agglomerates can be prepared without an additional deagglomeration step. The various methods used for preparation of TiO_2 powder as well as films are as follows.

The co-precipitation method involves the precipitation of hydroxide by addition of alkali solution (NaOH, NH_4OH, Urea) to the titanium precursor solution ($TiCl_3$ or $TiCl_4$).[34-37] The hydroxides obtained are calcined at certain temperatures in order to get the crystalline products. However the disadvantage of this method is that it is very difficult to obtain uniform distribution of nano sized TiO_2 because the fast hydrolysis or precipitation often causes the formation of larger particles instead of nanoparticles.

In hydrothermal or solvothermal method the various solvents like methanol, toluene, 1,4 butanol and water are used as reaction medium[38-40] and the chemical reaction is allowed to take place at low temperature under self generated pressure in a closed vessel. The calcination step can be avoided in this method because most of the times crystalline products are obtained. Also the method has advantages such as the nanosize product can be obtained , the grain size can be controlled and product obtained is uniform in size distribution. But the disadvantages such as requirement of long duration to complete the reaction, cost of the product, very difficult to commercialize the process are the main hurdles.

Microemulsion is another method which can be employed to prepare nanosize TiO_2 particles with low agglomeration.[41-42] In this an emulsion of two immiscible liquids which are thermodynamically stable, optically isotopic is prepared and microdomains of it stabilized by interfacial film of surfactant. This method can be used for preparation of TiO_2 in very small quantity and very rarely it has been used due to its limitation.

The fine, highly crystalline and large surface area anatase TiO_2 particles can be synthesized by combustion method. In this method , the sol containing redox mixture is heated rapidly and temperature reaches about 500-700 ^{0}C for short span of time. (may be for 1-5 minutes) This results in the formation of crystalline anatase TiO_2 powder. Since the material is at higher temperature only for few minutes, the particle growth of TiO_2 and transformation of anatase to rutile is hindered.

The fine particles can be produced by these methods in order to use it for photocatalytic applications. In previous studies many authors have used the powder TiO_2 for photo-

catalytic application. Various types of photo-reactors have been developed to study this catalyst powders. Initially the results obtained in photo-degradation of organic as well as inorganic pollutants were encouraging but latter it was observed that the catalyst separation after each experiment was a tedious and time consuming job. This is because to get better photo activity fine particles were used and it was very difficult to separate these particles by using various filtration techniques. In order to overcome this problem and further enhance the efficiency of TiO_2, researchers were of opinion that the use of TiO_2 thin films can be an attractive alternative for the pollution abatement. The extensive research in this field has generated plenty of publications in the area of thin films of TiO_2 for photo-catalytic applications. Thin films of TiO_2 can be deposited by using different techniques on verity of substrates. The techniques normally used are as follows.

Spray pyrolysis is an aerosol deposition technique for thin films and powders related to CVD . The metal organic compound or metal salt solutions[43-52] are used as precursor and they are converted into aerosol (small droplets). This aerosol is then focused on preheated hot substrate where either a film of TiO_2 or fine nanosize TiO_2 powder is formed. The technique has merits on other deposition techniques such as simplicity, low cost, reproducibility and fast deposition in large areas. However the films obtained by this techniques are non uniform in thickness as well as the films are not smooth enough.

The films of TiO_2 can also be obtained by electrochemical synthesis method. This method can be used to prepare advanced thin films such a epitaxial, superlattice, quantum dot and nanoporous. It is difficult to make the films using titanium inorganic

salts because of fast hydrolysis of these salts. In order to prevent the hydrolysis of titanium salts during the electrodeposition the films have been deposited either in oxygen free environment or in acidic medium. By following this method films have been deposited using inorganic salts such as $TiCl_3$[53,54] , $TiOSO_4$[55,56] and $(NH_4)_2TiO(C_2H_4)_2$[57,58]. In order to prevent hydrolysis during electrodeposition the use of non aqueous solvents will be an attractive option.[59]

The gas phase techniques such as chemical vapor deposition (CVD) and physical vapor deposition (PVD) can also be used to deposit TiO_2 thin films.

The chemical vapor deposition technique is mainly used in industrial application for fast deposition of thin films of semiconductor or ceramics on large surface area in short span of time. The films deposited by this techniques are lacking in properties such as smoothness and conductivity. However the films deposited by physical vapor deposition method are superior than prepared by CVD with respect to smoothness of the films, better conductivity, less contamination etc. In physical vapor deposition technique (PVD) the films are formed from gas phase of the precursor material and this technique can be used for substances which are stable in gas phase. The commonly used PVD technique is thermal evaporation where a material is evaporated and the vapors are allowed to condense on the substrate placed straight above the vapor source. Generally for deposition of TiO_2 thin films electron beam (E beam) is used as a source for thermal evaporation of substance. As mentioned above the films are superior in quality than prepared by CVD and other techniques but the film production is slow and laborious, so for deposition of thin films of TiO_2 for special applications this technique is very

suitable but for the applications such as photo-catalysis these gas deposition techniques may not be suitable due to their high cost as well as time consuming work.

Each of the technique reported above for the synthesis of nanosize fine TiO_2 as well as for deposition of TiO_2 thin films has certain advantages and disadvantages over each other. Hence depending on the application, cost and type of TiO_2 required the material can be produced by these techniques.

For applications like pollution control by degradation of pollutants using TiO_2 mediated photo-catalysis , the following qualities of the photo-catalyst as well as the degradation process may be considered while developing the method of catalyst preparation as well as treatment process.

1) Catalyst should be easily available
2) Cheap and cost effective
3) Efficient for photo-degradation of pollutant
4) Stable for long term application.
5) The process should be simple and easy for operation

To meet the above mentioned requirements, we have developed a very simple process for the deposition of thin films of TiO_2 on various substarstes using titanium peroxide based sol-gel dip coating technique.

The process consists of the preparation of thin films of TiO_2 by sol gel method, its characterization by various techniques and application as photo-catalyst. The reason for choosing the sol-gel method is that, it has potential to deposit the TiO_2 films on various substrates and has many advantages such as, easy for operation, the sol gets easily

anchored on the substrate and many more other advantages over the other film deposition techniques, like purity of TiO_2 films, homogeneity, felicity and flexibility, control over composition, ability to control microstructure and very useful for deposition of large and complex surface area substrates. The sol gel films can be prepared by using nonalkoxide and alkoxide precursors. The use of non alkoxide precursors such as nitrates, chlorides, acetates, carbonates, acetylacetonates[60-62] for TiO_2 thin film preparation have been reported but the removal of inorganic ions is necessary in these processes which is an additional step. The alkoxides (most preferably used in sol-gel methods) such as $Ti(OEt)_4$[63], $Ti(i\text{-}OP)_4$ and Ti $(O\text{-}nBu)_4$ can be used as a Ti-precursor for TiO_2 sol, gel and or precipitate.

The sol-gel process involves, the formation of metal-oxo-polymer network from molecular precursors such as metal alkoxides (titanium alkoxide) or metal salts.[64] In the case of titanium the titanium precursor such as titanium ethoxide, titanium isopropoxide or titanium butoxide are hydrolyzed as per equation (2.1)

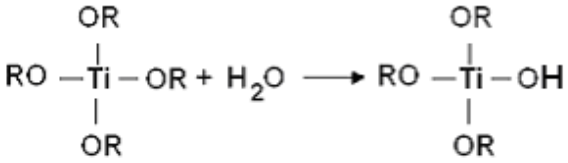

2.1

The control over this step is very important because if the hydrolysis is not controlled properly it results into separation of titanium hydroxide precipitate rather than a clear and transparent sol. The sol when kept for long duration, starts to form a polymer type gel by the process of polycondensation (Eq.2.2) as follows.

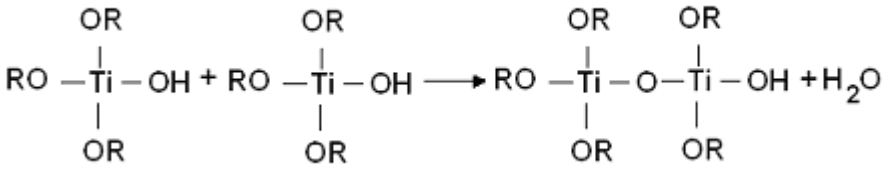

2.2

The relative rates of hydrolysis (Eq. 2.1) and polycondensation (Eq. 2.2), strongly influences the structure and properties of the resulting oxide. Factors affecting the sol-gel process are the reactivity of metal alkoxide, pH of the reaction medium, water : alkoxide ratio, reaction temperature and nature of solvent and additives. By varying the process parameters , materials with different microstructure and surface chemistry can be obtained. The films of TiO_2 as well as powder prepared by this method are normally amorphous in nature and it requires heat treatment at certain temperature to induce crystallization of TiO_2. In order to control the rate of hydrolysis of titanium precursor, the sol is prepared by using nonaqueous solvents i.e organic solvents because water induces the fast hydrolysis and results in formation of hydroxide of titanium rather than a sol. The water : alkoxide : solvent ratio plays an important role in the formation of transparent sol. Therefore, it is very essential to adjust the ratio in such a manner that the precipitate of titanium hydroxide should not form. Generally in this, the solvents added are in large quantity and during aging of the gel the solvent is allowed to evaporate in ambient atmosphere.

In view of the above, we have developed a sol-gel method, which is aqueous base instead of organic base and no organic impurities are released into the atmosphere during this sol-gel process. The process is based on the preparation of Ti-peroxy complex by

reaction of titanium alkoxide with hydrogen peroxide and subsequent gelation of the titanium peroxide sol after keeping for few hours. This method was previously reported to be used for detection of titanium and hydrogen peroxide content only. In 1988 Shimota[64] et. al have studied the optical and thermal properties of aqueous titanium isopropoxide-hyrogen peroxide solution and dry powder. Nogami [65] et. al have reported the preparation of titanium peroxide sol by reaction of titanium metal, hydrogen peroxide and dilute ammonia solution and the resultant solution has been utilized for deposition of TiO_2 films on ITO glass substrates using spray pyrolysis technique. In 2001 Niesen[66] et.al have reported to use this sol for preparation of self assembled monolayers on silicon substrates. Although the authors mentioned above have reported to use the titanium hydrogen peroxide sol for preparation of TiO_2 thin films, so far to the best of our knowledge no one has studied the sol-gel behavior of the titanium peroxide sol and thin film deposition using this sol by dip coating technique. We are the first to study in detail the sol-gel behavior of this system and used this process for deposition of thin films by sol-gel dip coating, a simplest technique for deposition of thin films.

2.3. Experimental

2.3.1 Materials

Titanium (IV)isopropoxide (TIP), and Titanium(IV) butoxide were obtained from Aldrich (Milwaukee, WI). De-ionized water was prepared from double distilled water using the de-ionized water unit (Millipore, Milli-Q-System) All chemicals and reagents were used as received without further purification. Glass substrates used for making

titania thin film were the microscope slides and other substrates such as silica rashig rings as well as glass helix were from VWR Scientific (Media, PA). These substrates were pretreated with acidic solution before use to remove sodium as well as other impurities on the surface of it .[67] First the substrates were put into a H_2SO_4 : H_2O_2 (3:1 v/v) mixture and kept immersed for 1 hr, followed by 2-3 washing with de-ionized water. The substrates were then kept in oven for drying at 100 ^{0}C.

2.3.2 Preparation of TiO_2 precursor sol

In the preparation of Ti-precursor sol, Titanium (IV) tetrabutoxide (4.8g, Aldrich chemicals) was hydrolyzed with deionized water (100ml) (as per eqn. 2.3), the resulting titanium hydroxide precipitate was separated by decantation and washed 2-3 times thoroughly with water to remove the alcohol generated during hydrolysis of titanium tetrabutoxide.

$$Ti(OR)_4 + 4\,H_2O \longrightarrow Ti(OH)_4 + 4\,R\text{-}OH \qquad (2.3)$$

The titanium hydroxide formed as per eqn.2.3 was allowed to react with aqueous hydrogen peroxide solution. This reaction results in formation of aqueous solution of titanium hydrogen peroxide complex hereafter referred as 'titanium peroxide' as per the equation 2.4

$$Ti(OH)_4 + H_2O_2 \longrightarrow Ti\,O_{2-x-0.5y}(O_2)_x(OH)y\,.H_2O + H_2O \qquad (2.4)$$

The reaction as per eqn.2.4, is highly exothermic and the heat generated during this reaction must be removed otherwise, it results in separation of precipitate of titanium peroxide rather than a sol. Films deposited by using this gelatinous precipitate are non

transparent and not uniform in thickness. Therefore the control over the sol temperature is very important in this stage of reaction in order to deposit the transparent, uniform in thickness and non scrachable films.

The sol prepared was initially like water but upon keeping for long time it slowly turns to dense and finally forms a dense transparent yellow colored gel. Under our deposition conditions where the pH of the sol was approximately 4, hydrolyzed cations would lead to hydrous oxide by condensing through both olation and oxolation[67a], which may be written schematically as follows.

$$M\text{-}OH + M\text{-}OH_2 \longrightarrow M\text{-}OH\text{-}M + H_2O \qquad \text{(Olation)}$$

$$M\text{-}OH + M\text{-}OH \longrightarrow M\text{-}O\text{-}M + H_2O \qquad \text{(Oxolation}$$

In order to study the variation of viscosity of the precursor sol with time, effect of concentration of Ti on viscosity and variation of film thickness with viscosity, it is very essential to know the sol-gel behavior of this titanium peroxide system. The schematic representation of the preparation of precursor sol by using titanium peroxide sol-gel method is given below in fig.2.3.

To study the variation of viscosity with time and effect of concentration on sol-gel behavior, Ti-precursor (Titanium peroxide) solutions of three different concentrations 0.01M, 0.005M and 0.001M (concentration with respect to TiO_2 content) were prepared. The viscosity of the three solutions was measured after every 30 minutes time interval.

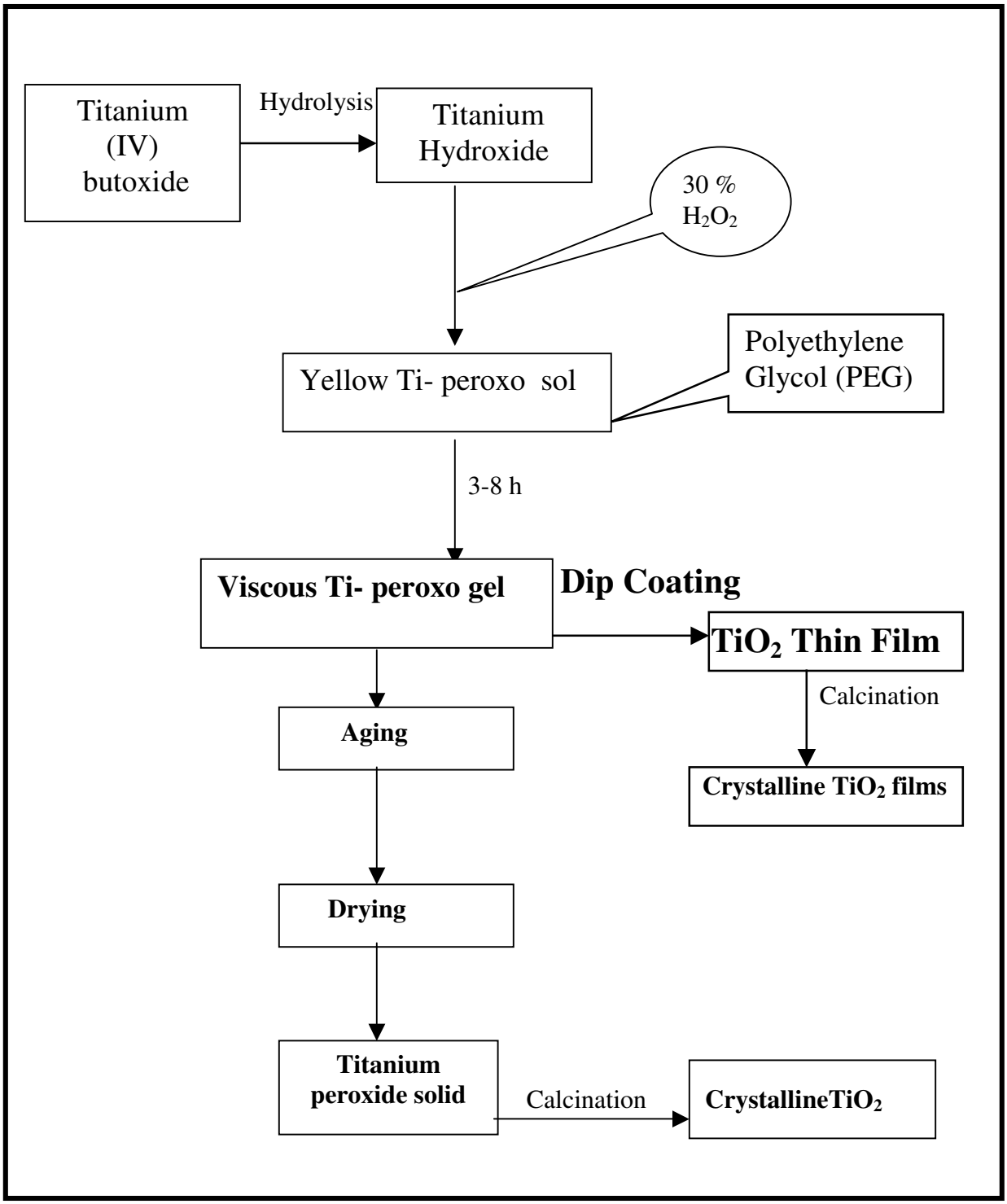

Fig. 2.3 : Schematic representation for preparation of TiO_2 thin film photo-catalyst in titanium peroxide sol-gel method.

The details of this study are discussed in section 2.5 with graphical presentation. However using titanium peroxide sol the films deposited are very thin and upon drying have very low wettability as a result the thickness of films can not be increased by performing more than one coating cycle. In order to increase the film thickness by coating substrate for more than one coating cycle, polyethylene glycol(PEG) has been added to the titanium peroxide sol.

2.3.3 Deposition of thin films of TiO_2 on glass plates

For the deposition of film, the substrates were first degreased, cleaned thoroughly and dried before deposition. The titanium peroxide sol of known concentration was prepared by using the method discussed in section 2.3.2. In the initial stage the sol releases oxygen by decomposition of unreacted excess hydrogen peroxide and if films are deposited at this stage the films are porous and non uniform. This is because during withdrawal of the glass plate, surface may contain bubbles along with sol film and these bubbles break during drying process leaving the surface with patches(uncoated). So the sol was allowed to stand for 3-8 hr depending on the concentration to ensure the complete decomposition of excess H_2O_2 and stabilize the sol of particular viscosity. Then the substrate was dipped in the viscous Ti- precursor sol of known viscosity as well as concentration and kept immersed in the sol for 2-5 minutes, then pulled out with uniform pulling rate of 1-2 mm/sec. The sol adhered to the substrate was allowed to dry in open atmosphere, due to atmospheric air and temperature the sol releases the solvent (water in this case) leaving a solid film of TiO_2 on the glass slide. After drying in open

atmosphere the films were then kept for further drying in an oven at 100 ^{0}C for complete removal of solvent. By following this the films obtained are very thin in thickness. The thickness of TiO_2 films can not be increased by coating the substrate for more coating cycles because after first coating cycle the film formed is hydrophobic, hence titanium peroxide sol does not adhere to substrate for second and subsequent coating cycles. In order to increase the film thickness as well as modification of surface, the polyethylene glycol (PEG) is added to the titanium peroxide sol (before gel formation). The sol containing PEG (0.1-2 gm)/g TiO_2 improves the adhesion of the sol to the substrate and using this sol comparably thick films can be deposited by coating substrate number of times. The films formed are then characterized by various techniques to study the properties. By using this method the substrates like glass plates, stainless steel plates and quartz plates were deposited. However these substrates can not be used for photo-catalytic study because of the size and shape of substrates. For photo-catalytic study of the catalyst, films are deposited on small sized and convenient substrates such as glass helix and silica ring.

2.3.4 Deposition of TiO_2 thin films on glass helix and silica rashig rings

The substrates such as silica/glass helix and silica rashig rings are small in dimensions and have a complex surface. Deposition of thin films of TiO_2 on each individual substrate one by one using above method may be tedious and time consuming job. Therefore for deposition on substrates like glass helix and silica rashig rings, the substrates were first cleaned and degreased by following the method used for cleaning

the glass plates. The known amount of substrates were taken and added into the titanium peroxide sol of particular viscosity. The viscous sol slowly turns into dense transparent yellow colored gel and it was allowed to dry completely. The TiO_2 gets deposited on the rings as well as helix from all sides, it was dried further in an electric oven. The substrates were heated in an electric furnace to induce the crystallization of TiO_2 before it is used for photo-catalytic experiments.

2.4 Photo-catalytic reactions using thin film photo-catalyst

The photo-activity of the thin film photo-catalyst was tested by decomposition of salicylic acid, methyl orange, phenol and methylene blue solution under UV light. The photo-reactor used in this study is as shown in fig.2.4, manufactured by Rayonet (UK) . The reactor system consists of a pyrex vessel (200 ml capacity) having jacket for water circulation for maintaining the constant temperature and a 150 watt UV lamp parallel to the vessel. The rector vessel also has an inlet for O_2 bubbling inside the reaction mixture and outlet for gases generated during the photo reaction. For this measurement, the silica rashig rings coated with TiO_2 and PEG-TiO_2 were used. The TiO_2 catalyst coated (approx.0.2g TiO_2 on 100 gm helix) in the form of thin films by following the method described in section 2.3.1 were heat treated at temperature 500 ^{0}C for 2 hrs first and then used for photo reactions.

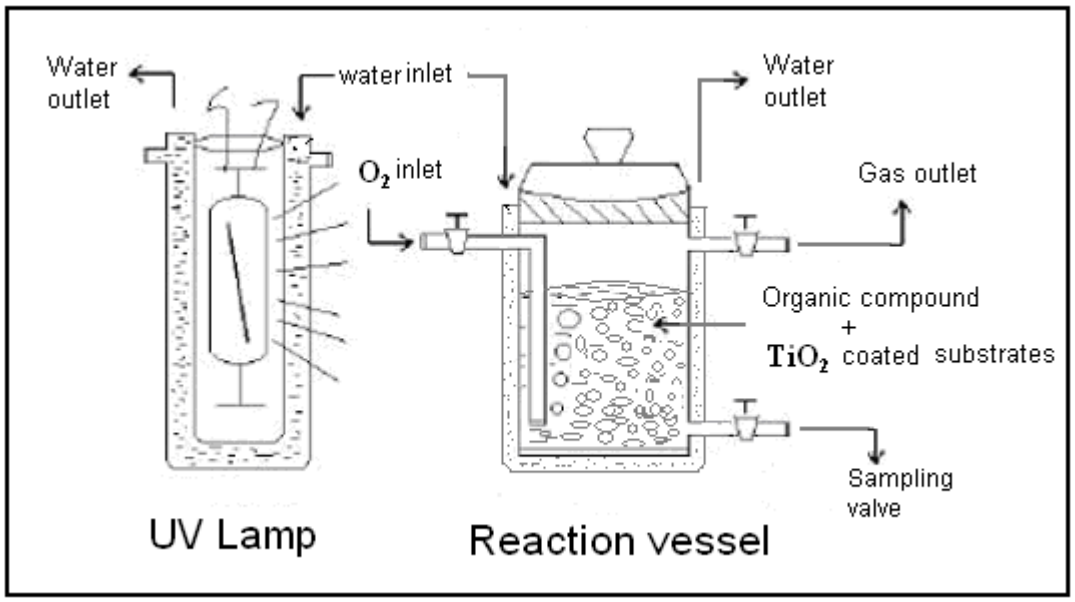

Fig. 2.4 **:** Schematic diagram of the photo-reactor used in the present study.

The 1.0 x 10^{-5} , 2.8 x 10^{-5}, 3.1 x 10^{-4} and 3.2 x 10^{-4} M stock solution of salicylic acid, methylene blue, methyl orange and phenol respectively used in this study were prepared by dissolving LR grade compounds in water and kept in air tight vessel in dark place. Throughout this study the same concentration of each pollutant compound and catalysts have been used.

For all photo-catalytic reactions, the reactor used and other reaction conditions were kept identical. The catalyst coated glass helix 100gm in weight were taken and fed into the reactor vessel. To this 100 ml of the salicylic acid (1.0 x 10^{-5} M) was added and kept for 30 minutes in dark place. After 30 minutes the sample was analyzed by UV-visible spectrometer to check the amount of adsorption and then the tube was irradiated with a 150 watt UV lamp (Hg lamp fitted in the reactor) for different time intervals. The samples were collected after irradiation of every 1hr and analyzed with UV-visible

spectrophotometer (Hitachi 3210). The differential absorbance at 296 nm for salicylic acid (absorption peak of salicylic acid) was measured. The change in the concentration of the salicylic acid of the irradiated sample as a function of time was compared with a sample kept in darkness.

For degradation of other compound studied such as methylene blue, methyl orange and phenol also the process described above has been followed and the samples were analyzed using UV-visible spectrometer. The differential absorbance of irradiated samples at 662.5 nm, 490 nm and 289.4 nm was measured for methylene blue, methyl orange and phenol respectively.

The UV-visible instrument was calibrated first for each compound used in this study by preparation of aqueous solutions containing various concentrations. The UV-visible spectra of the solutions for each concentration has been taken and the correlation between absorption at characteristic wavelength of that compound and concentration has been developed. The linear relationship between the absorbance (A) and the concentration (C) can be represented empirically by the equation.

$A = a. C$

where a is the calibration constant for each compound.

2.5 Characterization of thin films and powders

2.5.1 Measurement of viscosity of the sol

The titanium peroxide sol slowly becomes viscous due to internal chemical reaction. The change in viscosity with time was studied by measuring the viscosity of the sol at the

various stages of gel formation. The Brookfield make viscometer having RV type of spindles was used for this measurement. Depending on the viscosity, the spindle has been changed at various stages of polymerization of sol into gel. The viscosity in centipoises was calculated by multiplying the viscometer reading and the factor for that particular spindle.

2.5.2 Measurement of film thickness

The thickness of the Ti-peroxide films on glass plates was measured by Talley Step profilometer. For this measurement, the half surface of the plate was coated on one side and the height of the step i.e difference between the uncoated surface and coated surface was measured. In this measurement, the instrument works on the principle of height difference between coated surface and uncoated surface.

2.5.3 UV-visible spectroscopic characterization

The optical characterization of the gel as well as thin film photocatalyst was carried out using UV-visible spectrophotometer (Hitachi, U-3210) with wavelength range from 300-800 nm and scanning speed of 120 nm /min. For the UV-visible analysis of gel prepared is allowed to stabilize for 3-4 hr. During this time the unreacted H_2O_2 decomposes by releasing oxygen bubbles since it is light sensitive and the titanium peroxide sol stabilizes. This stabilized sol is then allowed to attain the viscosity around 240 cps and then filled in the quartz cuvette. The sample was then scanned with the scanning speed

of 120 nm/ min in the absorption mode. The spectrum obtained was recorded on thermal paper. By following this method all the samples were analyzed.

For the UV-visible characterization of thin films deposited on glass plates, the deposited thin films were first dried in open atmosphere at room temperature followed by drying in an electric oven at 100 ^{0}C. One set of the films was the subjected to heating at different temperatures from 200-500 ^{0}C in an electrically heated furnace in air. All these films were analyzed at the same scanning speed and wavelength range.

2.5.4 X-Ray diffraction studies

The powder diffraction is the most important technique used for the characterization of all crystalline materials. It furnishes vital information regarding the phase purity, structure type, isomorphous substitution, degree of crystallinity and estimation of particle size as well as unit cell parameters. The structural characterization was carried out using X- ray diffraction technique (Rigaku, Miniflex) with Cu Kα radiation. The titanium peroxide films deposited on glass plates were calcined at various temperature (200-600 ^{0}C) at the heating rate of 2-5 ^{0}C / min. After cooling the substrates, the films were peeled off from substrate with sharp edge blade and then utilized for XRD analysis. For dry gel samples, the gel was aged, dried in open atmosphere and then crushed using the agate pestle mortar to get powder of titanium peroxide. The sample was divided into 15-20 parts. From these 5 parts of the samples were taken separately and subjected to calcinations at different temperatures in the temperature range 200-600 ^{0}C at the heating rate of 10^{0}C/ min. The powder samples obtained after calcinations

and as prepared samples were dispersed and packed in the slot on the glass plate used for recording the powder diffraction pattern. The x-ray spectra were recorded using accelerating voltage of 35 kV and applied current of 20 mA. The x-ray pattern recorded were used to find out the structure, planes and particle size. In crystalline samples it was observed that, as the particle or crystallite size increases , the broadening of peak at particular theta value takes place. From the extent of broadening the peak, a particle size or crystallite can be estimated by using Scherrer Equation given below (Eq. 2.5) ,

$$d = \frac{0.9\lambda}{\beta \cos\theta} \qquad 2.5$$

Where d is the crystallite size, λ is the wavelength of the X-ray radiation (Cu Kα =0.154 nm),and β is the line width at half-maximum height, after subtraction of equipment broadening.

2.5.5 Thermo-gravimetric analysis

Thermal characterization of the titanium peroxide gel as well as films was studied by using TG/DTA technique (Metler Toledo, TG-DTA) with simultaneous DTA measurement. For this measurement, the dry gel was crushed using pestle-mortar or the films were peeled off using sharp edge knife and small quantity of it has been utilized. For each measurement 10-15 mg sample was used and heated at the heating rate of 5 ^{0}C / min in the temperature range of 40-900 ^{0}C under air atmosphere. The thermogram (TG curve) recorded was used to calculate the loss in weight with respect to temperature. The

DTA curve was utilized to understand the physical and chemical transformation taking place at various temperature.

2.5.6 Surface morphology

The crystallite size and morphology of the samples were analyzed using scanning electron microscopy technique. In this, high energy X-rays are bombarded on the sample and the scattered secondary electrons are used to form the image.

The surface properties Ti-peroxide powder as well as thin films were observed under Scanning Electron Microscope (SEM, XL-20, Philips) and Transmission Electron Microscope (TEM, JEOL). For SEM analysis, the Ti-peroxide films deposited glass plate was first cut into a small square size piece of 3 mm x 3 mm. Prior to analysis the surface of the sample glass piece was coated with Au by sputter coating technique in order to minimize the surface charging during the SEM analysis. Then the samples were mounted on aluminium stubs and observed under microscope. For TEM analysis, the dilute sol of Ti-peroxide with very low viscosity was used for deposition of thin films on copper grids. The sol adhered to the copper grid was dried in air at room temperature followed by further drying at 100 ^{0}C in oven. These samples were then observed under TEM.

2.5.7 Surface area analysis

The Brunner –Emmett- Tellor (BET) volumetric gas adsorption (nitrogen or argon) technique is a standard method for the determination of surface area and pore size

distribution of finely divided powder samples. The instrument used for this method was Quantahrome (Nova). The surface area of the sample is calculated using this technique. The general for of BET equation can be written as

$$1/ V_{ads}(P_0-P) = 1/ V_mC + [C-1/V_m] P/P_0$$

where V_{ads} = Volume of gas adsorbed at pressure P

P_0 = Standard vapor pressure

V_m = Volume of gas adsorbed for monolayer coverage

C = BET constant.

By plotting the left hand side of the equation against P/P_0, a straight line is obtained with slope (C-1) / V_mC and an intercept $1/V_mC$. The BET surface area was calculated using the following formula,

$$S_{BET} = X_m . N. A_m$$

Where N is Avagadro's number, A_m is the surface area of adsorbate molecule (For N_2 $A_m = 0.162$ nm^2) and X_m is the moles of nitrogen adsorbed.

2.5.8 Fourier transform infrared spectroscopy

This is a very good and important tool for the investigation of titanium dioxide. The FTIR (Perkin-Elmer, Spectrum 2000) instrument has been utilized for this study. The films on silica plates or glass have been directly used for FTIR measurement whereas for powder samples, the KBr pellets have been prepared and scanned in the range of 400-4000 cm^{-1}. This technique can be used to get information regarding the stretching and bending vibrations of hydroxyl groups as well as other functional groups. The surface

hydroxyl content of the TiO_2 films as well as powder can be investigated using this technique. The FTIR technique can also be used for investigating the Ti-O and Ti-O-O skeletal frequencies of anatase and rutile phases.

2.5.9 Chemical analysis of the photo-catalyst

Chemical analysis for Ti content of the films as well as powder was performed using Energy Dispersive X-ray Analysis (EDX) and Inductively Coupled Plasma-Optical Emission Spectroscopy (ICP-OES, P-1000, Perkin-Elmer).

For quantitative analysis using ICP-OES, a known quantity of the sample (0.1-0.5 gm) was taken using microbalance (Metler-Toledo, AT-201) in a glass beaker and the sample was dissolved in conc. H_2SO_4 : H_2O_2 (3:1 by volume) mixture solution. After complete dissolution the solution was diluted to 100 ml using freshly prepared double distilled water or deionized water (Millipore Milli Q system). This solution was used for analysis of Ti content in the films. The instrument was calibrated first for Ti using 1.0, 5.0 and 10.0 ppm standard solution at 334. 941 nm wavelength then samples were run as unknown.

2.6 Results and Discussion

2.6.1 Variation of viscosity of the sol with time

The change in viscosity of the precursor sol with time was studied at room temperature. Fig.2.5 shows the plot of change in viscosity of titanium peroxide solution having various concentration with time. The as prepared titanium peroxide solution was orange

colored and flows like water because initial viscosity of titanium peroxide sol with all concentrations was very low i.e 4-5 centipoise and attains highest within 12-70 hours depending upon the concentration of the titanium ion in the sol.

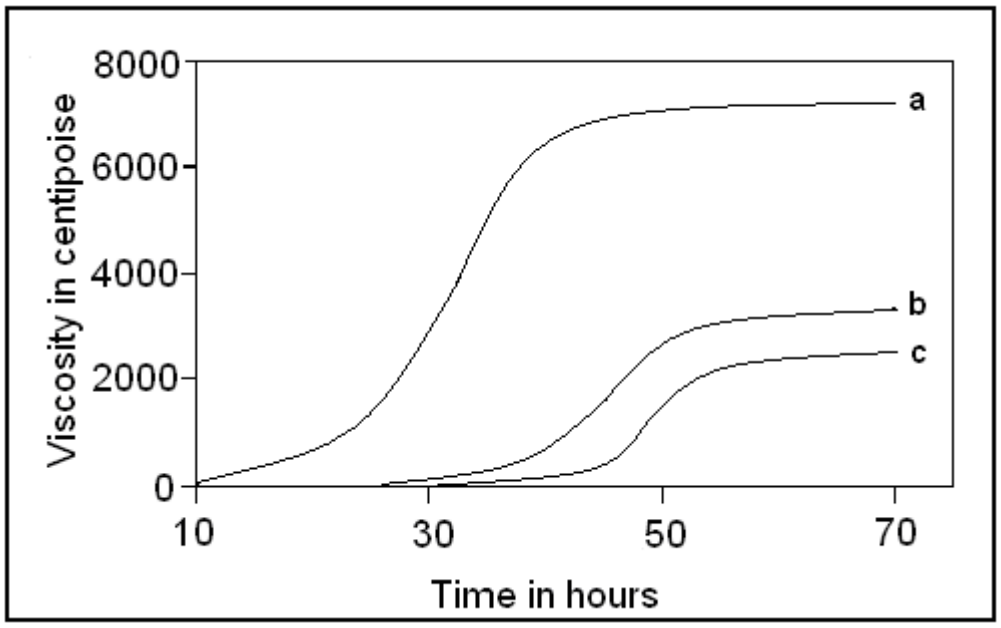

Fig. 2.5 : Variation in viscosity with time of titanium peroxide sol having titanium ion concentration a) 0.01 M b) 0.005 M and c) 0.001 M

Among the three solutions, the 0.01 M Ti containing sol starts to change the viscosity within 1hr and the rate of change in viscosity was also high as compared to other concentrations and within 3-4 hr time it attains a viscosity at which film deposition on glass slides can be started. However for 0.005M and 0.001M sol, for attaining the same viscosity 8-10 hr and 25-30 hr respectively are needed. So the viscosity of the TiO_2 sol and deposition of thin films are totally concentration dependent. The concentrated sol attains highest viscosity within 20-22 hr, medium sol takes 40-50 hr very dilute sol may attain its maximum viscosity in 60-70 hr and some times it results in separation of titanium peroxide precipitate rather than formation of gel. The effect of viscosity of the

sol on film thickness as well as on the quality of films has been observed during film deposition process. Films deposited by using the sol of viscosity within the range of 120-6000 cps were transparent, uniform in thickness and had very good adhesion to the substrate whereas films deposited using sol of viscosity below this range were transparent with good adhesion to the substrate but not uniform in thickness and having different colors at different spots. The films prepared by using sol of viscosity higher than this range were semi transparent with poor adhesion to the substrate, non uniform in thickness and after drying easily detaches. From this it can be concluded that the films deposited within viscosity range 120- 6000 cps were good in quality and useful for photo-catalytic experiments.

2.6.2 Variation of film thickness with viscosity

As discussed in previous section (section 2.6.1) the viscosity of TiO_2 sol plays an important role in the thin film deposition process. The viscosity is not only important in depositing the films but also to get proper thickness as well as good adhesion to the substrate. For this study the titanium peroxide sol of concentrations 0.001M, 0.01M and 0.05 M were used. The curve a - c in fig.2.6 represent variation in film thickness with change in viscosity of sample concentration 0.001M, 0.01M and 0.05M respectively. In the initial stage the viscosity of the sol was very low hence the films deposited were very thin. Using the Talley step profilometer, thickness below 30 nm can not be accurately measured. Therefore films deposited using the sol of viscosity above 300 cps and thickness more than 30 nm were used and studied.

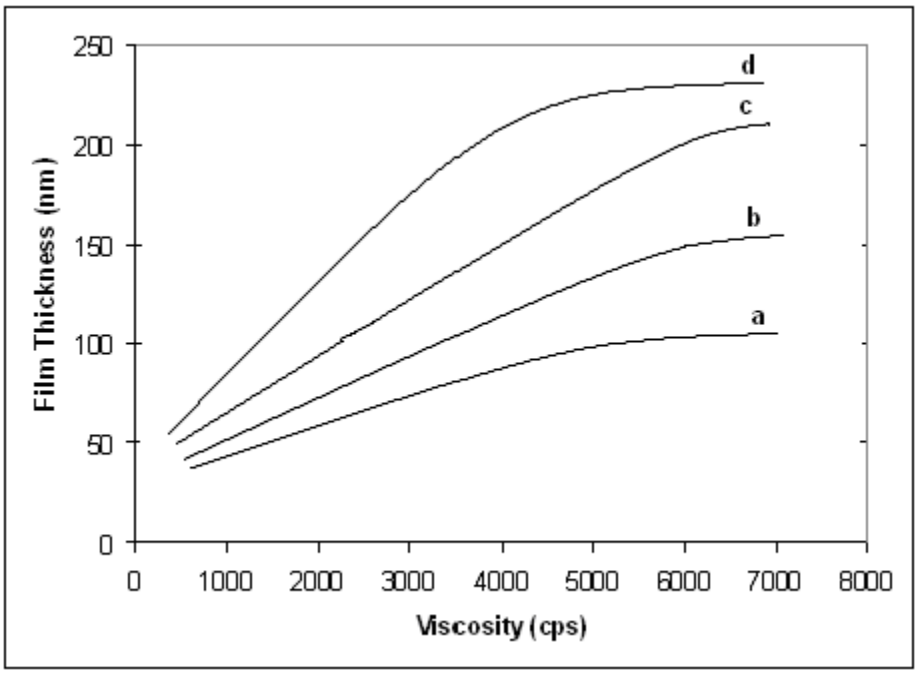

Fig. 2.6 : Variation of film thickness with viscosity of sol of concentrations a) 0.001 M, b) 0.01 M, c) 0.05 M, and d) 0.05 M containing 0.6g PEG/gTiO_2.

From the figure it is observed that the film thickness increases with increase in viscosity of titanium peroxide sol used for thin film deposition and this trend continues until the thickness reaches to 100-230 nm depending on the concentration of the sol used. After this it stabilizes and no much change in thickness was observed. This may be because in the viscosity range of 5500-6000 cps the sol almost turns to gel and once it forms gel the adhesivity or adhesiveness of it decreases, as a result there is no much increase in film thickness. Also when such gel is used for deposition of the substrate, it does not get adhered evenly, so after drying the surface looks unevenly coated and at the places where the film is thick it starts to get detached by simple rubbing with paper. This indicates if the films are deposited by using highly viscous liquid it looses its adhesion.

In the fig.2.6, it is also observed that, as the concentration of TiO_2 into the sol increases, the thickness also increases in the same viscosity range. It shows that, the thickness of the film is not only dependent on viscosity of the sol but also on the concentration of TiO_2 in the sol. In order to study the effect of PEG addition on the film thickness, 0.6 gm PEG was added into the sol of concentration 0.05M. Curve d in the fig.2.6 corresponds to the films deposited using PEG added Ti-peroxide sol. The results shows that, thickness of films deposited using PEG containing sol is more at particular viscosity than bare titanium peroxide sol. This shows that addition of PEG increases adhesion of film to the substrate.

The adhesion of the films was tested by performing scotch test using Scotch tape test method. In this test, the coated glass plate was cut into pieces of 5mm x 5 mm using the diamond glass cutter then a piece of commercial scotch tape was then applied firmly onto this piece. The tape was peeled off slowly from the film and the total portion of film gets peeled off has been used to see the extent of adhesion.

2.6.3 UV-visible spectroscopic characterization

The optical characterization of the titanium peroxide films deposited using the 0.05 M TiO_2 sol-gel aged for 8. 12, 18, 24 hrs and the PEG added sol aged for 24 hrs. Fig.2.7 shows UV-visible spectra of the TiO_2 films deposited on glass slides and calcined at 400^0C. The spectra show that, the films are transparent in visible region and shows characteristic absorption in UV region at around 325 nm wavelength which is typical absorption of TiO_2.

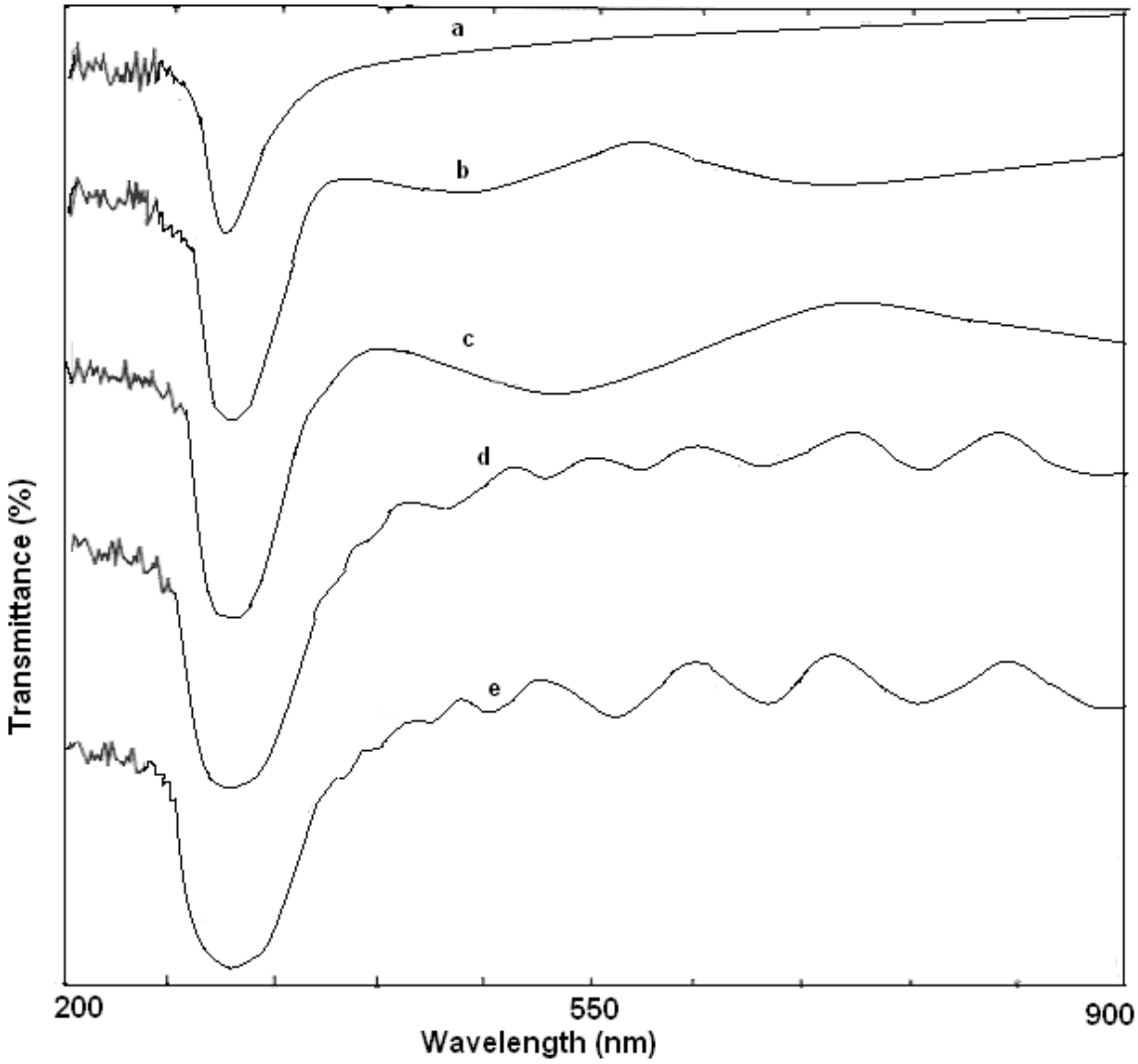

Fig. 2.7 : UV- visible spectra of thin films deposited on glass plates by dip-coating in the titanium peroxide sol aged for a) 8, b)12, c) 18, d) 24 hr and e) PEG added sol aged for 24 hr respectively.

The bulk TiO_2 shows absorption at around 380-400 nm depending on the structure and band gap. In this case the absorption edge of TiO_2 is shifted toward UV region (Blue shift) this may be attributed to the extremely small particles TiO_2 in thin films and

quantum size effect. The band at 305 nm slowly shifted toward the visible side for the films deposited using sol aged for longer duration and it increases with aging time. This is because film thickness increases with aging time of the gel used for deposition and variation in particle size of TiO_2. The spectra also shows absorption bands (maxima and minima) in 350-800 nm region. The number of maxima and minima increases with film thickness, this may be attributed to the absorption of the films due to interference color of the films.[66]

2.6.4 X-Ray diffraction studies of TiO_2 photocatalyst

The X-ray diffraction patterns of the as prepared dried at 100 ^{0}C gel and the samples heated at 200, 300, 400, 500, and 600 ^{0}C respectively are as shown in fig.2.8 (curves a - g). The XRD pattern of TiO_2 powder dried at 100 ^{0}C (curve a) shows it to be amorphous in nature. The sample were heated at 200 ^{0}C (curve b) shows an additional hump around 25.3 ^{0} which is the characteristic peak of 101 plane of anatase type of TiO_2 indicating the beginning of crystallization. Intensity of this peak increases with increase in heating temperature in samples heated at 200-500 ^{0}C (curve c ~ e) respectively. The additional peaks corresponding to 004 and 200 plane of anatase phase are also seen along with the predominant 101 peak in samples heated at 500 ^{0}C.

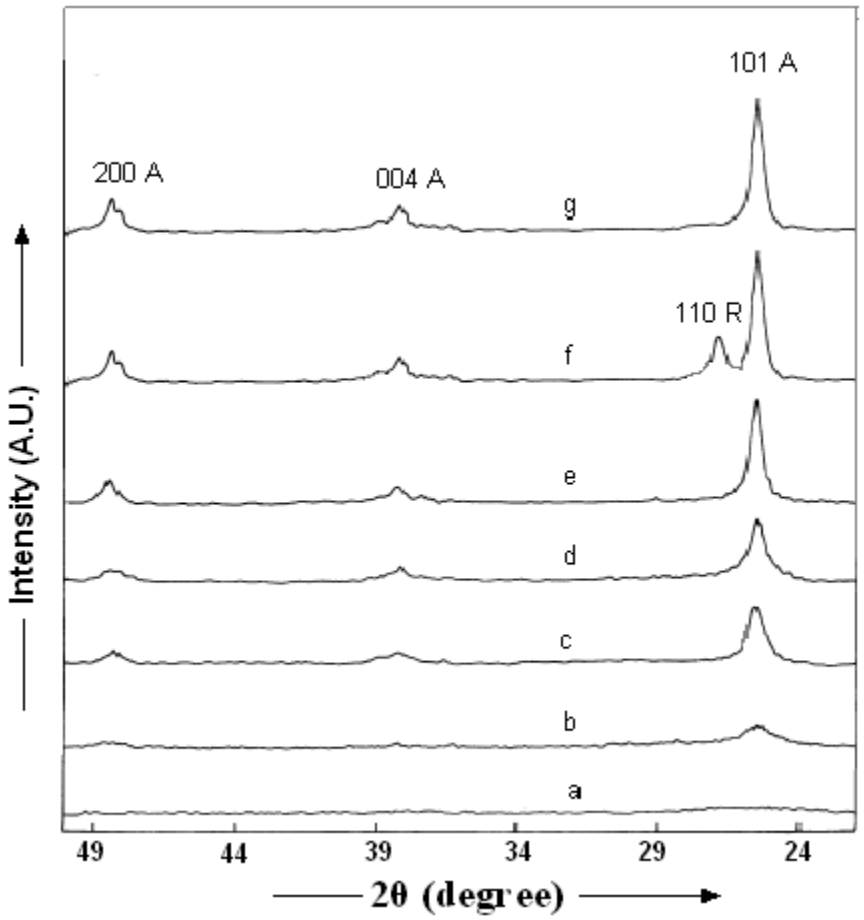

Fig. 2.8 : XRD patterns of titanium peroxide gel heated at a) 100, b) 200, c) 300, d) 400, e) 500 and f) 600 ^{0}C g) 0.6PEG/TiO_2 heated at 500 ^{0}C respectively.

All these peaks are broad in nature indicating that the particles are of nanosize. However the sample heated at 600 ^{0}C (curve f) shows an additional weak peak around 27.1^0 corresponding to 110 plane of rutile phase indicating the beginning of anatase to rutile transformation at this temperature. The curve 'g' which is of PEG added TiO_2 gel calcined at 500 ^{0}C shows pattern of pure anatase phase.

2.6.5 Thermo-gravimetric analysis

The thermal behavior of the dried gel powder was studied by using TG-DTA technique. TG curve of the sample dried at room temperature in air is as shown in fig. 2.9.

The curve shows two stages of loss in weight with a total weight loss of 37%. These two stages of weight loss are attributed to the loss of absorbed water in the titanium peroxide dry gel and the conversion of peroxide to oxide respectively. In DTA two endothermic peaks having minima at 130^0C and 255^0C respectively have been identified for the above weight loss. In the temperature range 270-1000 ^{0}C there is no further weight loss or weight gain but two broad exothermic peaks can be seen. The first peak is seen in the temperature range of 270-450 ^{0}C with maxima at around 375 ^{0}C and the other in the range 700- 1000^0C with a maximum at 900^0C. The first peak is attributed to the transformation of titanium peroxide to anatase form of TiO_2 and peak with maxima at 900 ^{0}C may be due to the slow conversion of anatase form of TiO_2 to rutile form. The beginning of such transformation at around 600^0C is also indicated in the XRD pattern of the sample. This suggests that the titanium peroxide is stable until 250 ^{0}C, then starts to transform to anatase phase first and then upon continued heating to rutile phase.

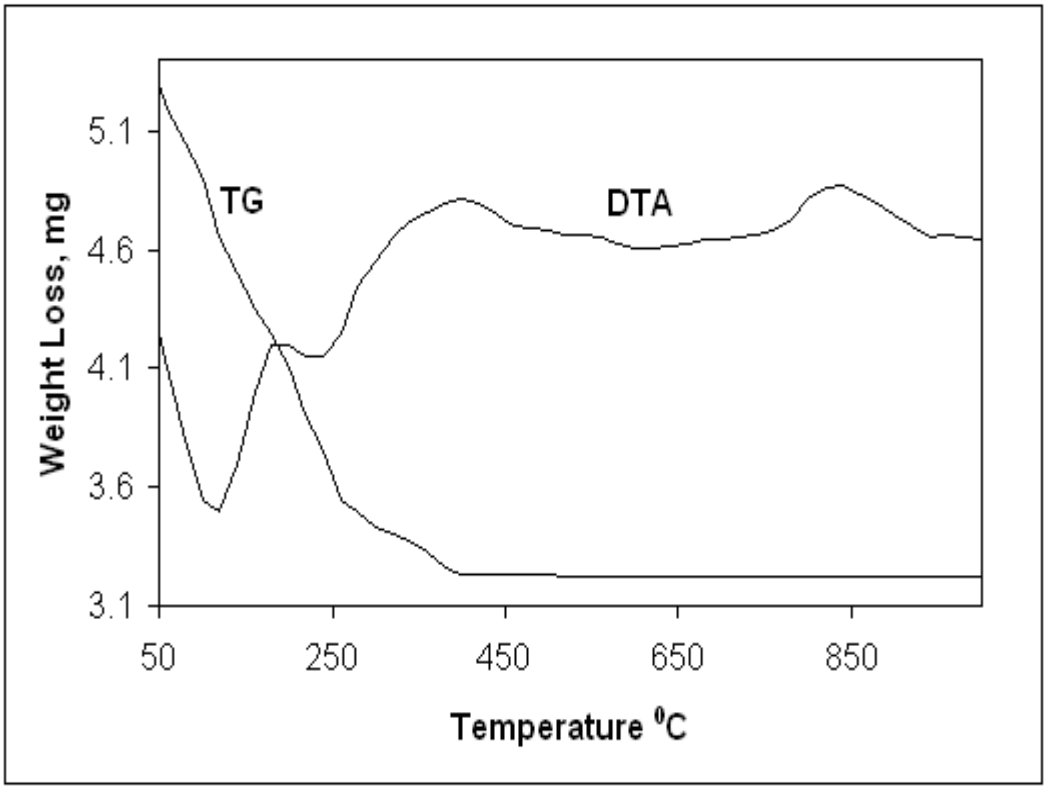

Fig. 2.9 : TG / DTA curves of titanium peroxide gel.

2.6.6 Surface morphology of titanium peroxide

Surface morphology of the films was studied by observing these films under scaning electron microscope(SEM). Fig.2.10 and fig 2.11 show typical images of as prepared titanium peroxide thin film on glass plate using a 0.001M sol after aging for 12 hr and the powder obtained by drying and calcining the gel at 400 ^{0}C in air. The SEM image of the thin film reveal that, the films deposited at different viscosities have a layer kind of structure. The films seem to be comparatively thinner at the edges of the slide and more thick at the central part.

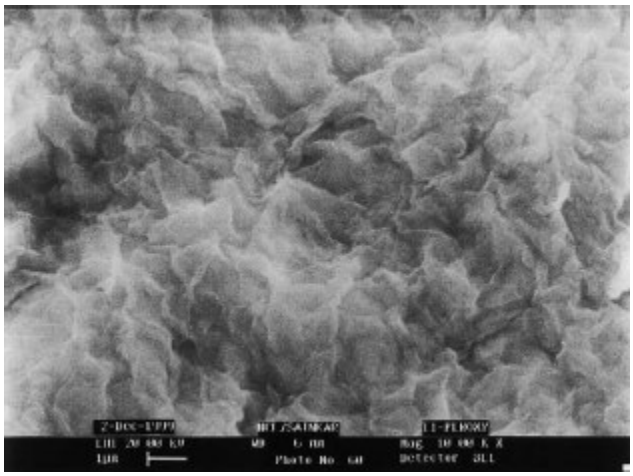

Fig. 2.10 : SEM photograph of titanium peroxide film of on glass dried in air at 100 ^{0}C.

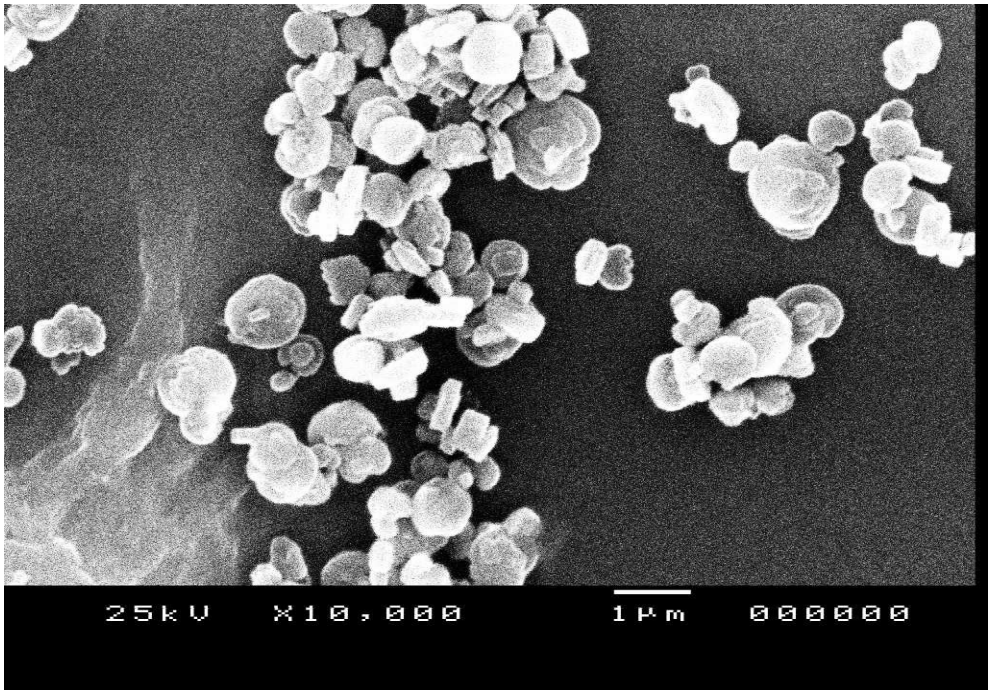

Fig. 2.11 : SEM photograph of titanium peroxide gel calcined in air at 400 ^{0}C.

This may be attributed to the slow evaporation of solvent during the drying of films. Water has higher boiling point (100 ^{0}C) and hence it evaporates slowly as compared to conventionally used organic solvents. In sol-gel dip coating, the drying of the film

starts at the edges and then slowly it spreads out to all parts, so there is force from edges which pushes liquid film to the central part of the substrate. This results in the films of titanium peroxide having bit more thick at the center as compared to edges of the substrate. In the image of titanium peroxide gel calcined at 400 ^{0}C(fig.2.11), the agglomerated TiO_2 particles can be seen which is generally observed in sol-gel methods because of fast drying. However the particle size estimation from XRD shows that, the TiO_2 obtained by using titanium peroxide sol-gel method is in the range of 15-60 nm.

2.6.7 Surface area of TiO_2 powder

Surface area of catalyst is very important parameter in all types of catalytic reactions because, with increasing surface area the number of active sites increases which ultimately results in an increase in activity of the catalyst.

Table 2.1

Effect of calcinations temperature on particle size and surface area of TiO_2.

Sr. No.	Calcinations temperature (^{0}C)	Surface area (BET) (m^2/g)	Crystallite size (XRD) (nm)
1	100	118	15
2	200	113	21
3	400	95	30
4	600	65	59

The surface area of titanium peroxide sample was analyzed by BET method and the are summarized in table. The surface area of sample calcined at various temperatures are given in table 2.1. The as prepared powdered gel sample(dried at 100 ^{0}C) shows a surface area at around 118 m^2/g. Upon heating the sample at various temperatures the surface area has shown decreasing trend because of particle growth at higher

temperatures. The TiO_2 powder with anatase as well as rutile phase having high surface area can be produced by using titanium peroxide sol-gel method.

2.6.8 Fourier transform infra-red spectroscopic analysis

The FTIR spectra of the titanium dioxide film and 0.6g PEG-TiO_2 film deposited on silica substrate are as shown in fig.2.12 (curves a - b). In both spectra, a broad peak appearing at 3100-3600 cm^{-1} is assigned to the fundamental stretching vibrations of OH groups (free or bonded)[67] which is further confirmed by a weak band at 1630 cm^{-1}.[68] This absorption band is caused by the bending vibrations of coordinated H_2O as well as Ti-OH. The bending vibrational mode of water may appear as shoulders on the spectrum such as that at 3240 cm^{-1}.[67] The peaks at located 500 and 430 cm^{-1} are likely due to the vibration of the Ti-O bonds in the TiO_2 lattice[69]. The peak centered at 900 cm^{-1} may be assigned to the characteristic O-O stretching vibration in H_2O_2[70] thus, the shoulder observed at 690 cm^{-1} may be due to the vibration of the Ti-O-O bond[70]. The FTIR spectrum definitely confirms the presence of Ti-O bonds, peroxo groups and OH groups in the precipitate. The intensity of peak at 3100-3600 cm^{-1} corresponding to fundamental stretching vibrations of OH groups and peak at 1630 cm^{-1} is more in 0.6gPEG-TiO_2 (curve 'b') than pure TiO_2 film (curve 'a'). This may be attributed to the more hydroxyl content in PEG-TiO_2 than pure TiO_2. This confirms that, the films containing PEG have more surface hydroxyl groups.

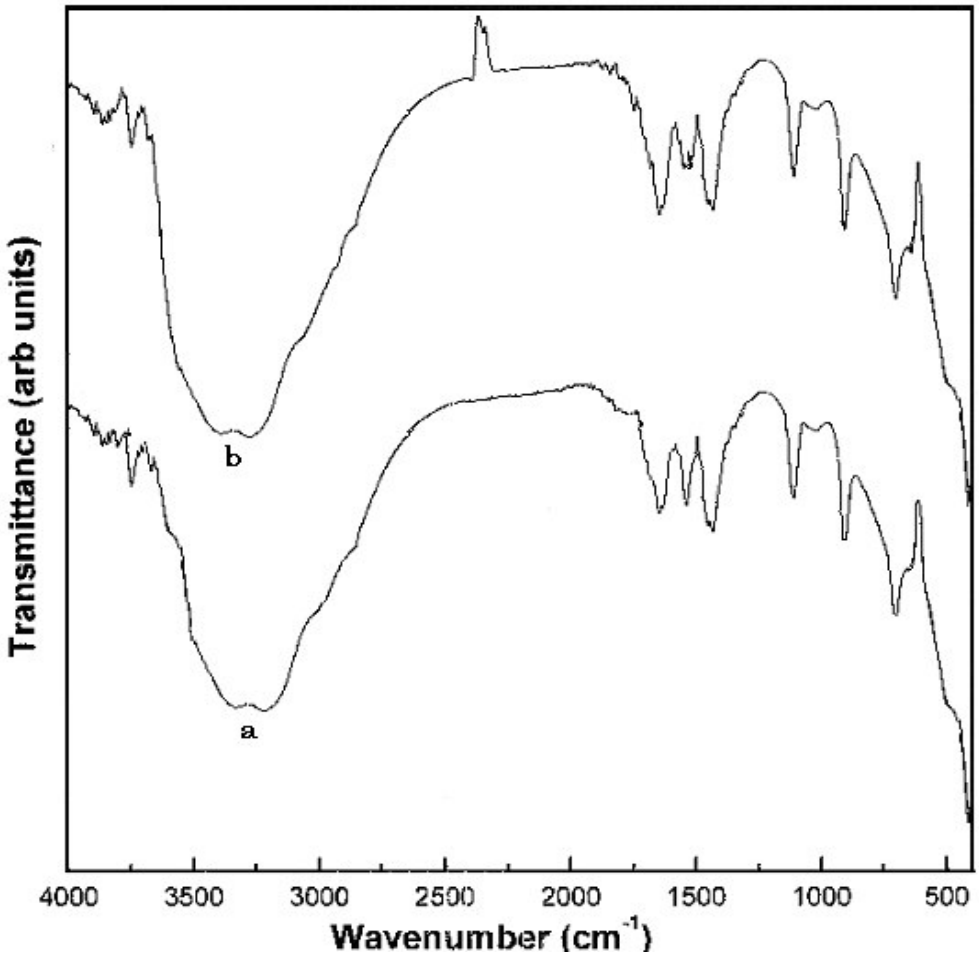

Fig. 2.12 : Infra-Red spectra of the a) titanium dioxide film and b) 0.6gPEG-TiO_2 deposited on silica plate using a sol aged for 12 hr.

2.6.9 Photo-catalytic activity of thin film TiO_2 photo-catalyst

In the photo-degradation of salicylic acid, the reaction products were analyzed before irradiation and after irradiation using UV-visible spectrophotometer. The typical UV-visible spectra of the salicylic acid irradiated for 0, 2, and 4 hrs. is as shown in fig.2.13. The residual % concentration of salicylic acid with time of irradiation without catalyst and with pure TiO_2 and PEG containing TiO_2 catalyst are shown in fig.1.14. (curves a-c respectively) The curve 'a' represents the sample kept in darkness which shows about

10% decrease in concentration in 4 hrs, it may be due to physical adsorption of salicylic acid on TiO_2 surface. The curve 'b' and 'c' suggests that, within 4 hr there is 80% degradation using pure TiO_2 and 90% degradation using PEG-TiO_2 catalyst. So there is an increase in photocatalytic activity for PEG-TiO_2 and it is attributed to the increase in surface hydroxyl content of TiO_2 due to addition of polymer.

In order to see the effect of surface modification on photocatalytic activity of TiO_2 thin films the films containing various concentrations of PEG (0.3g, 0.6g,0.9g and 1.2g/g TiO_2) have been used .Among these, the films containing 0.9g and 1.2g PEG /g TiO_2 are getting detached during the photocatalytic degradation. Hence they could not be studied in detail. The catalyst containing 0.6g PEG/ gTiO_2 showed good photocatalytic activity compared to other compositions. Hence it was studied in detail for all other reactions.

Based on the photoreactions the following reaction schemes for the degradation of salicylic acid and methylene blue respectively have been proposed.

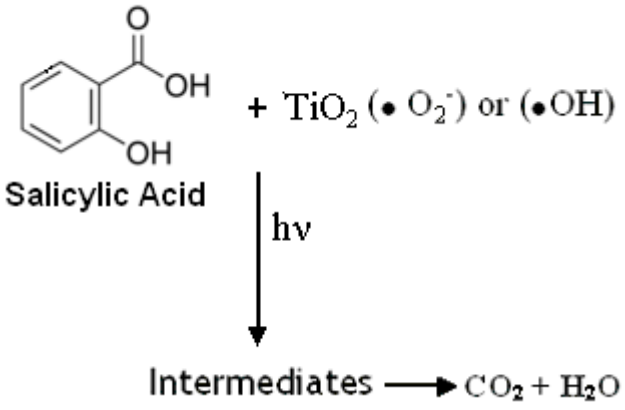

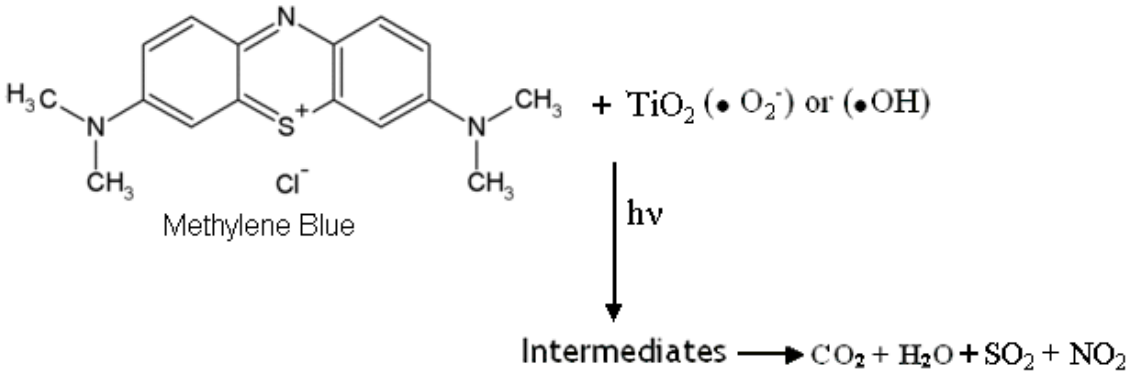

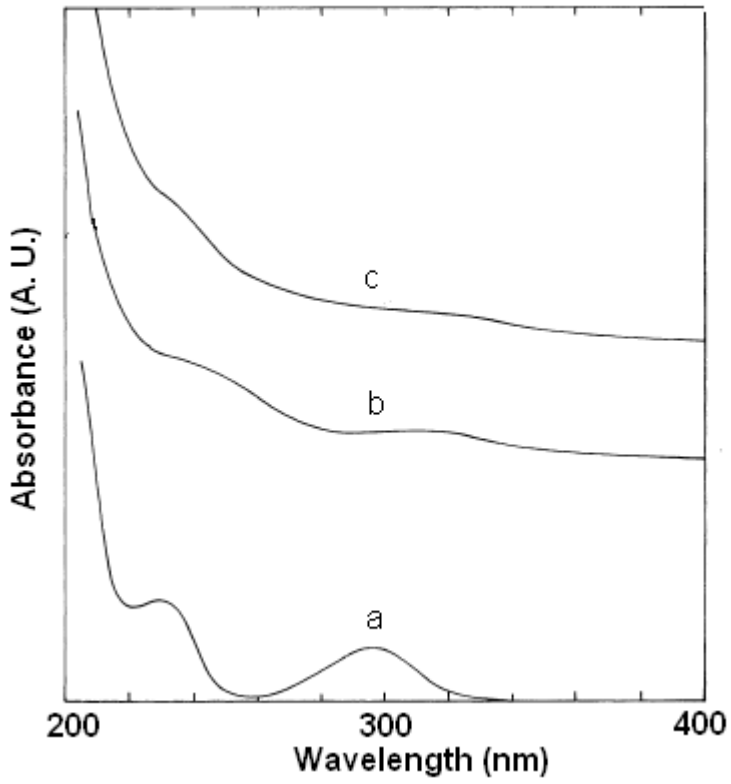

Fig. 2.13 : UV-visible spectra of reaction product of salicylic acid (6×10^{-5} M) solution photo-catalyzed by thin films of TiO_2 on glass helix, after UV irradiation of sample for a) 0, b) 2, and c) 4 hr.

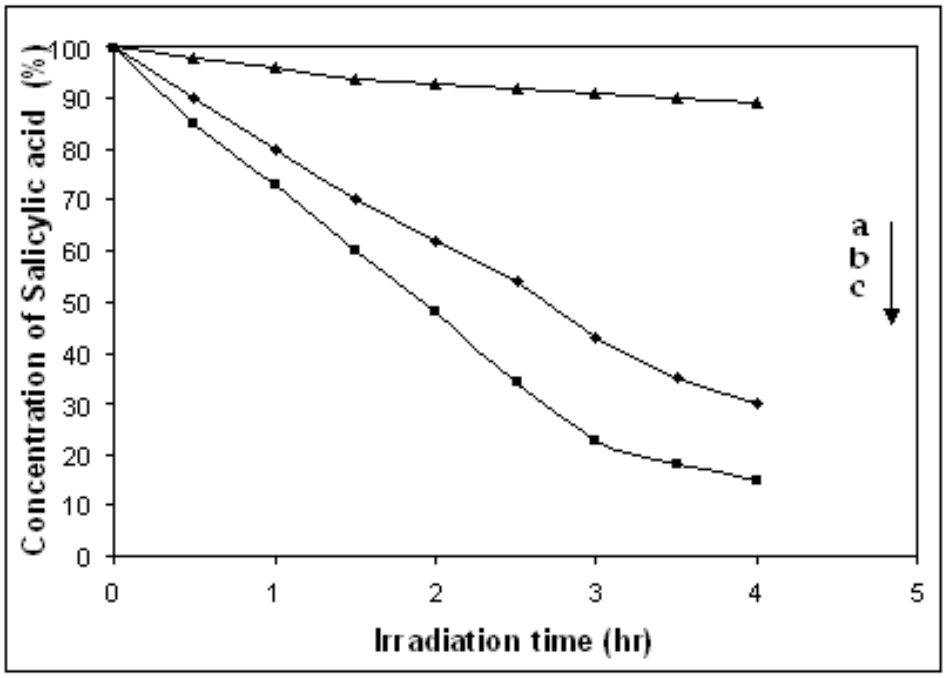

Fig. 2.14 : Change in concentration of salicylic acid with time using a) TiO_2 catalyst in darkness b) Pure TiO_2 and c) PEG TiO_2 .

In the photocatalytic reaction of methylene blue(MB), the UV spectra of methylene blue after UV irradiation for 0, 2, 4hrs. are shown in fig 2.15. The change in concentration of methylene blue with time for all the catalysts is shown in fig. 2.16. Similarly, photocatalytic degradation of methyl orange and phenol were also studied using these catalysts and the change in concentration with time of reaction are plotted in fig.2.16 and 2.17 respectively.

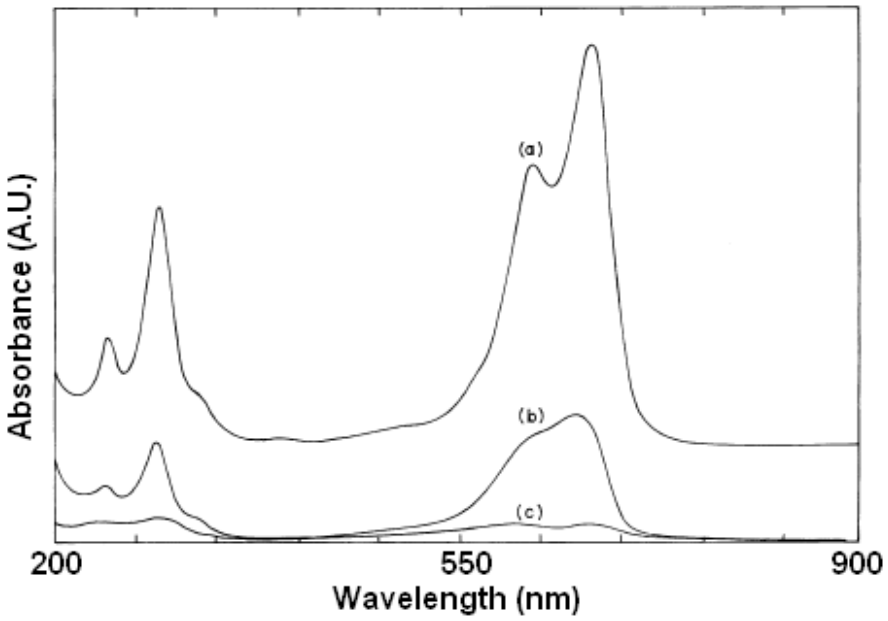

Fig. 2.15 : UV-Visible spectra of reaction product of methylene blue (6 x 10^{-5} M) solution photo-catalyzed by thin films of PEG-TiO_2 on glass helix, after UV irradiation of sample for a) 0, b) 2, and c) 4 hr.

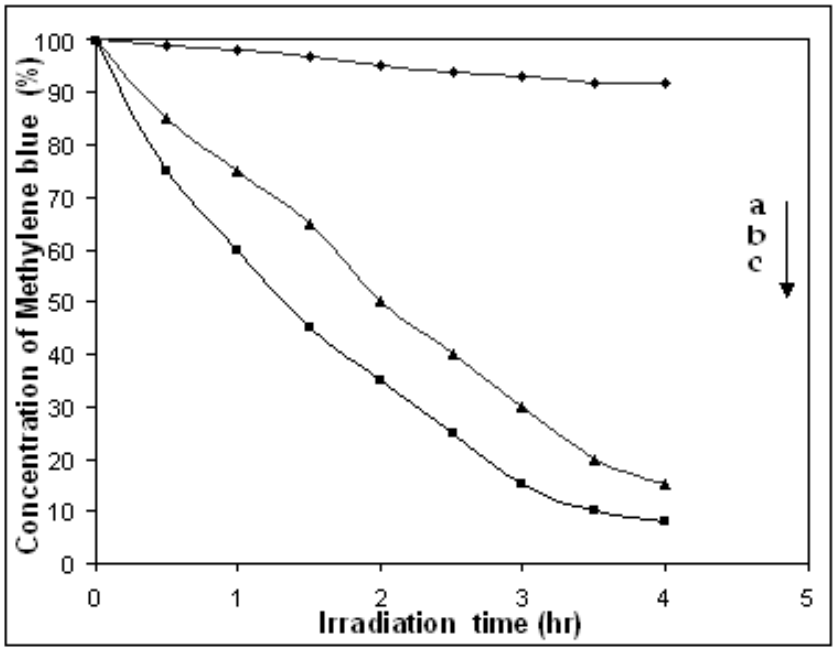

Fig. 2.16 : Change in concentration of methylene blue with time using a) TiO_2 catalyst in darkness b) Pure TiO_2 and c) PEG TiO_2.

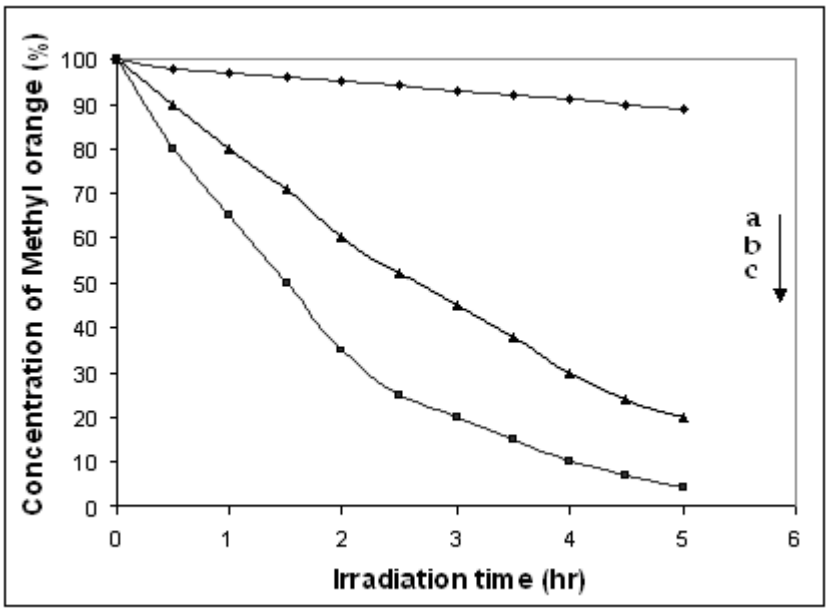

Fig. 2.17 : Change in concentration of methyl orange with time using a) TiO_2 catalyst in darkness b) Pure TiO_2 and c) PEG TiO_2.

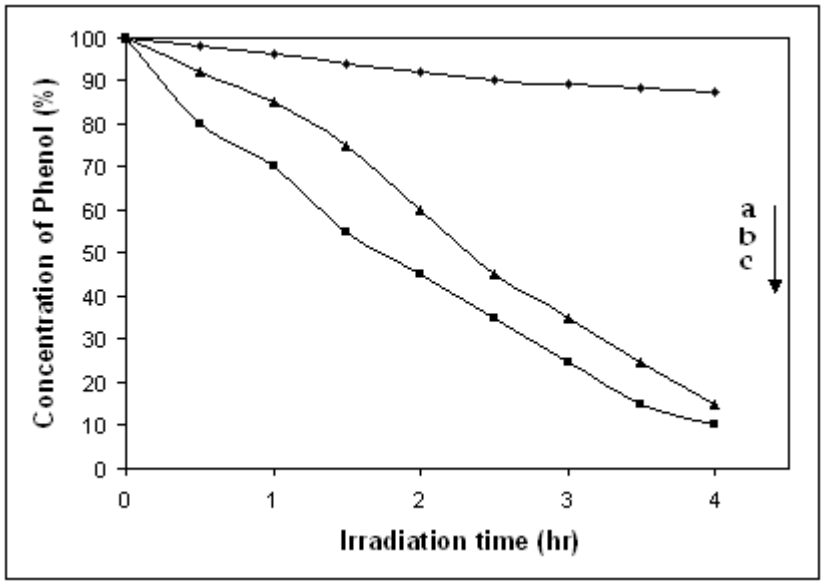

Fig. 2.18 : Change in concentration of phenol with time using a) TiO_2 catalyst in darkness b) Pure TiO_2 and c) PEG TiO_2.

It is well known that photo-catalysis experiments follow the Langmuir-Hinshelwood kinetics[46], where rate of reaction (R) is directly proportional to the surface coverage (θ)

$$R = -dc/dt = k_r \theta = k_r KC / (1 + KC) \quad (2.09)$$

Where, k_r is the rate constant, K is the adsorption coefficient of the reactant and C is the reactant concentration. In the case of very low concentration of reactant in solution (less than or in the range of 10^{-4} M) the product of K and C (KC) is negligible with respect to unity, so the equation Eq. 3.09 shows first order kinetics. The integration of Eq. 3.09 with limit condition that at the start of irradiation, t = 0 and C = C_0, gives equation,

$$- \ln (C / C_0) = k't \quad (2.10)$$

where, k' is the apparent first order rate constant.

The rate of reaction in photocatalytic degradation of salicylic acid, methylene blue, methyl orange and phenol over TiO_2 or PEG modified TiO_2 are plotted in fig. 2.19, 2.20,2.21 and 2.22 respectively.

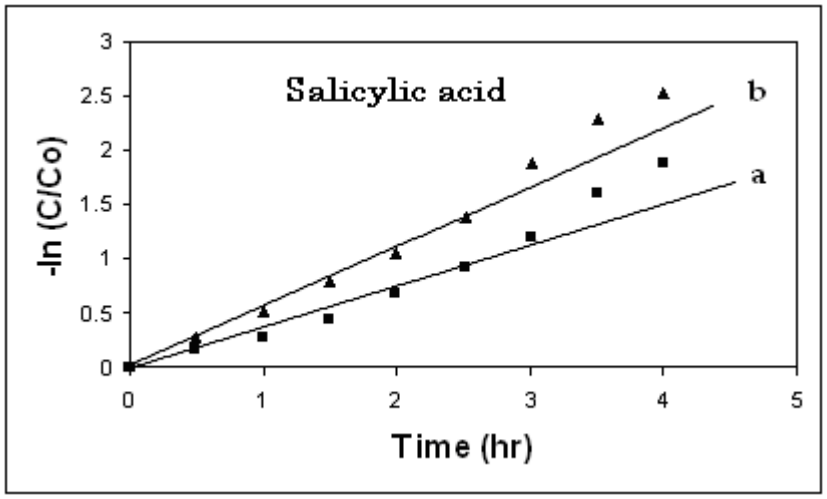

Fig. 2.19 : The first order kinetics of salicylic acid (SA) degradation using thin films of a) Pure TiO_2 and b) PEG TiO_2 .

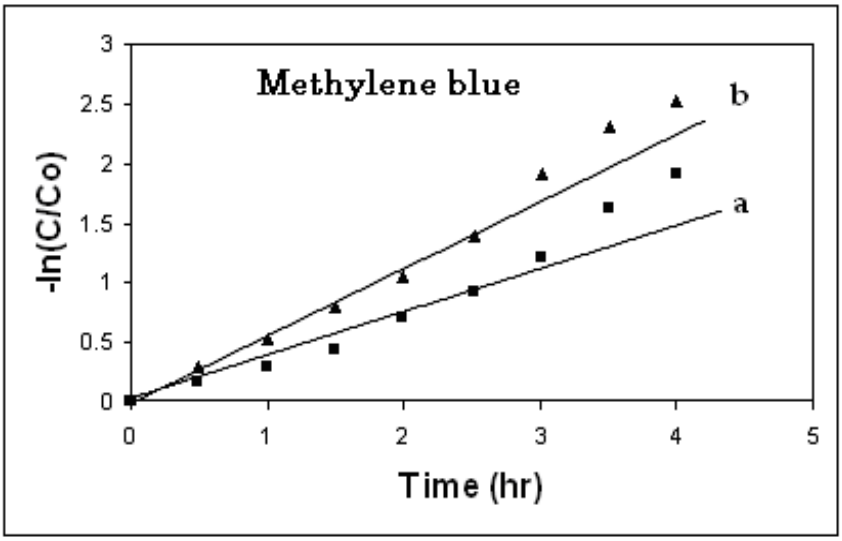

Fig. 2.20 : The first order kinetics of methylene blue (MB) degradation using thin films of a) Pure TiO_2 and b) PEG TiO_2.

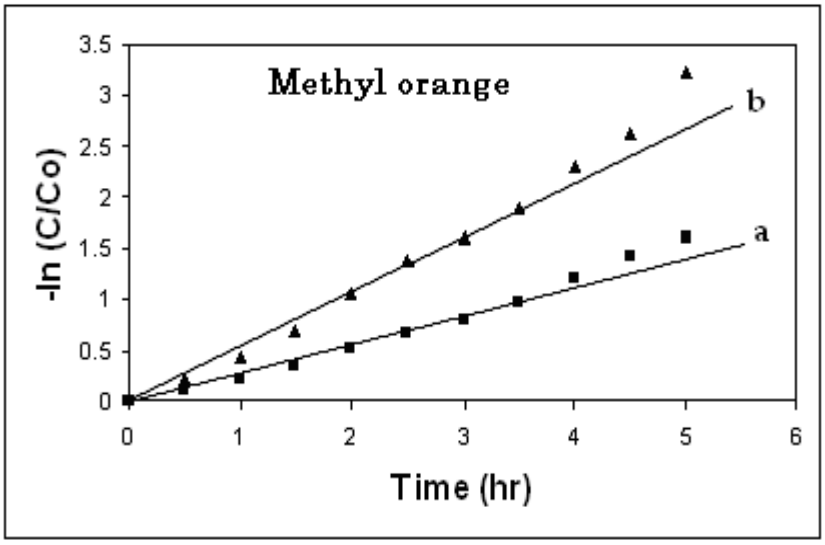

Fig. 2.21 : The first order kinetics of methyl orange (MO) degradation using thin films of a) Pure TiO_2 and b) PEG TiO_2.

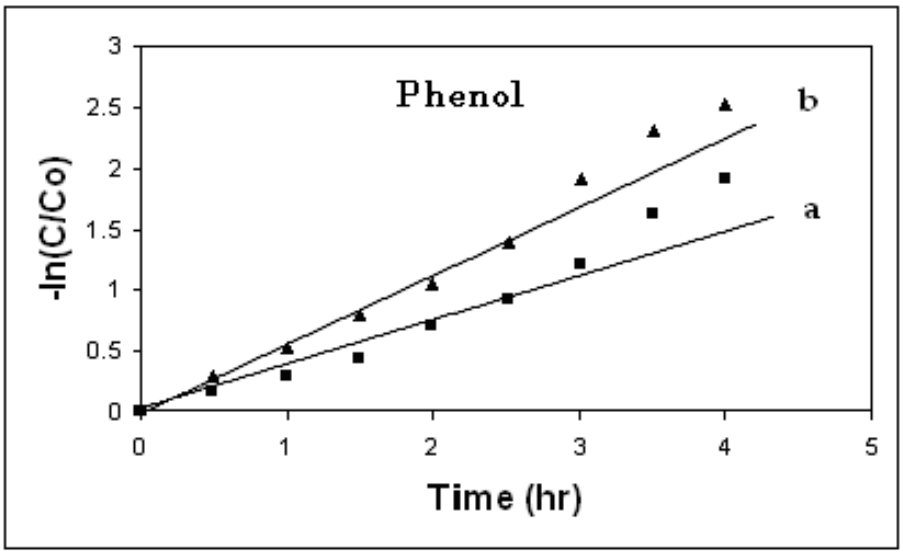

Fig. 2.22 : The first order kinetics of phenol (Ph) degradation using thin films a) Pure TiO_2 and b) PEG TiO_2 .

The kinetic parameters obtained from the above kinetic study for respective reactions are summarized in table 2.2 and 2.3.

Table. 2.2

Kinetic parameters and photocatalytic efficiency of films towards the degradation of SA, MB, MO and Ph in UV light using TiO_2 catalyst.

	SA	MB	MO	Ph
% pollutant remain after 1 hr	20	25	19	15
Time required for complete (90%) mineralization (hr)	---	4.5	---	5
Rate constant (min^{-1})	0.00423	0.0063	0.0048	0.0060

Table. 2.3

Kinetic parameters and photocatalytic efficiency of films towards the degradation of SA, MB, MO and Ph in UV light using PEG-TiO_2 catalyst.

	SA	MB	MO	Ph
% pollutant remain after 1 hr	40	27	35	30
Time required for complete (90%) mineralization (hr)	5	3.5	4	3.9
Rate constant (min^{-1})	0.0076	0.0091	0.0085	0.0068

From the above results it is observed that, for all these reactions, the rate of reaction is increased after modification of TiO_2 by PEG. It is clearly indicated by the significant increase in rate constant. The enhancement in rate of degradation of SA was found to be more and rate of degradation of Ph was found to least. Overall there was 1.1-1.9 times enhancement in photocatalytic activity after modification of TiO_2 by PEG. It may be attributed to the more hydroxyl content, porosity and surface roughness of the PEG-TiO_2 films as compared to pure TiO_2. In thin film photocatalyst, the photocatalytic activity reportedly depends on factors such as pore size , number of pores, surface area and the hydroxyl content of the TiO_2[71-72]. The TO_2 films prepared from titanium peroxide without PEG are less porous and the surface area of it is also less as a result reactant will not easily reach to the interior part of the film to capture the electrons and holes. Whereas PEG-TiO_2 films are porous in nature so the reactants can easily reach to the interior part of the films to capture the charge carriers. As the surface area of PEG

modified TiO_2 and the number of active sites the photoactivity of TiO_2 containing PEG is more. In TiO_2 mediated photocatalysis the hydroxyl radical formation is the key process because the hydroxyl radicals are strong oxidizing species which are responsible for the mineralization of organic compound landed on the surface of TiO_2. Due to addition of PEG the surface hydroxyl content of these films was found to be higher than the bare TiO_2 films

2.7 Conclusions

A very simple method for the deposition of thin films of TiO_2 on various substrates like glass plates, silica plates, stainless steel plates and glass/silica helix has been developed. The films are transparent, homogeneous, uniform and showed excellent adhesion to all the substrates. The film thickness is dependent on the concentration of titanium in the sol as well as the viscosity of the sol. It was found that, the films deposited in the viscosity range from 300 cps to 6000 cps are uniform and adhesion is also good than for viscosity below and above this range. Addition of polyethylene glycol in TiO_2 improves the adhesion of the TiO_2 films to substrate and film thickness can be increased by performing the number coating cycles. In the films heated at various temperatures i.e from 200 to 500 ^{0}C anatase phase incraeses. The films heated at 600 ^{0}C shows few weak peaks of rutile indicating the beginning of anatase to rutile transformation. The films of pure TiO_2 and PEG TiO_2 heated at 500 ^{0}C shows excellent photo-catalytic activity for the complete decomposition of salicylic acid, methylene blue , methyl orange

and phenol. The rate of photodegradation of all these organic compounds is found to be more when the surface of TiO_2 films is modified with polyethylene glycol.

References

1. O. Carp, C. L. Huisman, A. Reller, Progress in Solid State Chemistry 32 (2004) 33-177.
2. US Geological Survey Minerals Yearbook, 2002.
3. Greenwood N.N, Earnshaw A. Chemistry of the elements. Oxford: Butterworth Heinemann;1997.
4. Natara NC, Funaga N, No MG. Thin Solid Films 1998;322:6.
5. Kronos International, 1996.
6. Adams G. ECJ 1996;6:717.
7. Cotton, F. A.; Wilkinson, G. *Advanced Inorganic Chemistry*, 4th ed. John Wiley & Sons, New York, 1980, p 695.
8. Reddy, J. S.; Dicko. A.; Sayari, A. *Synthesis of Microporous Materials: Zeolites, Clays, and Nanostructures,* Occelli, M. L.; Kessler, H. (ed.), Marcel Dekker, New York, 1996.
9. Brittain, H. G.; Barbera, G.; DeVincetis, J.; Newman, W. *Anal. Prof. Drug Subs. Excip.* **1992**, *21*, 659.
10. Philips LG, Barbano DM. J Diary Sci 1997;80:2726.
11. Hewitt J. Cosmet Toiletries 1999;114:59.
12. Schulz J, Hohenberg H, Pfu¨ck F, Ga¨rtner E, Will T, Pfei.er S, et al. Adv Drug Deliv Rev 2002;54:157.

13. Schwaz VA, Klein SD, Hornung R, Knochenmuss R, Wyss P, Fink D, et al. Lasers Surg Med. 2001;29:252.

14. R. W. Matthews, , J. Phys. Chem. 91, 1987, 3328.

15. J. Herrmann and J. Mansot, J. Catal., 121, 1990, 340.

16. H. Gerisher and A. Heller, J. Phys. Chem. 95, 1991, 526.

17. S. Tunesi and M. Anderson, J. Phys. Chem. 95, 1991, 3399.

18. Y. Zhang, J. C. Crittenden, D. W. Hand and D. L. Perram, Environ. Sci. Technol., 28, 1994, 435.

19. M-C. Lu, G-D. Roam, J-N. Chen and C. P. Huang, J. Photochem. Photobiol., 76, 1993, 103.

20. I. Sopyan, S. Murasawa, K. Hashimoto and A. Fujishima, Chem. Lett., 1994, 723.

21. M. A. Aguado, M. A. Anderson and C. G. Hill, Jr., J. Mol. Catal., 89, 1994, 165.

22. A. Fernandez, G. Lassaletta, V. M. Jimenez, A. Justo, A. R. Gonzalez-Elipe, J. M.Herrmenn, H. Tahiri and Y. Ait-Ichou, Appl. Catal. B : Environ., 7, 1995, 49.

23. Y. Paz. Z. Luo, L. Rabenberg and A. Heller, J. Mater. Res. 10, 1995, 2842.

24 Tanaka, K.; Harada, K.; Murata, S. *Sol. Energy.* **1986**, *36*, 159.

25. (a) Bard, A. J.; Fox, M. A. *Acc. Chem. Res.* **1995**, *28*, 141. (b) Henderson, M. A. *Langmuir* **1996**, *12*, 5093. (c) Tabata, S.; Nishida, H.; Masaki, Y.; Tabata, K. *Catal. Lett.* **1995**, *34*, 245. (d) Michele Lazzeri, Andrea Vittadini, Annabella Selloni, Phy. Review B, 63, 155409.

26. Brus, L. E. *J. Chem. Phys.* **1984**, *80*, 4403.

27. Brus, L. E. *J. Phys. Chem.* **1986**, *90*, 2555.

28. Wang, Y.; Suna, A.; Mahler, W.; Kasowski, R. *J. Chem. Phys.* **1987**, *87*, 7315.

29. Sclafani, A.; Palmisano, L.; Schiavello, M. *J. Phys. Chem.* **1990**, *94*, 829.

30. Nishimoto, S.; Ohtani, B.; Kajiwara, H.; Kagiya, T. *J. Chem. Soc. Faraday Trans.* **1985**, *81*, 61.

31. Ohtani, B.; Ogawa, Y.; Nishimoto, S. *J. Phys. Chem., B* **1997**, *101,* 3746.

32. Thompson R. Industrial inorganic chemicals; production and uses. The Royal Society of Chemistry;1995.

33. Poznyak SK, Kokorin AI, Kulak AI. J Electroanal Chem 1998;442:99.

34. Pedraza F, Vasquez A. J Phys Chem Solids 1999;60:445.

35. Xie Y, Yuan C. Mater Res. Bull 2004;39:533.

36. Yin S, Fujishiro Y, Wu J, Aki M, Sato T. J Mater Proc Tech 2003;137:45.

37. Kang M. J Mol Catal A: Chem 2003;97:173.

38. Kim CS, Moon BK, Park JH, Son SM. J Cryst Growth 2003;254:405.

39. Zhang R, Gao L. Mater Res Bull 2002;37:1659.

40. Lim KT, Hwang HS, Ryoo W, Johnson KP. Langmuir 2004;20:2466.

41. Smith A, Rodriguez-Clemente R. Thin Solid Films 1999;345:192.

42. Sanchez-Juarez A, Tiburcio-Silver A, Ortiz A. Solar Energy Mater Solar Cells 1998;52:301.

43. Ahonen PP, Tapper U, Kauppinen EI, Joubert JC, Deschanvres JL. Mater Sci Eng A 2001;315:113.

44. Ahonen PP, Kauppinen EI, Joubert JC, Deschanvres JL, van Tendeloo G. J Mater Res 1999;14:3938.

45. Paraguay FD, Estrada WL, Acosta DRN, Andrade EM, Miki-Yoshida M. Thin Solid Films 1999,350, 192.

46. Veluchamy P, Tsuji M, Nishio T, Aramoto T, Higuchi H, Kumazawa S, et al. Solar Energy Mater Solar Cells 2001,67,179.

47. Zhang SZ, Messing GL. J Am Ceram Soc 1990,73,67.

48. Lyons SW, Ortega J, Wang LM, Kodas TT. Mater Res Soc SympProc 1992, 271, 907.

49. Ogihara T, Ookura T, Yanagawa T, Ogata N, Yoshida K. J Mater Chem 1991, 1, 789.

50 Dubois B, Ru.er D, Odier P. J Am Ceram Soc 1989;72:713.

51. Kavan L, O'Regan B, Kay A, Gra¨tzel M. J Electroanal Chem 1993;346:291.

52. Zhang X, Yao B, Zhao L, Liang C, Mao Y. J Electrochem Soc 2001;148:398.

53. Natarajan C, Nogami G. J Electrochem Soc 1996;143:1547.

54. Karuppuchamy S, Amalnekar DP, Yamaguchi K, Yoshida T, Sugiura T, Minoura H. Chem Lett 2001:78.

55. Matsumoto Y, Ishikawa Y, Nishida M, Ii S. J Phys Chem B 2000;104:4204.

56. Ishikawa Y, Matsumoto Y. Electrochim Acta 2001;46:2819.

57. Kamada K, Mukai M, Matsumoto Y. Electrochim Acta 2002;47:3309.

58. Iwasaki M, Hara M, Ito S. J Mater Sci Lett 1988;17:1769.

59. Bach U, Lupo D, Comte P, Moster JE, Weissortel F, Salbeck J. Nature 1998;395:583.

60. Sivakumar S, Krishna Pillai P, Mukundan P, Warrier K. Mater Lett 2002;52:330.

61. Matijevic E, Budnik M, Meites L. J Colloid Interface Sci 1997;61:302.

62. Okudera H, Yokogawa Y. Thin Solid Films 2003;423:119.

63. Sanchez C, Ribot F. New J. Chem. 1994, 18, 1007.

64. Shiota M. J. Mater. Sci. 1988, 23, 1718.

65 Natarajan C. Fukunaga N. Nogami G. Thin Solid films 1998, 322, 6.

66. Thomas P. Niesen, Joachin Bill, Fritz Aldinger Chem. Mater 13, 2001, 1552.

67. R. Zhang and L. Gao, Key Ehg. Mater. 2002, 224-226, 573.

68. B. Klingenberb and M. A. Vannice, Chem. Mater., 1996, 8, 2755.

69. T. Ivanova, A. Harizanova , M. Surtchev, Mater, lett. 2002, 55, 327.

70. Y. Gao, Y. Masuda, Z. Peng, T. Yonezawa, K. Koumoto, J. Mater. Chem. 2003, 13, 608.

71. Jiaguo Yu, Xiujian Zhao Mater. Res. Bull. 2000, 35, 1293.

72. Jiaguo Yu, Xiujian Zhao ,Qingnan Zhao, Thin Solid Films, 2000, 379,7-14.

CHAPTER-III

PREPARATION, CHARACTERIZATION AND PHOTOCATALYTIC ACTIVITY OF Fe/TiO_2 THIN FILMS

3.1 Introduction

As TiO_2 do not absorb in the visible region, it's use as a photocatalyst for wide spread applications has limitations. The other semiconductors such as CdS, CdSe and Fe_2O_3, have been investigated[1-3] for their use as photocatalyst in visible region. However it was observed that these materials are not stable under UV radiation, undergo degradation due to photocorrosion and they are reactive towards various chemicals normally available in the polluting materials.

Therefore there seems to be no other substance which is superior than TiO_2 for photo-catalytic applications. Since the photo-degradation efficiency of TiO_2 is less, in order to improve it, the composites of TiO_2 with other semiconductors such as ZnO, CdS, and Fe_2O_3 having different energy levels for conduction band and valence band have been utilized.[4-5] The intention was to improve the interfacial charge transfer process and efficient separation of charge carriers. In the composite, though TiO_2 was stable the other component semiconductor was not stable enough and the increase in photoresponse as well as photocatalytic activity was limited due to photo-corrosion of the other component semiconductor. So ultimately the catalyst could not be recycled

and the life of the catalyst was less. The scientists and technologists working in this area were of the opinion that the photo-response of TiO_2 itself should be increased to enhance the photo-catalytic activity. Numerous studies have been performed to extend the photo-response and photo-catalytic activity of TiO_2. In the attempt some workers have tried to enhance the efficiency by modifying its surface structure and surface properties using polymer such as polyvinyl alcohol and polyethylene glycol. These polymers as a surface modifier increase surface porosity as well as hydroxyl content of the catalyst. The hydroxyl ions play an important role in photocatalytic reactions because more is the hydroxyl content better is the activity of the catalyst.[6-11] There are many papers on modified TiO_2 with doping certain elements to increase surface properties and structure.

3.2 Iron Doped TiO_2 (Fe/TiO_2)

In 1977 Schrauzer and Guth[12] reported first time the preparation of Fe doped TiO_2 and it's application for the photo-reduction of molecular nitrogen to ammonia. This marks the beginning of doping in TiO_2 in order to improve it's photo-catalytic activity for various applications. Since then various elements like alkaline earth (Ca, Ba, Sr),[13] transition metal (Fe, Co, Cr, Mo)[14-19] and rare earth (La, Ce, Er, Pr, Gd, Nd Sm)[20] have been doped and useful results were obtained for degradation of various organic compounds. In some cases contradictory results were also obtained because the method of doping leads to different morphological and crystalline properties of the photo-catalyst. All earlier studies on the coupling of Fe with TiO_2 (Fe/TiO_2) or addition of Fe^{2+}

ions during the photo-degradation reaction along with catalyst has been found to be very useful due to the following reasons.

1. Presence iron (Fe) induces a Red shift or batho-chromic shift in optical properties.
2. Iron cations has a greater influence on the charge-carrier recombination process.
3. Use of iron-doped photocatalyst is efficient in several important photo-catalytic reduction and oxidation reactions.

Few authors have reported interesting results for photo-oxidation of organic substances using the Fe doped TiO_2 photo-catalyst. [21-24] However the method used for preparation of Fe doped catalyst is very important because just physical adsorption of Fe^{2+} ions on TiO_2 does not show much improvement in the activity of TiO_2. The Fe ions must occupy the substitutional sites of Ti^{4+} as a result the absorption spectrum of TiO_2 shifts to visible side and ultimately there is appreciable enhancement in photo-activity.. The common methods reportedly used for doping of Fe in TiO_2 are impregnation[22], co-precipitation[23], ion implantation[24-25] and sol-gel.[26-28]

In impregnation technique, known quantity of Fe solution prepared by dissolving ferric nitrate or ferric acetate in water was added into powder TiO_2 photo-catalyst. Whereas in co-precipitation the catalyst precursor solution (Titanium precursor, $TiCl_4$ or Ti-alkoxide) and dopant (Fe precursor) are mixed together followed by hydrolysis. This results in the formation of uniform mixture of titanium hydroxide and iron hydroxide precipitate which was then calcined for crystallization of TiO_2. This crystalline material was used for catalytic reaction.

The Fe doping by using co-precipitation and impregnation method is easy and cost effective because these method are vary simple in operation and requires very less time. However in many photo-reactions the rate of photo-oxidation or photo-reduction has shown very less improvement. This may be attributed to the physical adsorption of Fe ions on TiO_2 rather than substitution in TiO_2 structure. The presence of Fe^{3+} substituted ions on the surface of catalyst improves charge transfer process, efficient separation of electron-hole and improves absorption of TiO_2 in visible region. Although both physically adsorbed Fe and structurally incorporated Fe are beneficial for photo-catalytic reactions , the combined effect of both is much more.

The Fe doped TiO_2 can also be prepared by ion implantation technique. Anpo et. al[24,25] have reported this technique for implantation of various metal ions into TiO_2, in this technique a high energy metal ions are produced from metal source by applying high voltage and these ions are then bombarded on the TiO_2 target. Since the ions are having more energy they can penetrate into the TiO_2 lattice and occupy the substitutional Ti^{4+} sites in it. The doping of Fe by this technique shows improvement in many properties such as optical absorption in visible side (Red shift) and enhancement in photo-catalytic activity[26-34]. They have studied degradation of various pollutants using such catalysts and very good results have been reported, so the method could be very useful in pollution control. However the technique used needs a very special kind of equipment for doping the Fe cations and the Fe-TiO_2 catalyst obtained using this process is expensive which will directly affect on the cost of the treatment process. In conclusion, among the three methods for preparing Fe doped TiO_2, the first two

methods reported i.e impregnation and co-precipitation are mainly used for preparation of Fe- TiO_2 powder catalyst. Due to the problems associated with using catalyst in powder form (as described in Chapter.1) the photocatalyst in the form thin films is highly desired.

The most promising and widely used method for preparation of Fe doped TiO_2 powder as well as thin film is the sol-gel technique.[33-37] The advantages of sol-gel method are, it is very simple, cheap, easy for operation and sol gets easily anchored on the substrate during the thin film deposition. In sol gel method, the metal salts or metal organic salts are added into the TiO_2 precursor sol before the gelation or during gelation process. The Fe ion either occupies the substitutional position in TiO_2 structure because of the similar radius of Fe^{3+} and Ti^{4+}or gets adsorbed on the TiO_2 surface. The catalyst prepared by this technique has shown improvement in optical and structural properties. The TiO_2 shows shift in optical absorption to visible region. This shift in absorption edge and increased absorption in visible region results in an improvement in photo-catalytic activity of TiO_2 for photo-oxidation and photo-reduction of organic as well as inorganic pollutants. By following this sol-gel method many researchers have prepared Fe- TiO_2 thin films and used it for various applications.

In organic based sol-gel method[35-41] (as described in Chapter 1 and 2), the Ti-alkoxide precursor is diluted with organic solvent and hydrolyzed using small amount of water(controlled hydrolysis). The major part of the sol in this type of sol-gel methods is organic solvent which is used for deposition of TiO_2 thin films. However in our process the solvent is water. To the best of our knowledge, there are no reports on aqueous

titanium peroxide based sol-gel method as well as doping Fe into TiO_2 by using this (titanium peroxide based) process. Keeping in mind the above advantages more research needs to be done on this type of processes which are environmentally benign.

In view of the above, we have studied this process in detail. Various parameters such as effect of Fe addition on sol-gel behavior of titanium peroxide system, critical concentration of dopant, addition of organic modifier, variation of film thickness with viscosity etc. have been studied and optimized to get transparent , uniformly coated films with good adhesion to substrates such as glass slides, silica rings and glass helix. The films prepared were tested by various techniques in order to elucidate its thermal, structural and catalytic properties.

3.3 Experimental

3.3.1 Materials

Titanium (IV) isopropoxide (TIP), was obtained from Aldrich (Aldrich Chem. Co.). Polyethylene glycol (PEG Mol. Wt. 4000) and Ferric nitrate ($Fe(NO_3)_3.\ 9H_2O$) were obtained from local laboratory chemical manufacturer, Qualigen (Qualigen India Ltd.) De-ionized water was prepared from double distilled water using the deionised water unit (Millipore, Milli-Q-System) All chemicals and reagents were used as received without further purification. Glass substrates used for making titania thin film were the microscope slides and other substrates such as silica rashig rings silica/glass helix were from local supplier Perfect Scientific (Perfect Scientific Equipments, India). These substrates were pretreated with acidic solution before use to remove sodium as well as

other impurities on the surface of it.[42] First the substrates were put into a H_2SO_4 : H_2O_2 (3:1 v/v) mixture and kept immersed for 1 hr, followed by 2-3 washing with de-ionized water. The substrates were then kept in oven for drying at 100 ^{0}C.

3.3.2 Preparation of Fe doped TiO_2 sol.

In the preparation of Fe/TiO_2 sol, the Ti-peroxide sol was prepared as per the method reported in chapter.2. The titanium isopropoxide in place of titanium butoxide was used as titanium precursor. The titanium isopropoxide was hydrolyzed with the help of water, the resultant titanium hydroxide precipitate (as per eqn.3.01) was separated and washed 2-3 times with water. The precipitate was then allowed to react with dilute hydrogen peroxide solution(15% H_2O_2). To the orange colored sol obtained after complete dissolution of precipitate, required quantity of ferric nitrate solution(0.001M) was added drop wise with continuous stirring followed by dilution using water (50-100ml). This Fe/TiO_2 sol containing 1-2% (by weight) of Fe is allowed to stabilize and after attaining certain viscosity, it was used for deposition of the thin films.

In the preparation of PEG containing Fe/TiO_2, the titanium peroxide sol was prepared as described above. This sol was stirred with the help of magnetic stirrer and to this required quantity of polyethylene glycol solution was added drop wise (10% solution in water) followed by addition of 0.001M ferric nitrate solution. This Fe/TiO_2 sol was then allowed to equilibrate for 1-2 hr and then used for thin film deposition.

In this process, following reactions take place (eqn. 3.1 –3.3) during the Fe-TiO_2 sol preparation ,

$$Ti(O\text{-}ipr)_4 + 2H_2O \longrightarrow Ti(OH)_4 + Pr\text{-}OH \quad (3.1)$$

$$Ti(OH)_4 + H_2O_2 \xrightarrow{PEG} PEG\text{-}(Ti\,O_{2-x-0.5y}(O_2)_x(OH)y\,.H_2O) + H_2O \quad (3.2)$$

$$(Ti\,O_{2-x-0.5y}(O_2)_x(OH)y\,.H_2O)' \xrightarrow{Fe(NO_3)_3} PEG\text{-}Fe(Ti\,O_{2-x-0.5y}(O_2)_x(OH)y\,.H_2O) \quad (3.3)$$

The polymerization of PEG containing Fe/TiO_2 occurs by olation and oxolation process and the sol slowly transforms to gel as per following scheme.

$$n\,[PEG\text{-}Fe(Ti\,O_{2-x-0.5y}(O_2)_x(OH)y\,.H_2O)] \longrightarrow \underset{(sol)}{PEG\text{-}Fe/TiO_2} \longrightarrow \underset{(viscous\ sol)}{PEG\text{-}Fe/TiO_2} \longrightarrow \underset{(gel)}{PEG\text{-}Fe/TiO_2}$$

3.3.3 Deposition Fe/TiO_2 thin films on glass plates

The iron doped titanium peroxide sol (Fe/TiO_2) of various concentrations of Fe was prepared by using the method discussed in section 3.3.2. The sol was kept for 1-2 hr depending on the concentration of Fe and Ti. The change in viscosity was monitored by measuring the viscosity at various stages using brookfield viscometer. In the initial stage the sol releases oxygen by decomposition of unreacted excess hydrogen peroxide and if films are deposited at this stage the films are porous and non uniform. So the sol was allowed to stand for 1-2 hr depending on the concentration to ensure the complete decomposition of excess H_2O_2 and stabilize the sol of particular viscosity. Then the substrate was dipped in the viscous Fe/TiO_2 precursor sol of known viscosity as well as concentration and kept immersed in the sol for 2-5 minutes, then pulled out with uniform pulling rate of 1-2 mm/sec. The sol adhered to the substrate was allowed to dry in open atmosphere and at room temperature, during drying film releases the solvent (water in this case) leaving a yellow colored solid film of Fe/TiO_2 on the glass slide. After drying in open atmosphere the films were then subjected for drying in an oven at 100 ^{0}C for

complete removal of solvent. By using this method the substrates like glass plates, stainless steel plates and quartz plates were deposited.

By following the method described above the films of PEG containing Fe/TiO_2 were prepared using PEG containing Fe/TiO_2 sol of various viscosity.

3.3.4 Deposition of Fe/TiO_2 thin films of glass helix and silica rashig rings

For the deposition of Fe/TiO_2 and PEG containing Fe/TiO_2 thin film catalyst on the substrates such as glass helix and silica rashig rings, the method described in chapter.2 has been utilized. The films were then calcined at certain temperature and used for photocatalytic reactions.

3.3.5 Photo-catalytic reactions using Fe/TiO_2 thin film photo-catalyst

Photocatalytic activity was determined using the reactor and the procedure as described below. The natural energy source sunlight was utilized for this study. All the experiments were performed on very sunny day with solar irradiation of about 4.5–5 Wm^2/day between 9.00 a.m. and 17.00 p.m. in the month of April and May 2004. The photo-catalytic activity of the catalyst was tested using an in-house fabricated quartz reactor. The reactor consists of a quartz tube of dimensions 20mm diameter×250mm length having arrangement for bubbling air during the reaction. For this measurement, the silica rashig rings coated with Fe/TiO_2 and PEG-Fe/TiO_2 were used. The Fe/TiO_2 and PEG-Fe/TiO_2 catalysts coated (approx.0.2g TiO_2 on 100 gm helix) in the form of thin films by following the method described in section 2.3.1 were first heat treated at temperature 500 ^{0}C for 2 hrs and then used for photo reactions.

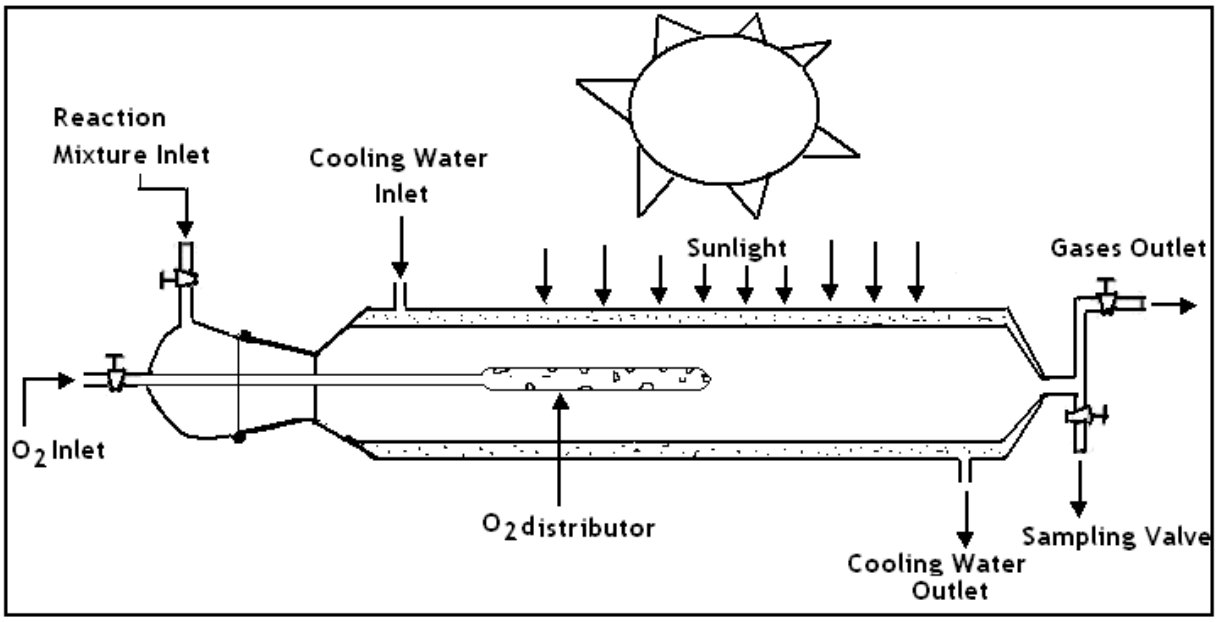

Fig. 3.1 **:** Schematic diagram of the quartz photo-reactor used in sunlight.

The 100 gm silica rashig rings were loaded into the reactor column. The solution of salicylic acid was fed into the reactor column and kept in dark place for 30 min. After 30 min the reactor was irradiated with sunlight for different time intervals. The oxygen gas was bubbled throughout the experiment at the rate of 10 ml min^{-1}. The samples were collected after irradiation of every 1hr and analyzed with UV-visible spectrophotometer (Hitachi 3210). The differential absorbance at 296 nm for salicylic acid (absorption peak of salicylic acid) was measured. The change in the concentration of the salicylic acid of the irradiated sample as a function of time was compared with a sample kept in darkness.

For degradation of other compounds such as methylene blue, methyl orange and phenol also the process described above has been followed and the samples were analyzed

using UV-visible spectrometer. The differential absorbance of irradiated samples at 662.5 nm, 490 nm and 289.4 nm for methylene blue, methyl orange and phenol respectively was measured.

The UV-visible instrument was calibrated first for each compound used in this study by preparation of standard solutions containing various concentrations. The UV-visible spectra of the solutions for each concentration have been taken and the correlation between absorption at characteristic wavelength of that compound and concentration has been developed. The linear relationship between the absorbance (A) and the concentration (C) can be represented empirically by the equation.

$A = a. C$

where a is the calibration constant for each compound.

The samples were characterized using different techniques as described in chapter.2.

3.4 Results and Discussion

3.4.1 Effect of Fe addition on sol –gel behavior

In the sol-gel transformation of $FeTiO_2$ and PEG containing Fe/TiO_2 the change in viscosity with time is presented in fig.3.2 and compared with that of pure TiO_2. The viscosity plays an important role in the deposition of thin films using sol gel dip coating process[43]. It was observed that the film thickness increases with the increase in the viscosity of the Fe/TiO_2 precursor sol. The variation of viscosity of 0.05M sol of pure titanium peroxide, $0.5\%Fe/TiO_2$ and PEG $0.5\%Fe/TiO_2$ with time has been studied and

presented in fig.3.2. In the figure, curve a ~ c represents the change in viscosity of pure titanium peroxide, 0.5%Fe/TiO_2 and PEG 0.5%Fe/TiO_2 respectively.

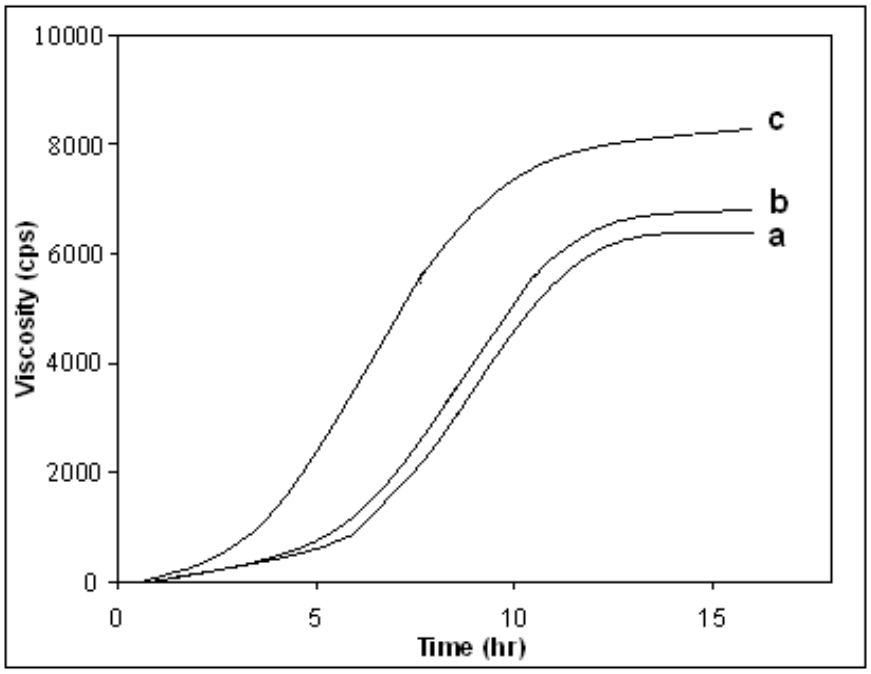

Fig. 3.2 : Variation of viscosity with time of 0.05M sol of a) titanium peroxide, b) 0.5% Fe/TiO_2 and c) PEG-0.5% Fe/TiO_2.

The 0.05M titanium peroxide sol starts changing viscosity (curve a) within 2-3 hrs and turns to gel in 12-14 hrs. In the initial stage the viscosity increases very slowly but after completion of 6 hrs it increases very rapidly and after completion of 12 hrs it slows down again due to the formation of dense gel. The 0.5%Fe/TiO_2 sol also behaves in similar manner and very small difference in viscosity change (curve b) was observed as compared with titanium peroxide. However in PEG containing Fe/TiO_2 sol (curve c), the increase in viscosity is very fast and within a period of 10 hrs it turns to dense gel.

Addition of Fe within 0.5-2% by weight does not show significant change in sol-gel behavior but as concentration of Fe increases it starts formation of slight turbid gel and beyond 2% Fe addition it starts to separate the gel into two layers, the upper layer is clear transparent solvent (water) with dirty yellow colored gelatinous precipitate at the bottom rather than remaining homogeneous gel. This two layered sol on keeping for 1-2 days turns into turbid viscous gel and if it is used for film deposition, the films were non uniform and opaque. The adhesion of these films was also poor and it can be easily peeled off or scracheable. In previous studies [11,47] the polymers such as polyethylene glycol, polyvinyl alcohol and other polymers are reported to be used for surface modification and to increase the porosity of the TiO_2 film. The polymers such as PVA and PEG have been used in our system for improving the sol-gel behavior and to prepare thin films without cracks. Among the two polymers used, we found polyethylene glycol to be better in our system hence it was used and studied in detail.

3.4.2 Film thickness measurement

The thickness of the Ti(IV) oxide films on glass and silica plates was measured by Talley Step profilometer. For this measurement, the half surface of the plate was coated on one side and the height of the step i.e difference between the uncoated surface and coated surface was measured. The effect of change in viscosity of the Fe/TiO_2 and PEG-Fe/TiO_2 sol on film thickness has been studied in detail and the results are summarized in table.3.1.

3.4.3 Addition polyethylene glycol (PEG) in Fe/TiO_2 sol

In order to see the effect of PEG addition in Fe/TiO_2 sol, the polyethylene glycol of molecular weight 4000 has been used further. The addition of polyethylene glycol at 0.3 –1.2 g/g TiO_2 level has been studied. This polymer addition into Fe containing titanium peroxide changes the sol-gel behavior and also increases adhesion property of the film. As described in chapter.2, in titanium peroxide sol-gel process, the film thickness was adjusted by depositing film at particular viscosity in a single attempt because once the first layer of the film dries, the second layer does not adhere to the surface. The films prepared using Fe/TiO_2 sol also shows similar behavior. However the polyethylene glycol added sol can be used for many coating-drying cycles and film thickness can be adjusted as per requirement by increasing the number of coating cycles. The results of change in film thickness with and without addition of PEG are summarized in Table3.1. Apart from the improvement in adhesion, addition of 0.6 g PEG/g TiO_2 has shown a positive effect and it improved the gel formation process in Fe doped sol. As described in previous section, the addition of Fe ion solution more than 2% disturbs the TiO_2 sol and subsequent gel as well. However addition of PEG prohibits the separation behavior of Fe/TiO_2 sol and stabilizes the sol as well as gel. By addition of PEG the sol containing 4% Fe (by weight) can be prepared and this sol can be stable for long time and there is no separation of two layers. However if the concentration of Fe into the sol is increased beyond 4% (by weight), the layer starts to separate even though quantity of PEG in sol is increased. The Fe/TiO_2 sol containing 1-4% of Fe and various PEG content (0.1-1.2g/g TiO_2) were prepared. Films were deposited by using these sol. However it is observed

that, the films containing 0.6 g PEG/g TiO_2 are found to be the most suitable for characterization as well as photocatalytic activity .

Table.3.1

Effect of PEG addition on the thickness of Fe/TiO_2 thin films on glass plates.

Composition of sol	Viscosity in Centipoise	Number Coating Cycles	Thickness (nm)
2%Fe/TiO_2 sol	1280	1	65
	1280	2	65
	1530	1	80
	1530	2	82
	2300	1	94
	2300	2	95
2%Fe/TiO_2 sol containing 0.6 gm PEG	1280	1	70
	1280	2	85
	1280	3	95
	1530	1	80
	1530	2	100
	1530	3	115
	2300	1	100
	2300	2	130
	2300	3	155

The films containing more PEG does not have much influence on surface properties and photocatalytic activity. In addition to this, the films containing higher PEG content are not suitable for photo reactions because the films start to detach from the surface during photocatalytic experiment and separation of this becomes the problem.

3.4.4 Chemical composition of Fe/TiO_2

The iron (Fe) content of the thin film catalyst was analyzed by using Energy Dispersive X-ray analysis (EDX) as well as Inductively Coupled Plasma Optical Emission Spectrometer (ICP-OES) technique. The results are given Table.3.2.

Table. 3.2

Chemical composition of Fe/TiO_2 photo-catalyst powders by ICP-OES and SEM-EDAX techniques.

Catalyst	% Iron added in the sol	Iron estimated by ICP-OES	Iron estimated by EDX
2% Fe/TiO_2	2	1.93	2.15
4% Fe/TiO_2	4	3.90	4.18
0.6gm PEG, 2% Fe/TiO_2	2	1.89	2.07
0.6gm PEG, 4% Fe/TiO_2	4	3.95	4.10

The concentration estimated by EDX analysis is slightly high (2-5%) as compared to the expected values. To get accurate data, the results were confirmed by analyzing the samples using ICP-OES which are in good agreement with the expected values.

3.4.5 UV-visible spectroscopic characterization

In order to see the effect of Fe doping on the optical properties of TiO_2 films, the films were prepared on glass plates by depositing sol of titanium peroxide containing 0.6g PEG/g TiO_2 and 0, 1, 2, 4 % Fe respectively. The films were calcined first at 500^0C in an

electric furnace at the heating rate of 0.5 ^{0}C/ min and then characterized by UV-visible spectroscopy.

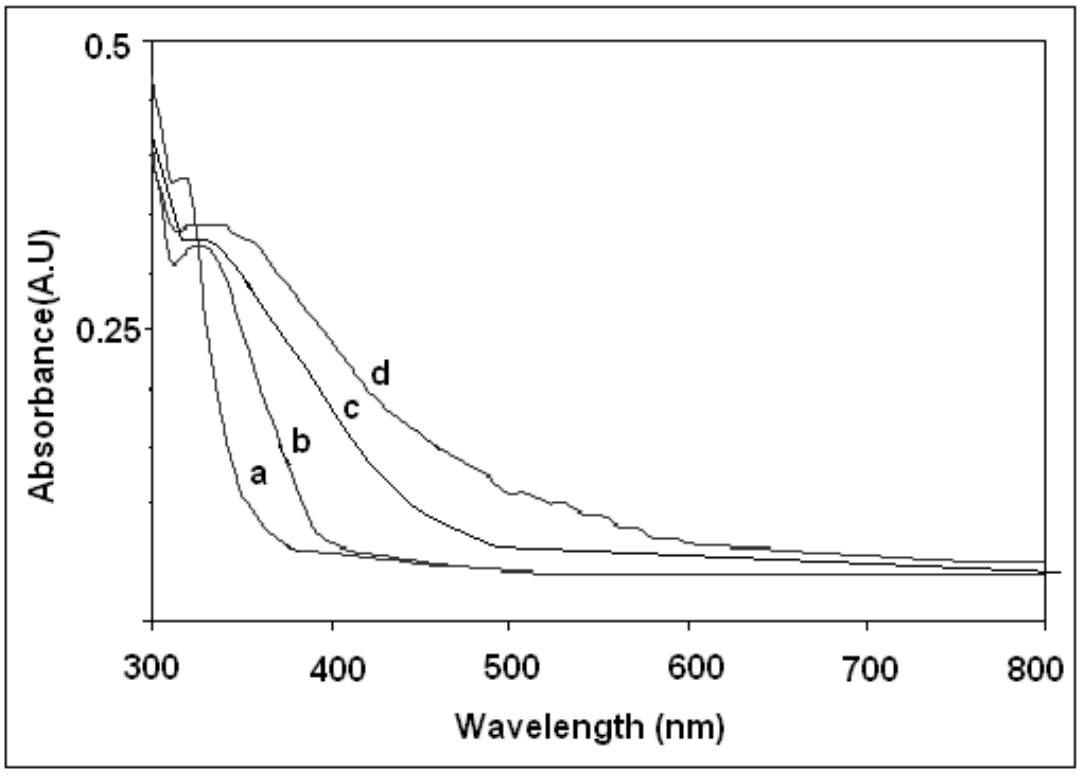

Fig.3.3 : UV-visible spectra (in absorption mode) of the films deposited using a) Titanium peroxide sol , b) 1% Fe/TiO_2 sol and c) 2% Fe/TiO_2 sol d) 4% Fe/TiO_2 sol containing 0.6PEG/g TiO_2.

The UV-visible spectra of these samples are shown in fig.3.3. In the spectra, curves a-d represent the UV spectra of thin films prepared using doped TiO_2 containing 0, 1, 2, 4 % Fe respectively. The undoped TiO_2 sample(curve 'a') show a peak having absorption edge at around 340 nm in UV region rather than 390nm of bulk TiO_2, it may be due to the particle size of TiO_2 in the film. In sol-gel powder or in thin film the particles are in nanosize range which ultimately show a blue shift in absorption edge than its bulk form

(quantum size effect). The 1% Fe doped sample (curve 'b') shows a small shift in absorption to visible side (absorption edge at around 380 nm) indicating that there is a shift (Red) in optical absorption edge. The curve 'c' and 'd' samples show further shift in absorption (430 nm and 460 nm). The increase in the concentration of dopant shows not only shifts the absorption edge towards the visible but also shows slight increase in the absorption of TiO_2 in whole visible range (400-800 nm). This shift may be ascribed to formation of substitutionally doped Fe/TiO_2 mixed oxide or mixture of simple and mixed oxides.[44-47] The Fe cations occupy the substitutional positions, because the ionic radius of both iron (Fe^{3+}) and titanium (Ti^{4+}) are nearly equal, leading to the easy formation of solid solution.

3.4.6 XRD studies of Fe/TiO_2 photocatalysts

The films deposited as well as the dried gel powder was heat treated at different temperatures and XRD patterns were recorded. (Fig.3.4) The 2%Fe-TiO_2 containing 0.6g PEG/g TiO_2 has been employed for the XRD studies in the 2θ range 20-80 ^{0}. Curve 'a' represents the pattern of as prepared gel dried at 100 ^{0}C which shows only humps and no distinguished peaks corresponding to anatase phase indicating that the powder sample is semicrystalline in nature. Curve 'b' shows the pattern of sample heated at 250 ^{0}C in air for 2 hr, which shows a prominent diffraction peak at 2θ - 25.2^0, corresponding to the (101) plane of anatase phase. Along with the prominent peak the peaks of other planes are also seen. The intensity of all peaks increases with calcination temperature.

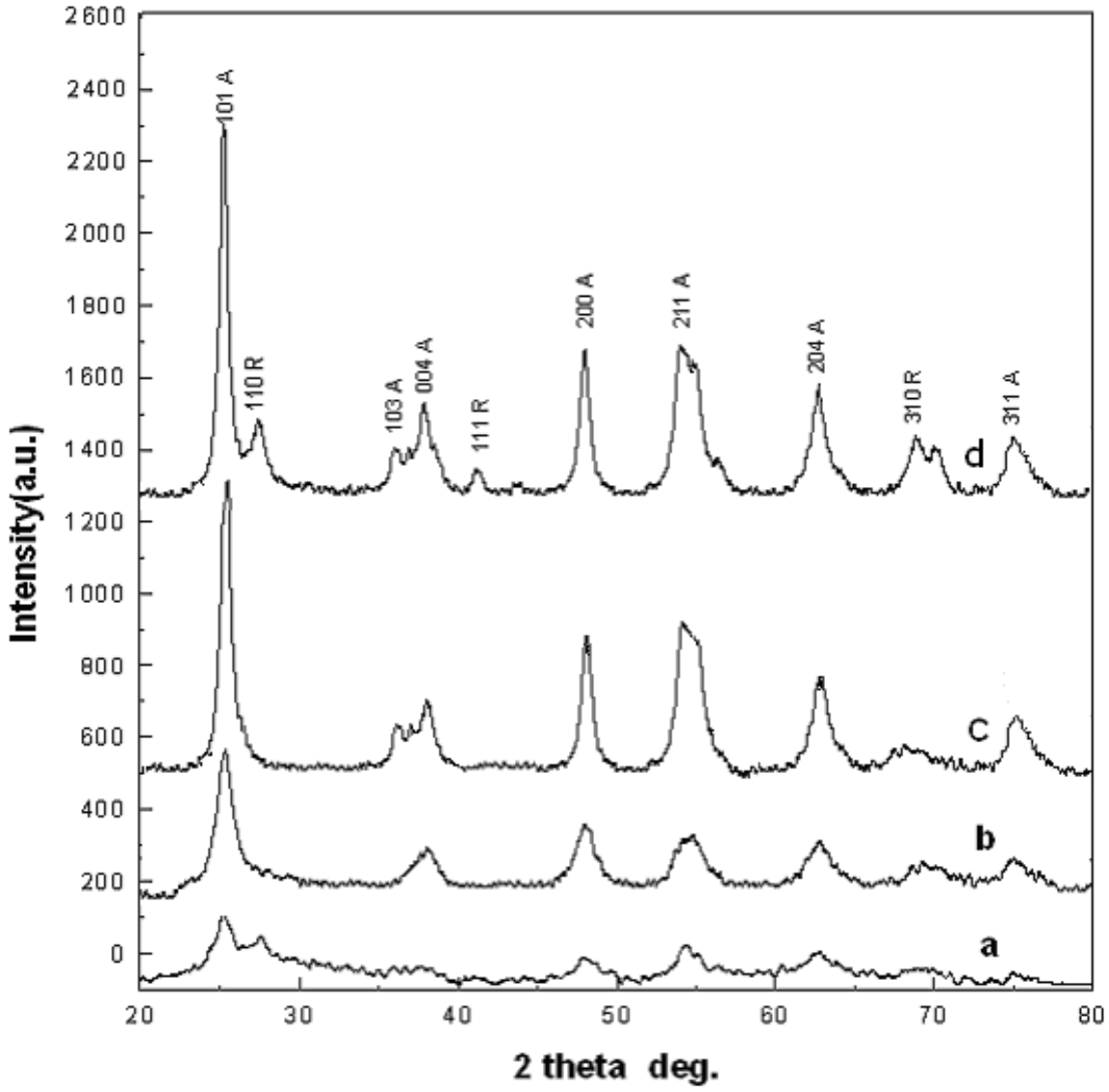

Fig. 3.4 : X-Ray diffraction pattern of the 2% Fe/TiO_2 sample calcined in air atmosphere at temperature a) 100 ^{0}C , b) 250 ^{0}C c) 400 ^{0}C and 500 ^{0}C respectively.

The sample calcined at 400 ^{0}C (curve c) shows complete transformation of amorphous to anatase phase. This suggests that, complete transformation of amorphous to anatase crystal structure appears at or less than 400 ^{0}C. Curve 'd' corresponds to the sample

heated at 500 ^{0}C. In this pattern along with the anatase peaks some weak peaks corresponding to rutile phase also appeared. From the above, it can be easily understood that, anatase is stable until 400 ^{0}C and after that rutile starts to grow. As compared to pure TiO_2 the crystallization temperature of amorphous Fe/TiO_2 is found to lower. Such lowering in crystallization temperature of anatase in Fe doped TiO_2 has been reported by Peral and Ollis et.al[50]. The crystal phases of TiO_2 are reported[49-50] to depend on the particle size as well. We have found that, the particle size of Fe/TiO_2 is bigger than pure TiO_2. In all the patterns recorded it is also observed that, the XRD peaks of samples calcined at lower temperature are broad due to smaller size of TiO_2 crystallites and the sharpness of the peaks increases with increase in the calcination temperature which can be attributed to the crystal growth of TiO_2 particles at higher temperature.

3.4.7 Thermo-gravimetric analysis

The TG/DTA curve for the sample of 2%Fe/TiO_2 gel is shown in Fig.3.5. In TG curve the sample shows a total weight loss of around 39-40% in two stages. In the first stage a gradual weight loss of around 21% in the temperature range of 40-200 ^{0}C was observed whereas in the second stage a sharp weight loss of around 18% in the temperature range of 201-325 ^{0}C has been observed. In DTA, the curve shows an endothermic peak at around 100-150 ^{0}C and two exothermic peaks in the temperature range of 225-325 ^{0}C and 475-600 ^{0}C. The endotherm in the range of 100-150 ^{0}C centered at 125 ^{0}C may be attributed to the loss of absorbed water in the titanium peroxide gel. The first exotherm with considerable weight loss in the temperature

region of 225-325 ^{0}C centered at 250 ^{0}C is attributed to the conversion of amorphous titanium peroxide to crystalline anatase type titanium dioxide.

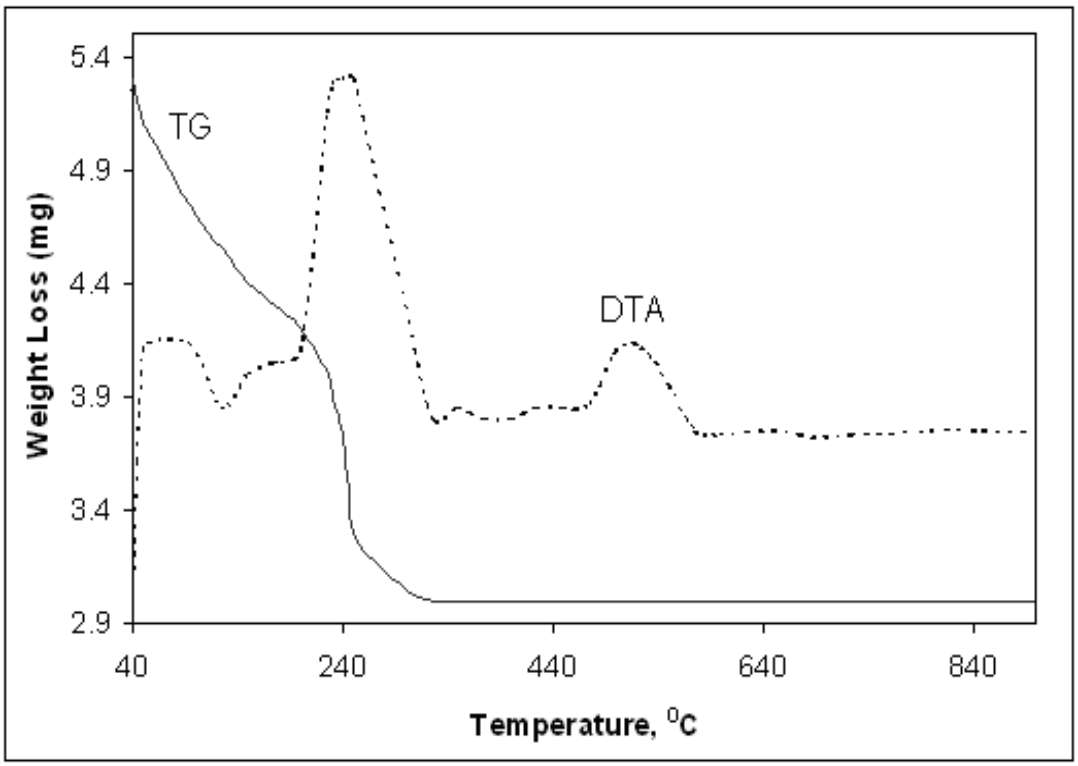

Fig. 3.5 : TG-DTA Curve of 2% Fe/TiO_2 sample in air atmosphere.

The another exotherm with no further weight loss in the temperature region of 475-600 ^{0}C centered at 525 ^{0}C may be due to the slow conversion of anatase to rutile phase of TiO_2. These thermal results are in good agreement with the structural transformation results observed in X-ray diffraction studies.

3.4.8 Surface morphology of Fe/TiO_2 films

The effect of PEG addition on the surface microstructure of the films was investigated by Scanning Electron Microscope (SEM). The fig.3.7, 3.8 and 3.9 shows the SEM

images of pure 2%Fe-TiO_2, 0.3g PEG/g 2%Fe-TiO_2, 0.6g PEG/g2%Fe-TiO_2 films calcined at 500 ^{0}C respectively.

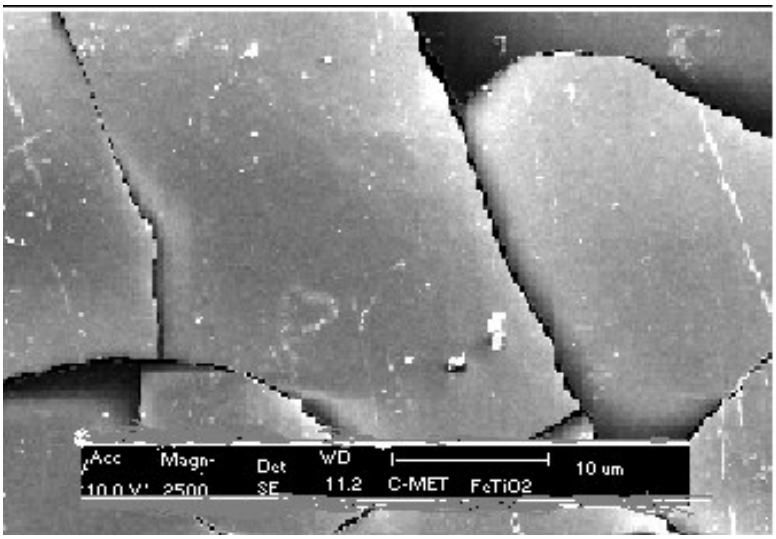

Fig.3.6 : Scanning Electron Micrograph (SEM) of the thin film deposited on soda lime glass plate using pure 2%Fe/TiO_2 sol.

It is observed that, 2%Fe-TiO_2 film prepared without addition of PEG (fig.3.6) is not uniform in thickness and having cracks at many places. Such cracking of thin films during calcinations has been observed previously. Soga and coauthors[11a] have reported that, the TiO_2 films prepared by sol-gel coating get cracked due to stress induced during the crystallization of TiO_2. In order to prepare films without cracks , they have used polyethylene glycol as a surface modifier. In titanium peroxide based sol-gel also, the film prepared by addition 0.3g PEG into titanium peroxide the sol is uniform with granular texture and without cracks (Fig.3.7). If the concentration of PEG into Fe/TiO_2 sol is increased further, the films obtained are uniform in thickness without any fracture

as well as pores but after calcinations at 500 ^{0}C or more the films become porous in nature.

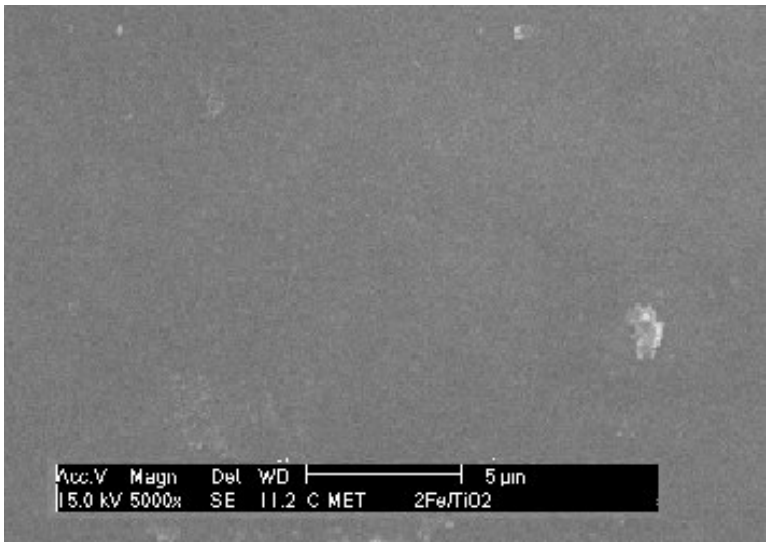

Fig. 3.7 : Scanning Electron Micrograph (SEM) of the thin film deposited on soda lime glass plate using 0.3 g /g PEG containing 2%Fe/TiO_2 sol.

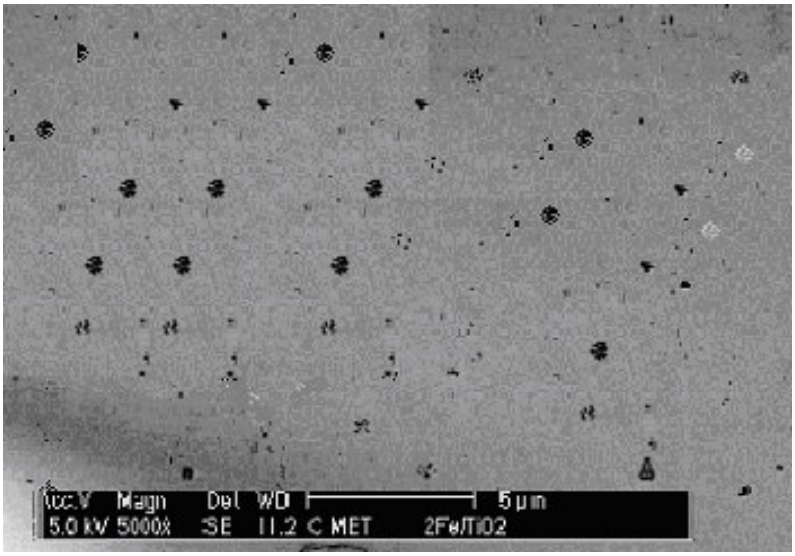

Fig. 3.8 : Scanning Electron Micrograph (SEM) of the thin film deposited on soda lime glass plate using 0.6 g PEG containing 2%Fe/TiO_2 sol

Fig.3.8 shows the SEM picture of 0.6PEG-2%Fe/TiO_2 film on soda lime glass plates. The picture shows many pores on the surface of the film and it may be due to the decomposition and desorption of PEG from the surface at 500^0C. The number of pores and size of pores on the surface of the film increases with increase in PEG content. In actual photograph of the films shown below suggests that the film containing PEG has pores on the surface.

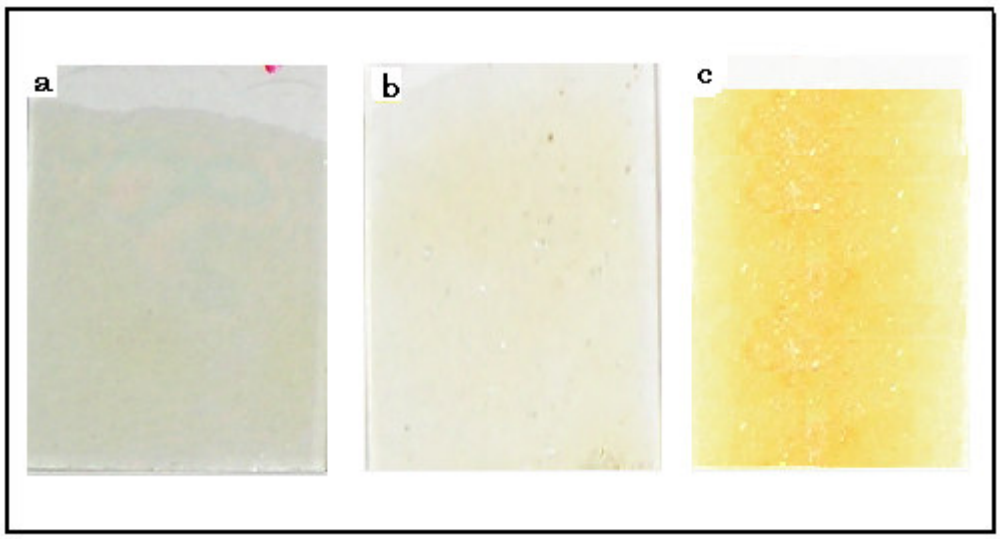

Photograph : Typical photograph of the films prepared on glass plates using sol a) Titanium peroxide, b) 0.5%Fe/TiO_2, and c) PEG-4%Fe/TiO_2

3.4.9 Fourier transform infra red spectrometric analysis

It is reported by J. Yu and coworkers[11b] that, addition of PEG in TiO_2 increases the surface hydroxyl content and it ultimately helps in improving the photo-catalytic activity. In order to investigate the effect of PEG addition on hydroxyl content of the films, the films were characterized by FTIR spectroscopy. The FTIR spectra of the thin

film samples of nearly equal thickness (150 nm) have been taken. The FTIR spectra of the films deposited on glass plates using Fe/TiO_2 sol containing various amount of PEG is as shown in fig.3.9.

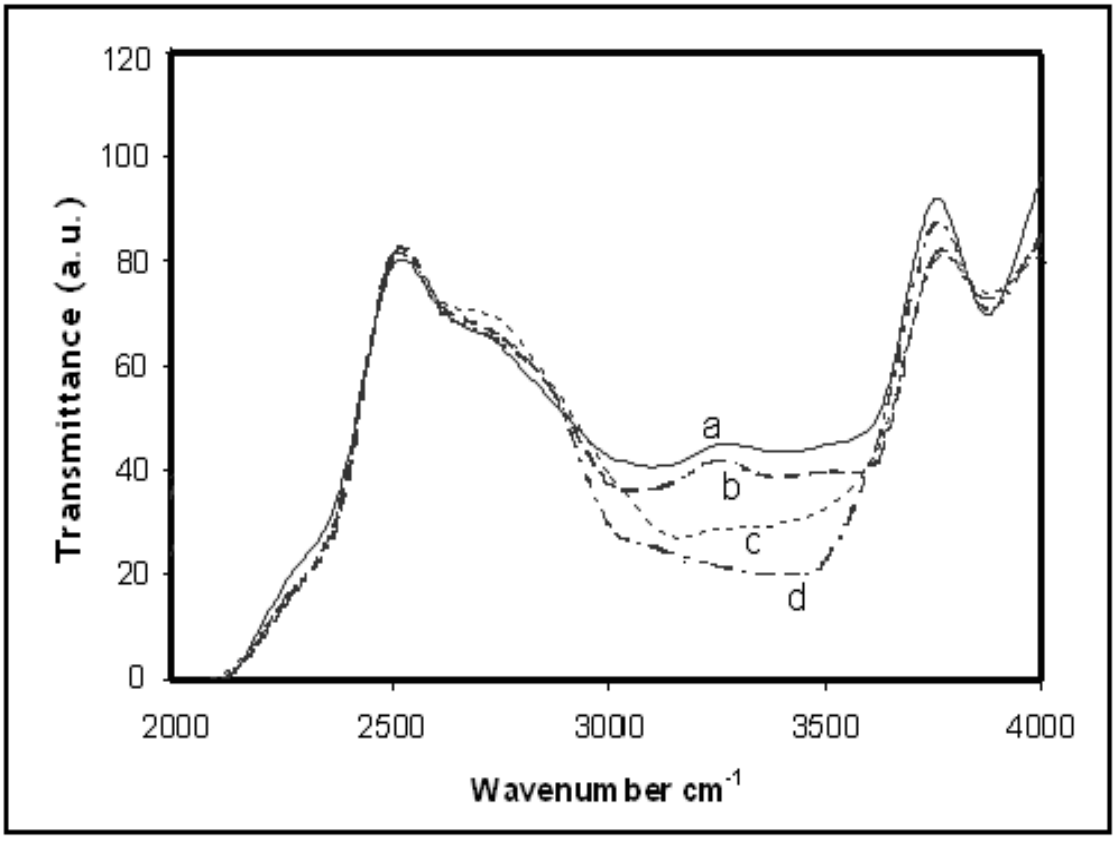

Fig. 3.9 : FTIR reflectance spectra of the films deposited on glass plates using titanium peroxide sol containing a) 0 g , b) 0.6 g , c) 1.0 g and d) 2.0 g of PEG/g 2%Fe/ TiO_2.

The glass sample without TiO_2 coating was utilized as a blank in all FTIR measurements. The curves a - d in figure corresponds to the thin film samples deposited by using sol containing 0g , 0.6g. 1.0g and 2.0g PEG respectively. All samples were initially scanned in the range of 400-4000 cm^{-1} but the glass shows complete absorption in the region of 400-2000 cm^{-1} hence the spectra were recorded in 2000-4000 cm^{-1}region

only. The curve 'a' in the figure shows a broad band in the region of 3600-3200 cm^{-1} (O-H stretching) with maximum centered at around 3420 cm^{-1} and a shoulder at around 3230 cm^{-1}. The band at 3420 cm^{-1} can be ascribed to the basic hydroxyl groups[49]. Since the glass shows absorption in region of 400-2000 cm^{-1} where the skeletal frequencies of Ti-O and Ti-O-O are generally observed these frequencies can not be distinguished in these spectra. The nature of spectra for all samples are qualitatively identified and it indicates that, the surface of Fe/TiO_2 films is hydrated and hydroxylated. The intensity of the broad band in the region of 3600-3200 cm^{-1} (O-H stretching) shows increasing trend in curves 'b-d' i.e with increase in PEG content of the sol used for deposition, similar to earlier reports The increase in hydroxyl groups is expected to improve the photo-catalytic activity of the Fe/TiO_2 thin film photo-catalysts.

3.4.10 Photo-catalytic activity of thin film Fe/TiO_2 photo-catalyst

Photo-degradation of organic compounds using $Fe\text{-}TiO_2$ as catalyst occurs when catalyst is illuminated with light in presence of water containing dissolved oxygen and organic compound. The organic species are decomposed to CO_2 and H_2O under these conditions.

$$Fe\text{-}TiO_2 \xrightarrow{h\nu} Fe\text{-}TiO_2\,(e^- + h^+) \qquad (3.5)$$

$$h^+ + OH^-_{ad} \longrightarrow OH_{ad} \qquad (3.6)$$

$$h^+ + H_2O_{ad} \longrightarrow OH_{ad} + H^+ \qquad (3.7)$$

$$e^- + O_2 \longrightarrow O_2^- \qquad (3.8)$$

where, h^+ represents the hole with positive charge generated at the surface of catalyst.

The organic molecules like salicylic acid, methyl orange, methylene blue and phenol in water are attacked by hydroxyl radicals formed as given in the above equations and generates organic radicals or other intermediates. Finally the parent compounds and intermediates are oxidized into CO_2, SO_2^{2-}, NO_3^- and H_2O.

The residual % concentration of salicylic acid with varying time intervals in the blank experiment (kept in darkness) is shown in fig.3.10 (curve 'a'). The variation of concentration of salicylic acid with time during photocatalytic decomposition using pure 2%Fe/TiO_2, 0.6gPEG-2%Fe/TiO_2 and 0.6gPEG-4%Fe/TiO_2 catalysts are depicted fig. 3.10, curves 'b-d' respectively. The curve a (blank experiment with the sample kept in darkness) shows about 11% decrease in concentration in 4hrs which may be due to the physical adsorption of salicylic acid on the surface of catalyst. The curves b, c and d suggest that, within 4 hrs there is 88%, 92% and 96% degradation of salicylic acid using 2%Fe/TiO_2, 0.6gPEG-2%Fe/TiO_2 and 0.6gPEG-4%Fe/TiO_2 catalyst respectively.

Similarly photo-catalytic degradation of methylene blue was also studied using these catalysts and the plots of change in concentration of methylene blue with time is shown in fig3.11. From the figure it is seen that, there is 90% , 93% and 95% degradation of methylene blue in 4 hrs. using 2%Fe/TiO_2, 0.6gPEG-2%Fe/TiO_2 and 0.6gPEG4%Fe/TiO_2 catalyst respectively.

In the photo-catalytic reaction of methyl orange, the typical UV-Visible spectra of the reaction products of the sample of methyl orange irradiated for 0, 2 and 4 hrs. is as shown in fig.3.12.

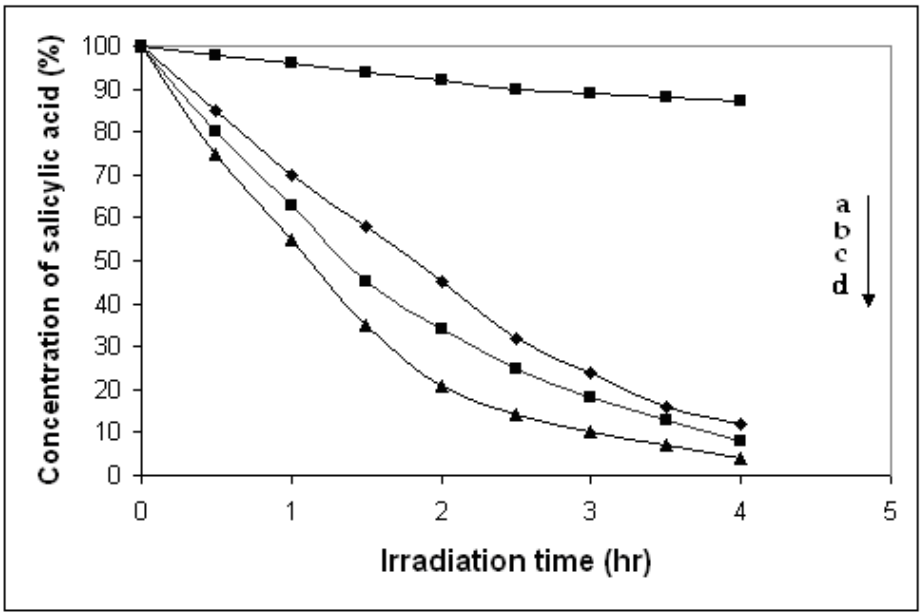

Fig.3.10 : Change in concentration of aqueous salicylic acid with time using a)2%Fe TiO_2 catalyst in darkness b) 2%Fe TiO_2 c) PEG 2%Fe TiO_2 and d) PEG -4%Fe TiO_2

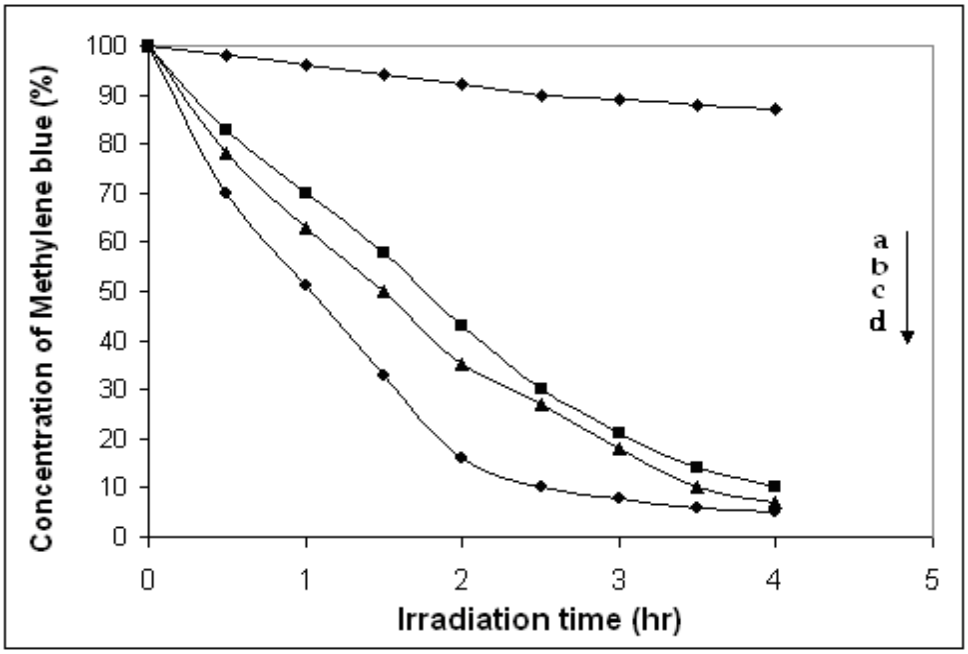

Fig.3.11 : Change in concentration of aqueous methylene blue with time using a)2%Fe TiO_2 catalyst in darkness b) 2%Fe TiO_2 c) PEG 2%Fe TiO_2 and d) PEG- 4%Fe TiO_2

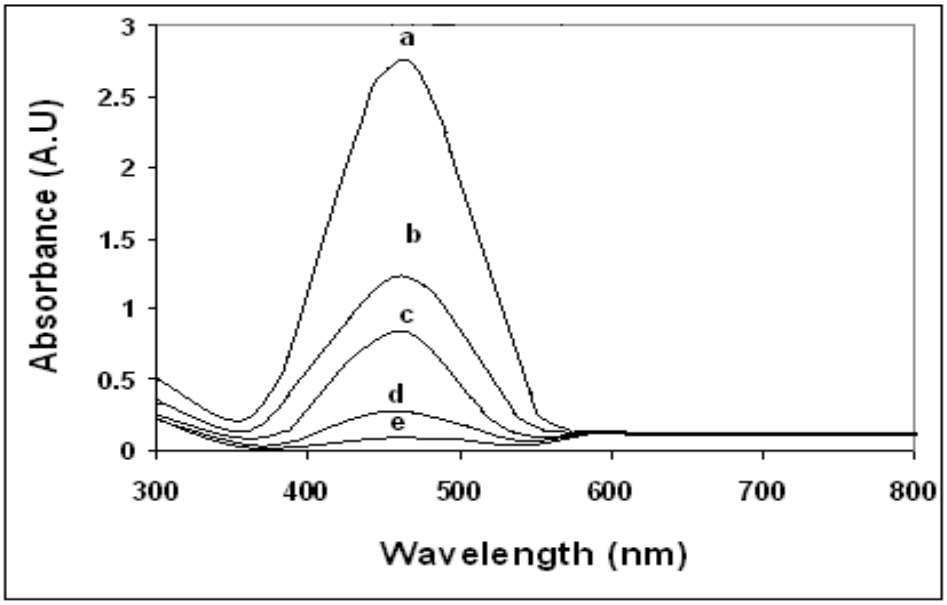

Fig. 3.12 : UV-Visible spectra of reaction product of methyl orange solution photo-catalyzed by thin films of PEG 2%Fe/TiO_2 on silica rings after irradiation sample for a) 0 hr, b) 1 hr, c)2 hr, d) 3 hr and e) 4 hr.

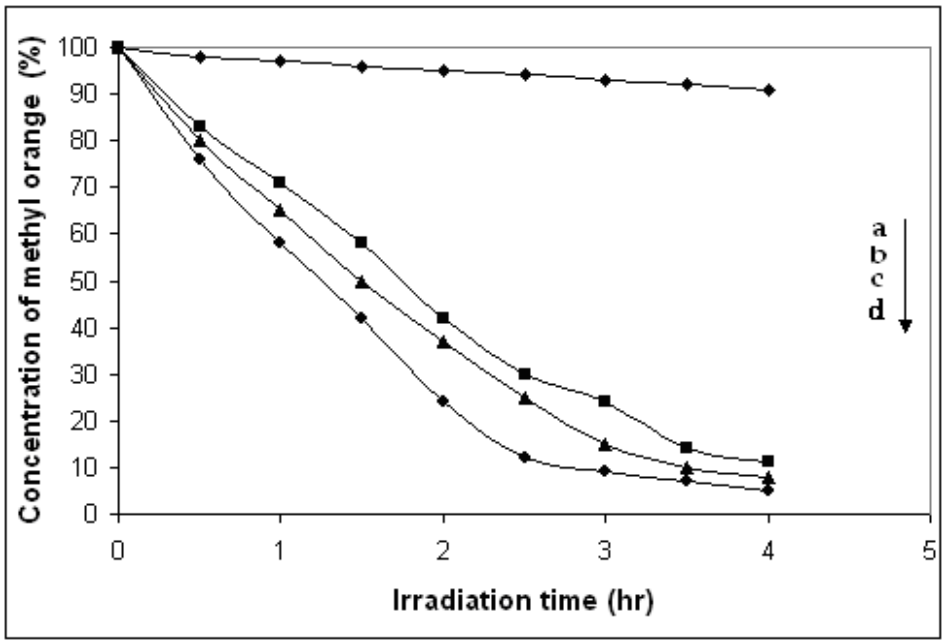

Fig.3.13 : Change in concentration of aqueous methyl orange with time using a)2%Fe TiO_2 catalyst in darkness b) 2%Fe TiO_2 c) PEG -2%Fe TiO_2 and d) PEG -4%Fe TiO_2.

The plot of change in concentration of methyl orange with time of irradiation is shown in fig.3.13. It suggests that 89%, 92% and 95% degradation of methyl orange degraded in 4 hrs using 2%Fe/TiO_2, PEG-2%Fe/TiO_2 and PEG-4%Fe/TiO_2 respectively. Similarly photo-catalytic degradation of phenol was also studied using these catalysts and the plot of change in concentration of phenol with time is shown in fig3.14. From the figure it is observed that, there is 88%, 91% and 95% degradation of phenol in 4 hrs. using 2%Fe/TiO_2, PEG-2%Fe/TiO_2 and PEG-4%Fe/TiO_2 respectively.

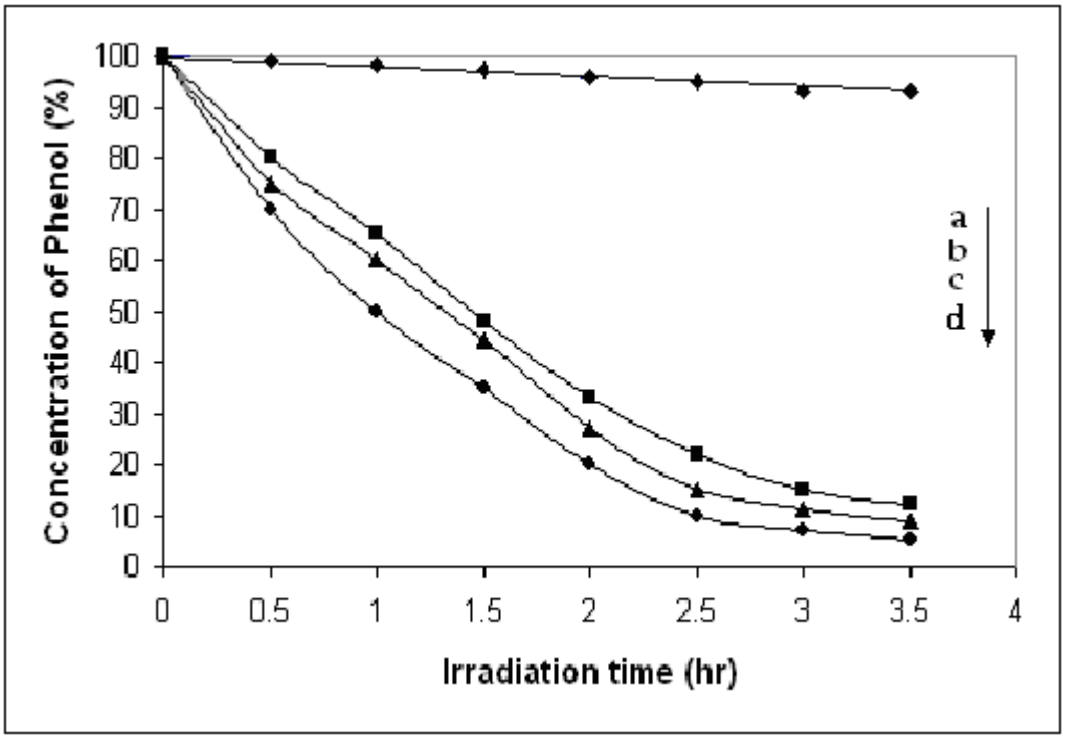

Fig.3.14 : Change in concentration of aqueous phenol solution with time using a)2%Fe/TiO_2 catalyst in darkness b) 2%Fe/TiO_2 c) PEG -2%Fe/TiO_2 and d) PEG -4%Fe/TiO_2.

It is well known that photo-catalysis experiments follow the Langmuir-Hinshelwood kinetics[54-57], where rate of reaction (R) is directly proportional to the surface coverage (θ)

$$R = -dc/dt = k_r \theta = k_r KC / (1 + KC) \qquad (3.9)$$

Where, k_r is the rate constant, K is the adsorption coefficient of the reactant and C is the reactant concentration. In the case of very low concentration of reactant in solution (less than 10^{-4} M) the product of K and C (KC) is negligible with respect to unity, so the Eq. 3.09 shows first order kinetics. The integration of Eq. 3.9 with limit condition that at the start of irradiation, t = 0, the concentration is the initial one, $C = C_0$, gives equation,

$$- \ln (C / C_0) = k't \qquad (3.10)$$

where, k' is the apparent first order rate constant. The rate constant can be obtained by linear regression.

The rate of reaction in photocatalytic degradation of salicylic acid, methylene blue, methyl orange and phenol over 2%Fe/TiO_2 , PEG-2%Fe/TiO_2 and PEG-4%Fe/TiO_2 are plotted in fig.3.15, 3.16, 3.17 and 3.18 respectively.

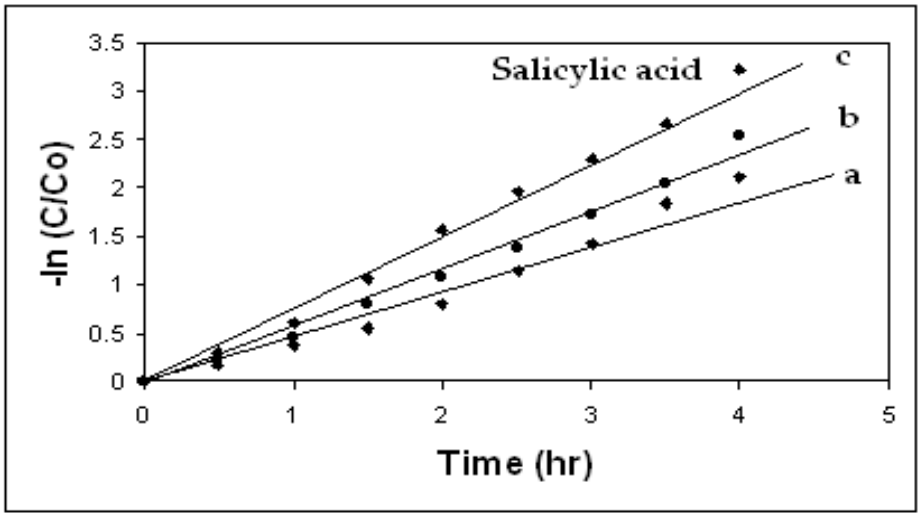

Fig. 3.15 : The first order kinetics of salicylic acid (SA) degradation using thin films of a) 2%Fe/ TiO_2, b) PEG 2%Fe/TiO_2 and c) PEG 4%Fe/TiO_2.

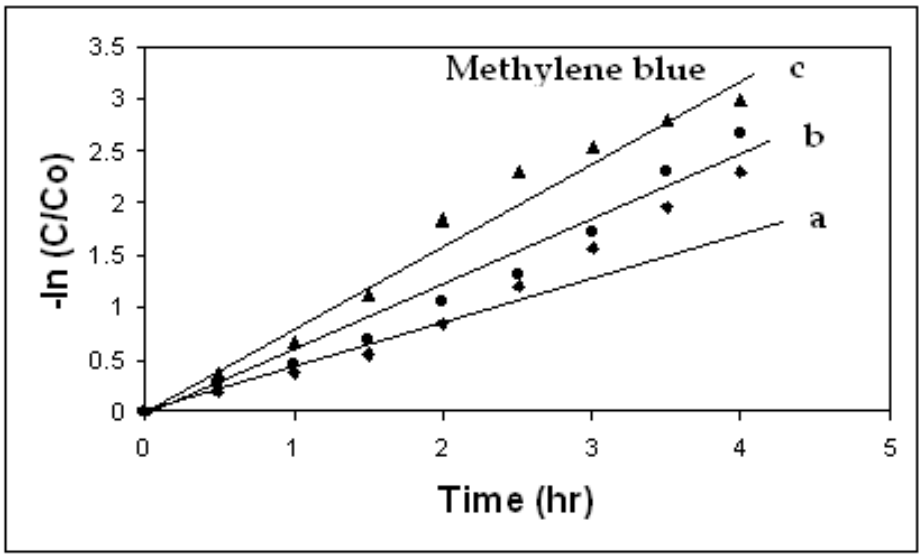

Fig. 3.16 : The first order kinetics of methylene blue (MB) degradation using thin films of a) 2%Fe/ TiO_2, b) PEG 2%Fe/TiO_2 and c) PEG 4%Fe/TiO_2.

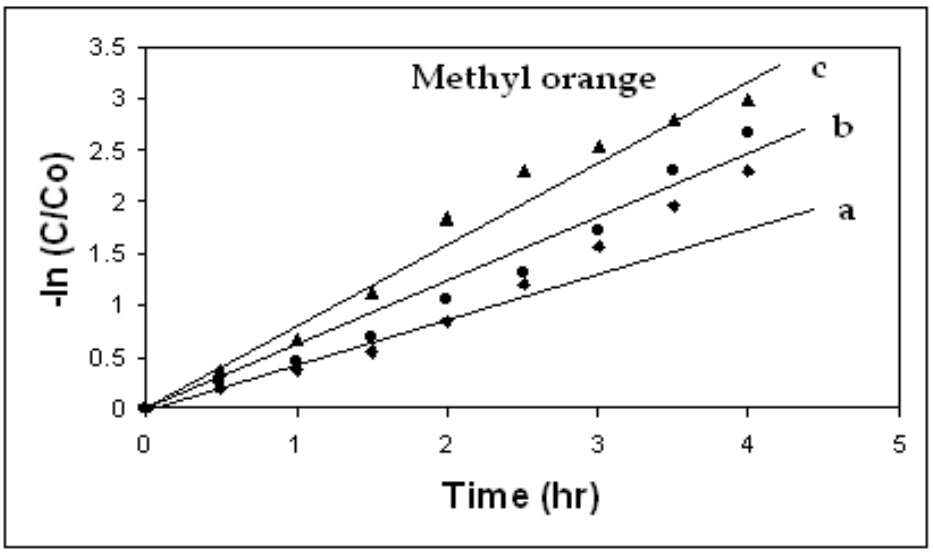

Fig. 3.17 : The first order kinetics of methyl orange (MO) degradation with using thin films a) 2%Fe/ TiO_2, b) PEG 2%Fe/TiO_2 and c) PEG 4%Fe/TiO_2.

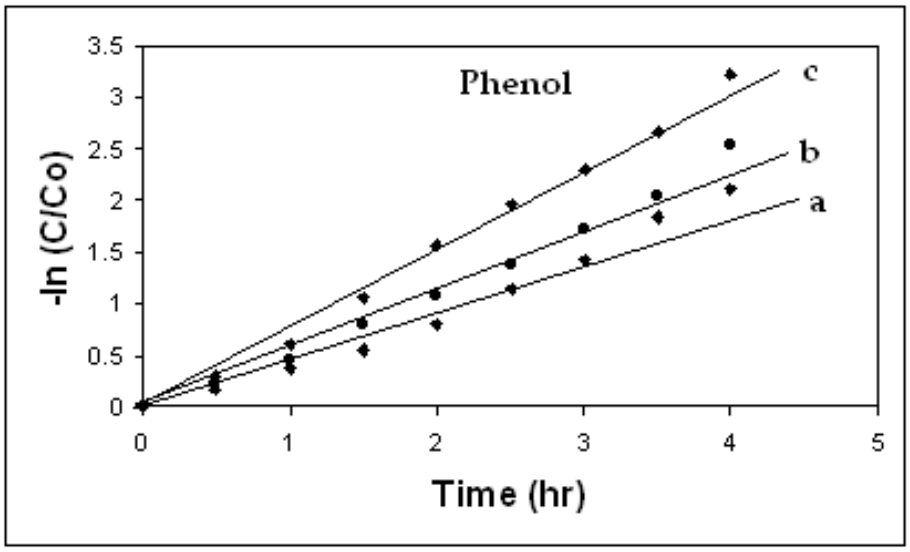

Fig. 3.18 : The first order kinetics of phenol (Ph) degradation using thin films a) 2%Fe/ TiO_2, b) PEG 2%Fe/TiO_2 and c) PEG 4%Fe/TiO_2.

From the kinetic study of degradation of salicylic acid, methylene blue, methyl orange and phenol the parameters such as degradation of compound after 1 hr, time for more than 90% degradation of each compound and rate constant were obtained. In table 3.3, 3.4 and 3.5, the kinetic parameters for the respective reactions are summarized.

Table. 3.3

Kinetic parameters and photocatalytic efficiency of films towards the degradation of SA, MB, MO and Ph in sunlight light using 2%Fe/TiO_2 catalyst.

	SA	MB	MO	Ph
% pollutant remain after 1 hr	29	31	35	27
Time required for complete (90%) mineralization (hr)	4	4.5	---	4
Rate constant (min^{-1})	0.0096	0.0083	0.0098	0.0096

Table. 3.4

Kinetic parameters and photocatalytic efficiency of films towards the degradation of SA, MB, MO and Ph in sunlight light using PEG-2%Fe/TiO_2 catalyst.

	SA	MB	MO	Ph
% pollutant remain after 1 hr	37	36.5	40	35
Time required for complete (90%) mineralization (hr)	4	3.5	3.5	3.5
Rate constant (min^{-1})	0.0109	0.0105	0.0111	0.0110

Table. 3.5

Kinetic parameters and photocatalytic efficiency of films towards the degradation of SA, MB, MO and Ph in sunlight light using PEG-4%Fe/TiO_2 catalyst.

	SA	MB	MO	Ph
% pollutant remain after 1 hr	45	48.5	50	42
Time required for complete (90%) mineralization (hr)	3	2.5	2.4	3
Rate constant (min^{-1})	0.0124	0.0136	0.01467	0.0116

From the experimental results of degradation of organic compounds and kinetic study it was observed that, the doping of Fe in TiO_2 increases the rate of photodegradation reactions. The activity of the catalyst increases by doping the TiO_2 with Fe as well as by addition of PEG. In the case salicylic acid, the rate constant has increased from 0.0096

min^{-1} for 2%Fe/TiO_2 to 0.0109 min^{-1} for PEG-2% Fe/TiO_2, so there is ~ 1.2 fold enhancement in rate of photodegradation. As compared to pure TiO_2 films (rate constant 0.00425 min^{-1}), approximately 2.6 fold enhancement in rate of degradation of SA using PEG-2%$FeTiO_2$ has been observed. For MB degradation reactions, the rate constant obtained are 0.00628 min^{-1}, 0.0083 min^{-1} and 0.0136 min^{-1} for undoped TiO_2, 2%Fe/TiO_2 and PEG-2%Fe/TiO_2 respectively. There is an enhancement of 1.3 and 2.2 fold in rate of photodegration of MB for 2%Fe/TiO_2 and PEG-4%Fe/TiO_2 respectively as compared to pure TiO_2 has been observed. Similarly in MO degradation using pure TiO_2, 2% Fe/TiO_2 and PEG-2% $Fe\text{-}TiO_2$, the enhancement in rate of reaction is found to be 2 and 2.3 fold respectively than pure TiO_2 obtained. However for phenol degradation the enhancement of 1.6 and 1.8 times respectively was obtained for 2% Fe/TiO_2 and PEG-2%Fe/TiO_2 than pure TiO_2. The following scheme has been proposed for degradation of methyl orange in sunlight as a typical example of degradation of organic compounds.

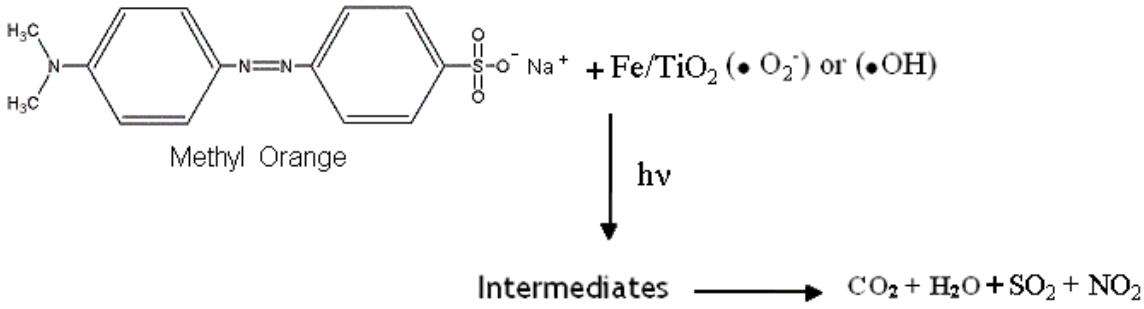

From the above results it can be concluded that, there is an increase in photo-activity of Fe doped TiO_2 catalyst and it increases with increase in concentration of Fe as well as by addition of PEG in TiO_2. In Fe doped catalyst, this increase in activity is attributed to the shift in absorption edge of TiO_2 towards visible side as well as increase in life time of charge carriers.[50-53] The shift of absorption edge in metal ion doped TiO_2 has complex origin but the researchers are of the opinion that if the shift is dependent on concentration of Fe it may be due to substitution of Ti^{4+}. Since the ionic radius of both Fe^{3+} and Ti^{4+} are nearly same, it forms the solid oxide solution easily at low concentrations. The samples of Fe/TiO_2 containing 2-4% iron and 0.6g PEG shows higher activity than the Fe/TiO_2 samples without PEG. It was reported earlier[58,59] that, photo-catalytic activity of the TiO_2 films has been increased by surface modification using polymers such as polyvinyl alcohol (PVA) and polyethylene glycol (PEG). In our case, the aim of addition of PEG was to improve the adhesion properties of TiO_2 thin films as well as surface modification.. The addition of 0.6g PEG in 2% Fe-TiO_2 and 4% Fe-TiO_2 increased the photo-catalytic activity of the catalyst further so the time required to 90% degradation of each compound has decreased. This can be attributed to the more hydroxyl content, porous nature of the films as well as surface roughness. The Fe/TiO_2 thin film samples containing PEG have shown more hydroxyl content as per FTIR analysis than the Fe/TiO_2 samples without PEG and the hydroxyl content of the films increases with the increase in PEG content of the film. Since the hydroxyl ions are very important in photocatalytic reaction, the increase in hydroxyl content will be beneficial in improving photoactivity. This is because, in heterogeneous photocatalysis,

the illumination of semiconductor produces electrons(e^-) and holes (h^+). The holes (h^+) are combining with OH^- ions and there is formation of hydroxyl radicals ($h^+ + OH^- \rightarrow {}^\bullet OH$). These surface hydroxyl radicals formed on the surface of the photo-catalyst are oxidizing species which ultimately affects the photo-catalytic activity.[58,59] It is also reported that, porous nature as well as surface roughness are also helping in improving the photo-activity. In high surface area rough titania films, the ability to efficiently capture photons is high as compared to the films with smooth surface. The rough surface is acting in a 'sponge' like way[60] throughout a thick semiconducting network and helps in improving the photocatalytic activity of the film. The surface porosity is also an important parameter because in porous films the adsorption of the organic reactants is more than that of non porous films. The combined effect of all these parameters results in improving the photo-catalytic activity of PEG added Fe/TiO_2 thin film photo-catalysts.

3.5 Conclusions

A very simple method for the deposition of thin films of Fe/TiO_2 on various substrates like glass plates, silica rashig rings and glass helix has been developed. The film thickness is dependent on the concentration of titanium in the sol and the viscosity of the sol. The addition of PEG into TiO_2 sol improves the adhesion of the sol to substrate, gel formation behavior of the sol and photocatalytic property. The films are transparent, homogeneous, uniform and showed excellent adhesion to all the substrates. The films of pure TiO2 are colorless but Fe doped films are brownish in colour due to presence of Fe

ions. The addition of Fe into the titanium peroxide lowers the crystallization temperature as well as phase transition temperature. The Fe doped TiO_2 sol and films prepared using this sol shows the shift in absorption of TiO_2 towards visible side(Red shift). The structural and thermal properties of the Fe doped catalyst have been changed due to addition of Fe ions. In pure Ti-peroxy powder the transformation of anatase to rutile begins at 600 ^{0}C whereas in Fe doped TiO_2 the same transition begins at 450 ^{0}C. The films heated at various temperatures i.e from 200 to 450 ^{0}C are mostly of phase pure anatase type. We have reported here a photocatalytic thin film system which can decompose almost completely complex organic molecules like SA, MB, Mo, and phenol which are often contaminating candidates in polluted water. The PEG-Fe/TiO_2 thin films calcined at 500 ^{0}C have shown excellent catalytic activity. An enhancement of 1.2-2.6 fold in photocatalytic activity has been observed for PEG-Fe/TiO_2 films than pure TiO_2 films in sunlight.

References

1. G. Hodes, Nature, 1980, 285, 29.
2. A. Heller, Acc. Chem. Res. 1995, 28, 503.
3. A. Mills, S. L. Hunte, J. Photochem. Photobiol. A : Chem. 1997, 108, 1.
4. Z. Yuan, J. Jia, l. Zhang Mater. Chem. Phys. 2002, 73, 326.
5. N. Nogishi, T. Iyoda, K. Hashimoto, A. Fujishima, Chem. Lett. 1995, 841
6. M. R. Hoffamnn, S. T. Martin, W. Choi, D. W. Bahnemann, Chem. Rev. 1995, 95, 69.

7. P. V. Kamat, in Nanoparticles and Nanostructured Films, ed. J. H. Fedler, Wiley-VCH, New York (1998).
8. M. I. Litter and J. A. Navio, J. Photochem. Photobiol. A 98 (1996) 171.
9. C. C. Wang, Z. Zhang and J. Y. Ying, Nanostruct. Mater. 9 (1997) 583.
10. G. H. Li, L. Yang, Y. X. Jin and L. D. Zhang, Thin Solid Films 368 (2000) 168.
11. a) K. Kajihara, K. Nakanishi, K. Tanaka, K. Hirao, N. Soga, J. Am. Ceram. Soc. 1998, 81(10) 2670. b) Jiaguo Yu, Xiujian Zhao and Qingnan Zhao Thin Solid Films 379 (2000) 7.
12. Schrauzer G.N, Guth T.D. J Am Chem Soc 99 (1977) 7189.
13. Al-Salim NY, Abagshaw S, Bittar A, Kemmett T, McQuilla AJ, Mills AM, J Mater Chem. 10 (2000) 2358.
14. M. Kang J. Mol. Catal. A: Chem 2003, 97,173.
15. J. Wang, S. Una, K.J. Klabunde, Appl. Catal. B: Environ 2004, 48, 151.
16. K. Wilke, H.D. Breuer J. Photochem. Photobiol. A: Chem. 1999, 121, 49.
17. F. Garcia, J.P. Holgado, F. Yubero, A.R. Gonza´lez-Elipe, Surf. Coat. Technol. 2002,158–159, 552.
18. Y. Yang, X.J. Li, J.T. Chen, L.Y. Wang. J Photochem. Photobiol. A: Chem 2004, 163, 517.
19. A.W. Xu, Y. Gao, H.Q. Xu. J Catal. 207 (2002) 151.
20. S.T. Martin, C.I. Morrison, M.R. Hoffman, J. Phys. Chem. 1994,98,13695.
21. C.Y. Kwan, W. Chu Water Res. 2003,37,4405.

22. J.A. Navýo, M. Garcýa Gomez, M.A. Pradera Adrian, J. Fuentes Mota ,Guisnet M, editor. Heterogeneous catalysis and fine chemicals II. Amsterdam: Elsevier; 1991, p. 445.

23. J. Aran¡a, O. Gonzalez-Dýaz, M. M. Saracho, J. M. Dona-Rodrýquez, J.A. Herrera-Melian, J. Perez-Pena, et al. Appl. Catal. B: Environ. 2002,36,113.

24. B. Pal, T. Hata, K. Goto, G. Nogami J. Mol. Catal. A :Chem 2001,169,147.

25. M. R. Dhannanjayan, V. K. Kandavelu, R. Renganathan J. Mol.Catal. A: Chem. 2000, 151, 217.

26. H. Yamashita, M. Harada, J. Misaka, M. Takeuchi, B. Neppolin, M. Anpo Catal. Today, 2003, 84, 191.

27. M. Anpo, Y. Ichihashi, M. Takeuchi, H. Yamashita, Stud. Surf. Sci. Catal. 1999, 121, 305.

28. K.E. Karakitsou and X. E. Verykios, J. Phys. Chem. 97 (1993) 1184.

29. M. Graetzel and R. F. Howe, J. Phys. Chem. 94 (1990) 1566.

30. J. Soria, J. C. Conesa, V. Augugliaro, L. Palmisano, M. Schiavello and A. Sclafani, J. Phys. Chem. 95 (1991) 274.

31. J. Kiwi and C. Morrison, J. Phys. Chem. 88 (1984) 6146.

32. Yu-Hong Zhang, Armin Reller, J. Mater. Chem. 11(2001) 2537.

33. Misook Kang, J. Mol. Catal. A: Chemical 197 (2003) 173.

34. B. Pal, M. Sharon, G. Nogami, Mater. Chem. and Phys. 1999, 59, 254.

35. J. Novio, G. Colon, M. Macias, C. Real, M. Litter Appl. Catal. A: Gen 1999, 177, 111.

36. R. Phani, S. Santucci , Mater. Lett. 2001, 50, 240.

37. Yuan Z.H, Jia H.J, Zhang L.D. Mater Chem Phys 2002, 73, 323.

38. Chen-Chi Wang, Jackie Y. Ying Chem. Mater. 1999, 11, 3113.

39. S. S. Watson, D. Beydoun, J. A. Scott, R. Amal Chem. Eng. J. 2003, 95, 213.

40. Y. Haga, H. An, R. Yosomiya, J. Mater. Sci. 1997, 32, 3183.

41. K.J.Y. Yung, S. B. Park, J. Photochem. Photobiol. A: Chem, 1999, 127, 177.

42. Hanprasopwattana A, Rieker, T. Sault, A. G. Datye, A. K. C*atal. Lett.* **1997**, *45*, 165.

43. C. J. Brinker, G. W. Scherer, Sol-Gel Science, Academic Press San Diego, 1990.

44. J.S. Thorp, H.S. Eggleston. J Mater Sci Lett 1985, 4, 1140.

45. A. Amorelli, J.C. Evans, C.C. Rowlands. J Chem Soc Faraday Trans I 1989, 85, 4031.

46. R. D Shannon, J.A. Pask. J Am Ceram Soc 1965, 48,391.

47. K. Kato, A. Tsuzuki, Y. Torii, H. Taoda, T. Kato, Y. Butsungan, J. Mater. Sci. 1998, 30, 2259.

48. Y . Iida, S. Ozaki J. Am. Ceram. Soc. 1961,44,120.

49. Jr. A. Nobile, Jr. M.W. Davis. J. Catal. 1989,116, 383.

50. J. Peral, D.F. Ollis. J. Catal. 1992,136, 554.

51. A.V. Vorontsov, E.N. Kurkin, E.N. Savinon, J. Catal. 1999,186, 318.

52. S.B. Kim, S.C. Hong, Appl. Catal. B: Environ 2002, 35, 305.

53. D. Cordischi, N. Burriesci, F. D'Alba, M. Petrera, G. Polizzetti, M. Schiavello. Solid State Chem1985,56,182.

54. A.R. Bally, E.N. Korobeinikova, P.E Schmid, F. Le´vi, F. J. Bussy, Appl Phys 1998,31,1149.

55. F.C. Gennari, D.M. Pasquevich, J Mater Sci 1998;33:1571.

56. J. Moser, M. Gra¨tzel. Helv. Chim. Acta. 1982,65,1436.

57. D. F. Ollis, E. Pelizzetti, N. Serpone, Environ. Sci. Technol. 25(1991) 1523

58. M. Takahashi, K. Mita, H. Toyoki, M. Kume, J. Mater. Sci. 1989,24, 243

59. Y. Takahashi, Y. Matsuoka, J. Mater. Sci. 1988, 23, 2259.

60. I. M. Arabatzis, T. Stergiopoulos, D. Andreeva, S. Kotova, S. G. Neophytides, P. Falaras, J. Cat. 220 (2003) 127.

CHAPTER-IV

PREPARATION, CHARACTERIZATION AND PHOTOCATALYTIC ACTIVITY OF Au/TiO_2 THIN FILMS

4.1 Introduction

The major goal of designing the metal-semiconductor composite system is to tailor photo-electrochemical properties of semiconductor nanomaterials. A series of metal-semiconductor composite materials have been shown to facilitate charge rectification in the semiconductor nanostructures.[1-9] The deposition of metals especially noble metals on semiconductor is beneficial for maximizing the efficiency of photocatalytic reactions.[10-16]

The various metals(Pt, Pd, Ag and Ru) supported on TiO_2 have shown improvement in catalytic activity because of improvement in charge transfer process between semiconductor and metal.[17-20] It is reported that there is a quick charge transfer between platinum metal and semiconductor observed due to ohmic type of contact between metal and semicoductor.[21] The TiO_2 nanoparticles modified with precious metals have also been employed in photo-catalytic splitting of water.[22-24] A direct correlation between the work function of the metal and the photocatalytic activity has been developed for metal-TiO_2 system. Recent studies have shown that metal or metal ion doped semiconductors exhibit a shift in fermi level to more negative potentials.[25-28] Such a shift in the fermi

level improves the energetic of the semiconductor metal system and enhances the interfacial charge transfer process which ultimately improves the photocatalytic activity. Among the noble metals, gold (Au) has been paid less attention because of the low activity due to high ionization potential and poor affinity towards reactant molecules. The conventional supported Au catalysts (Au on TiO_2) prepared by imprignation method were less active than other metal supported catalysts (Pt or Pd on TiO_2). The less activity may be attributed to the comparably large size of Au particles than other metal particles prepared by this method. The melting point of the metal decreases with decrease in particle dimensions accordingly the Au particles of size 30 nm has melting point 1063 ^{0}C whereas the melting point of 2 nm Au particles is lowered to 300 ^{0}C. There is drastic change in thermal properties as well as other properties due to size quantization. Bond and Sermon[29-30] have reported that highly dispersed small Au particles on silica support have been shown to improve the catalytic activity for hydrogenation reactions. Highly dispersed tiny Au particles on magnesia and alumina[31-32] have been found to be very useful for hydrogen and oxygen transfer. These studies mark the beginning of dispersed small Au particles supported on various supports for hydrogenation and oxidation reactions. Since then many researchers have reported the different methods for preparation of highly dispersed Au particles on various supports such as TiO_2, MgO, SiO_2, Al_2O_3, ZrO_2 and many more. All are of the opinion that, the Au particles within the 2-10 nm are showing high catalytic activity towards the hydrogenation, oxidation of CO, and reduction of NO_x. Although the Au/TiO_2 in a highly dispersed state has been used for various catalytic reactions, it has been very

rarely used for the photo-catalytic application. The reason may be the same as mentioned above and now papers have started to appear in this important area of pollution abatement. In TiO_2 mediated photo-catalysis, the illumination of catalyst excites electron from VB to CB leaving a positively charged hole in VB (formation of charge carriers). The formation of charge carriers and subsequent formation of hydroxyl radicals by trapping the electrons as well as holes are important steps. If the charge carriers are not trapped, there is possibility of electron-hole recombination which ultimately reduces the efficiency of the catalyst. The charge carrier separation and fermi level equilibration in metal TiO_2 nanocomposites is as shown in fig.4.1[33]

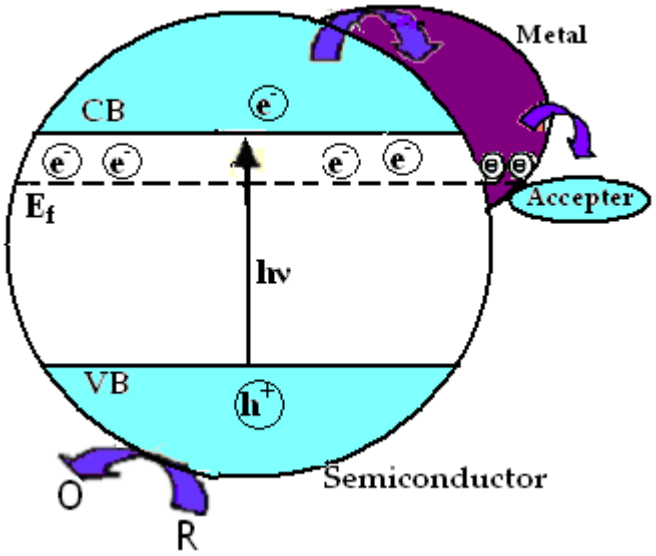

Fig. 4.1 Charge carrier separation and Fermi level equilibration in a semiconductor-metal nanocomposite system[33].

The small Au particles not only improves the charge carrier separation by trapping the electron on the surface of TiO_2 but also it increases the absorption of TiO_2 in visible region due to its characteristic surface plasmon band at around 520-530 nm[34]. This

increased absorption in visible region makes it possible to use TiO_2 under visible radiation as well and also increases the efficiency of it. By using these metal composites, the photo-catalytic efficiency can be improved but the composites prepared are in powder form and using powder catalyst has disadvantages like need of stirring during the experiment and separation of catalyst powder after each experiment. Use of thin film catalyst will overcome these problems and also improves the photo-catalytic activity. In many studies, doping of transition metal ions or noble metals by simple methods such as impregnation or sol-gel does not show much increase in photo-activity whereas by using ion implantation the photo-activity has been reported to be increased but the method of doping may not be easy for operation. So there is a need to develop a simple method for preparation of thin film photo-catalyst which can be effective in UV as well as visible light and it can be easily prepared. Keeping in mind the above requirements, we have attempted to develop a thin film photo-catalyst which can be used in UV as well as visible light or rather sunlight, the cheapest and easily available source of energy.

In the present study, the aim was to develop thin film catalyst which can be efficiently used under UV-visible or sunlight for the decomposition organic compounds. Gold doped TiO_2 films were prepared by sol-gel dip coating method using titanium peroxide as titanium precursor. To the best of our knowledge no such work has been reported earlier. We are the first to report preparation Au/TiO_2 thin films as well as powder using titanium peroxide sol-gel route. The advantages of this method which we have illustrated in the earlier part are, it is very easy to operate, it requires no complicated

instruments and TiO_2 is easily anchored on the substrates. The thin film catalyst was characterized by various techniques to elucidate the structure, morphology and stability. Effect of Au addition on the sol-gel behavior of titanium peroxide and ultimately on the films has been investigated. The efficiency of both undoped and doped catalyst was tested by decomposition of various compounds such as salicylic acid, methylene blue, methyl orange and phenol as model examples under solar light. The effect of Au addition on photo-catalytic efficiency has been studied and compared with undoped TiO_2. The kinetic study was performed and the data obtained was fitted to a equation to find out the rate of decomposition of salicylic acid, methylene blue, methyl orange and phenol and other parameters.

4.2 Experimental

4.2.1 Materials

Titanium (IV) isopropoxide (TIP), was obtained from Aldrich (Milwaukee, WI). $HAuCl_4$ and $NaBH_4$ were obtained from Qualigen (Qualigen India Ltd.) De-ionized water was prepared from double distilled water using the de-ionized water unit (Millipore, Milli-Q-System). The high purity Argon gas(UHP grade 99.99%) was obtained from local gas supplier (Inox Air Products Ltd.). All chemicals and reagents were used as received without further purification. Glass substrates used for making titania thin films were the microscope slides and other substrates such as silica rashig rings as well as glass helix were obtained from Perfect Scientific Equipments (Pune).

4.2.2 Preparation of colloidal Au solution

The gold colloidal solution was prepared by reduction of $HAuCl_4$ solution with $NaBH_4$ solution as a reducing agent. The formation of Au^0 was monitored using UV-visible spectrophotometer. The yellow $HAuCl_4$ (10 mM) solution shows an intense absorption band in UV region at 290 nm. Prior to use the $HAuCl_4$ (10 mM) solution was purged with high purity argon gas to remove the oxygen and air dissolved in the solution. During the addition of $NaBH_4$ solution the $HAuCl_4$ solution was continuously stirred with help of magnetic stirrer. The addition of $NaBH_4$(5 mM) in $HAuCl_4$ solution starts to change color from yellow to red and finally attains red due to complete reduction of Au^{3+} available in the solution to Au^0 (colloidal gold solution). The $HAuCl_4$ solution shows absorption band at 290 nm in UV region. The samples collected at various time intervals during the addition of reducing agent shows a new band emerging at 530 nm in visible region and it intensifies. At one stage the intensity of this band at 530 nm stabilizes, this indicates the complete reduction of $AuCl_4^-$ ions to Au^0. This solution was kept in air tight vessel and it was sufficiently stable for long period i.e for months

4.2.3 Preparation of Au/TiO_2 sol

The Ti- peroxide sol was prepared by method described in our previous chapter.(Chapter.II) It was initially red colored and this was stable until 1-4 hours depending on the concentration of titanium in the sol. As time passes, the color intensity of the sol decreases, the viscosity of the sol increases and finally sol turns into dense gel after 10-24 hours. The gel formed was transparent, light yellow colored and stable

for 5-10 days. If $AuCl_4^-$ solution (10 mM) is added immediately after preparing titanium peroxide sol before it forms gel the sol-gel behavior drastically changes. Initially during the addition of $AuCl_4^-$ solution into the sol there is no any separation of precipitate but the sol after keeping for 1-2 hr starts formation of translucent solution due to separation of Ti- hydroxide precipitate rather than formation of transparent gel. This may be attributed to the Au^{3+} ions catalyzed decomposition of titanium peroxide into titanium hydroxide precipitate. In place of Au^{3+} ion solution, if the colloidal Au solution where Au is having no charge on it is used, it gives a very stable transparent red colored gel for doping upto 0.5-2% of Au in titanium peroxide. Therefore all other experiments were performed using colloidal Au solution instead of Au^{3+} solution.

The yellow Ti-peroxide sol prepared by above method was stirred with the help of magnetic stirrer and to this the required quantity of gold colloidal solution was added dropwise. The addition of gold solution into yellow Ti-peroxide sol changes the color of the sol to redish or violet. In this process, following reactions take place (Eq. 4.1 – 4.3) during the preparation Au/TiO_2 sol

$$Ti\,(O\text{-}ipr)_4 + 2H_2O \longrightarrow Ti\,(OH)_4 + Pr\text{-}OH \qquad (4.1)$$

$$Ti\,(OH)_4 + H_2O_2 \longrightarrow (Ti\,O_{2-x-0.5y}(O_2)_x(OH)y\,.H_2O)_n + H_2O \qquad (4.2)$$

$$(Ti\,O_{2-x-0.5y}(O_2)_x(OH)y\,.H_2O) \xrightarrow{\text{Au-sol}} Au\,(Ti\,O_{2-x-0.5y}(O_2)_x(OH)y\,.H_2O) \qquad (4.3)$$

This sol was allowed to stand for 1-2 hr before using for film deposition, this slowly starts to polymerize and then it turns to gel by olation and oxolation process. (Eq. 4.4)

$$n\,[Au\,(Ti\,O_{2-x-0.5y}(O_2)_x(OH)y\,.H_2O)] \longrightarrow [Au\,(Ti\,O_{2-x-0.5y}(O_2)_x(OH)y\,.H_2O)]_n \qquad (4.4)$$

The Au/Ti-peroxide sol obtained by above method is hereafter referred as Au/TiO_2 sol and it has been used for deposition of films before it turns to a thick gel as per following scheme.

Au/TiO_2 (sol) ⟶ Au/TiO_2 (viscous sol) ⟶ Au/TiO_2 (gel)

4.2.4 Deposition of Au/TiO_2 thin films on glass plates

The Au/TiO_2 sol, prepared by this method starts to form viscous liquid after 1-2 hrs. The liquid after attaining the particular viscosity range 300- 2800 cps was used for deposition of thin films on soda lime glass. The soda-lime glass plate was dipped into Au/ TiO_2 sol of required viscosity and kept for 5 minutes. After 5 minutes, the plate was pulled out at approximate pulling rate of 2 mm/sec. The sol adhered to the substrate upon drying at room temperature in air forms a uniform thin film. These plates were further dried at 100 ^{0}C in an electric oven for 2 hrs. and used for characterization. For deposition on substrates like glass helix and silica rashig rings the procedure as described in chapter.2 has been followed. The physicochemical characterization of thin films as well as dried gel was performed as per characterization techniques described in chapter 2. The evaluation of photocatalytic activity of the Au/TiO_2 thin film catalyst under sunlight was done as per procedure described in chapter 3.

4.3 Results and discussion

4.3.1 Effect of Au addition on sol-gel behavior

The Ti-peroxide sol is sufficiently stable for long time, the sol is having viscosity almost equal to water since the concentration of Ti is very low. It remains transparent red colored for 1-4 hr and then it starts to become viscous. The viscosity of the sol starts to change depending on the concentration of Ti^{4+} species in it and finally the sol turn to a transparent yellow colored thick gel. Addition of foreign ions (Au^{3+}) even at low concentration level(0.5-4%) into this sol alters the sol-gel behavior and it rapidly turns to a gelatinous precipitate rather than a stable gel. This gelatinous precipitate after keeping for 12-14 hrs starts separating from the solvent (water in this case) which can not be used for film deposition. It gives a non uniform translucent film of doped TiO_2. These films were poor in adhesion and not useful for photo-catalytic experiments. However addition of colloidal gold solution in place of Au^{3+} ion solution allows the formation of stable Au/TiO_2 sol and this sol after keeping for long duration turns to transparent gel. The separation behavior may be explained on the basis of more reactivity of Au^{3+} ions than Au^0. The Au in ionic state has more affinity towards the oxygen in the titanium peroxide sol than as Au^0, which hinders the formation of gel network via olation and oxolation process. It means Au restricts formation Ti-O-Ti network hence there is

separation of precipitate rather than formation of gel.

The formation of transparent stable gel was limited only upto 0.5-2% of Au colloidal solution. Further addition of Au colloids results in to precipitation of $Au/Ti(OH)_4$. The

Au addition at 1-2 percent does not show much change in gel behavior except the time required for gel formation and color. But increase in Au content more than 2% results in redish gelly precipitate rather than a perfect transparent violet colored gel. After keeping this gel for 12-15 hours the gelly precipitate separates into two layers the upper solvent layer (water in this case) and gelatinous precipitate at the bottom layer. The formation of precipitate may be attributed to breakage of gel network by free Au. In more than 2% Au containing sol, part of the gold added is inserted into TiO_2 lattice and some may remain as a free atomic gold into gel. This free atomic gold in TiO_2 matrix increases with increase in percentage of addition of gold. The availability of oxidizing species(H_2O_2) results in oxidation of free atomic gold to gold ions and these ions are more reactive species. The Au ions try to attach to the bridging oxygen (Ti-O-Ti) in the gel network. This leads to the breakage of gel network and ultimately formation of gelly precipitate rather than a perfect gel. Films deposited by using this gelly precipitate are opaque, non uniform in thickness and poorly adhesive to the substrate.

4.3.2 UV-visible spectroscopic characterization

The UV-visible spectra of the colloidal Au sol prepared by reduction of $HAuCl_4$ solution using $NaBH_4$ solution is presented in fig.4.2 . In the figure it is seen that with the addition of $NaBH_4$ solution the intensity of peak at 530 nm increases gradually. The absorption peak at 530 nm is the well known SPR of spherical gold nanoparticles.[35-37] This absorption is due to collective oscillation of free conduction band electrons of the gold particles in response to optical excitation. Position of this band totally depends on

the size and shape of the gold particles[38] and this band may not observed in bulk material of same composition.

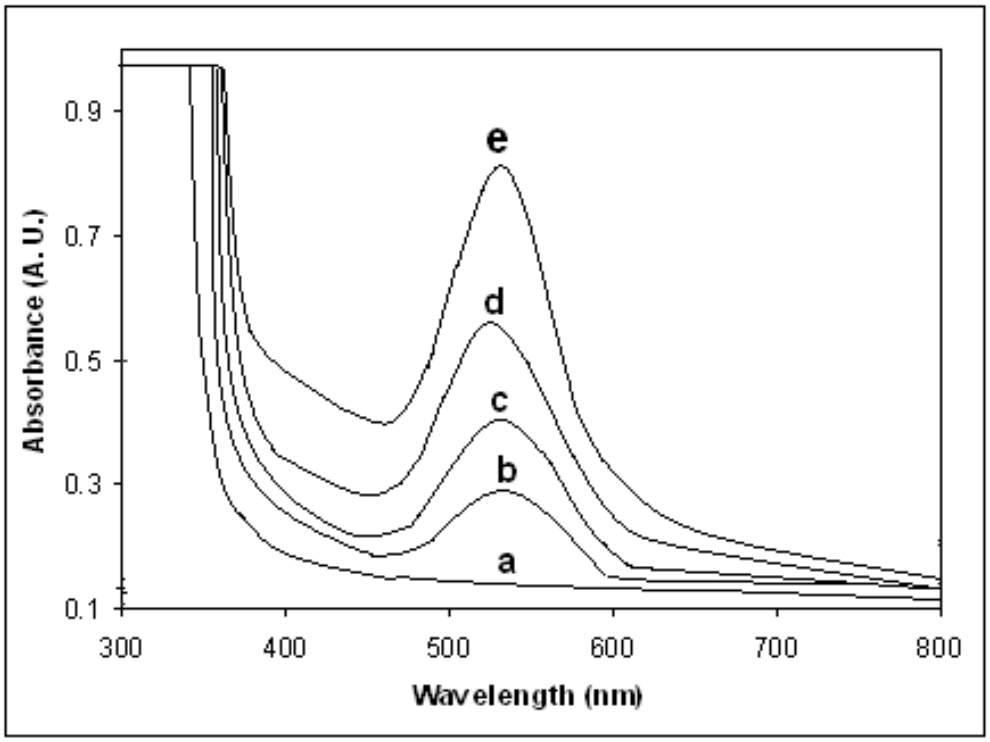

Fig. 4.2 : UV-visible absorption spectra of Au sol prepared by reduction of aqueous $HAuCl_4$ solution using a) 0 ml , b) 2 ml c) 4 ml d) 6 ml and e) 8 ml $NaBH_4$ (5 mM) solution.

Fig. 4.3 (curves a ~c) shows the UV-visible spectra of the pure titanium peroxide gel and titanium peroxide gel containing different amount of Au (1% and 2%) aged for 4 hrs. From the figure it is observed that, pure titanium peroxide gel (curve a) shows an absorption edge at around 360 nm whereas titanium peroxide gel containing 1% Au (curve 'b') and 2% Au (curve 'c') shows absorption edge at around 450 nm. In addition, the intensity of band at 530 nm in the visible region increases with increase in Au content.

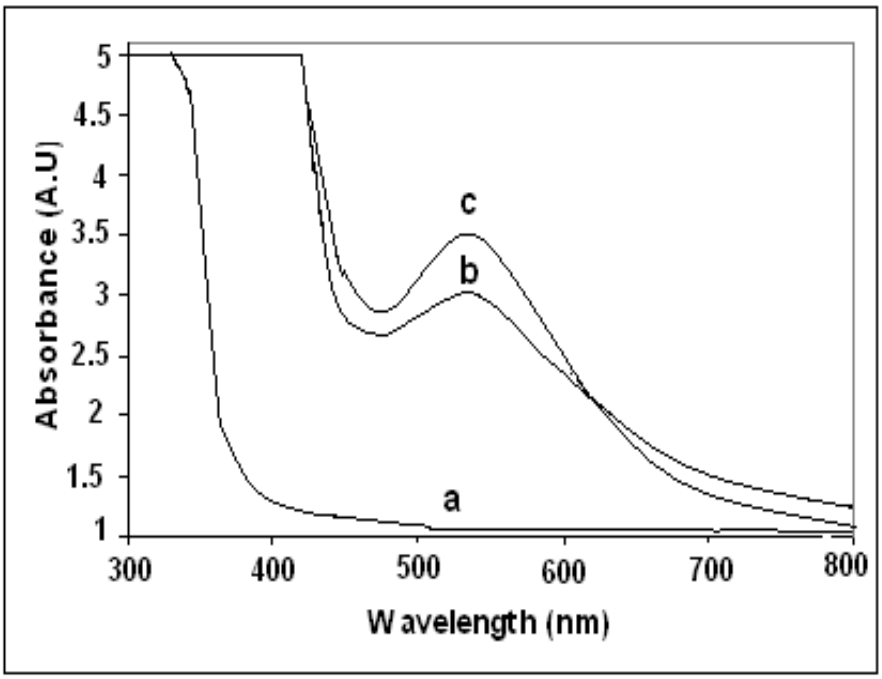

Fig. 4.3 : UV-visible absorption spectra of the a) Ti-peroxide sol b) 1% Au/TiO_2 sol c) 2% Au/TiO_2 sol aged for 4 hrs.

It is also observed that, there is slight red shift in SPR band of Au which is initially at 530 nm (for pure Au colloids) is shifted to 540 nm after addition into the titanium peroxide sol which is attributed to the surrounding TiO_2 medium. The red or blue spectral shift of SPR band depends on the dielectric constant of the embedding medium.[38,39] A strong red shift in the SPR of Ag nanoclusters incorporated in SiO_2 or TiO_2 matrix was reported by Kribig & co-workers[34,36]. The dependence of shift on the chemically differing embedding medium indicates the high sensitivity of SPR band to cluster-matrix interface properties.

Fig.4.4 (Curves a~c) shows the UV-visible spectra of TiO_2, 1% Au/TiO_2 and 2% Au/TiO_2 thin films calcined at 275 ^{0}C respectively. Pure TiO_2 shows an absorption

edge at around 360 nm whereas the 1% Au/TiO_2 shows at 410 nm and 2% Au/TiO_2 at around 450 nm.

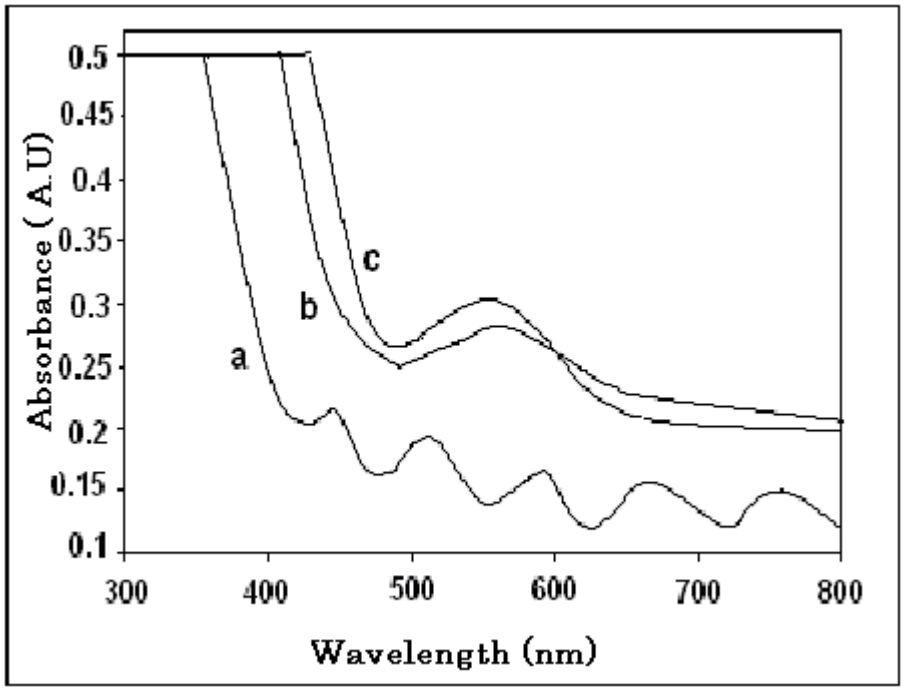

Fig. 4.4 : UV-Visible absorption spectra of the a) Ti-peroxide film b) 1% Au/TiO_2 c) 2% Au/TiO_2 films.

4.3.3 XRD Characterization of Au/TiO_2 photocatalyst

In the Fig.4.5 and Fig.4.6, the X-ray diffraction patterns of 1%Au/TiO_2 and 2%Au/TiO_2 calcined at different temperatures are presented. The curves 'a' in fig. 4.5 and 4.6 show the diffraction patterns of as prepared gel which suggest that the Au as well as titanium peroxide are in amorphous state. This is commonly observed in most samples prepared by sol-gel.

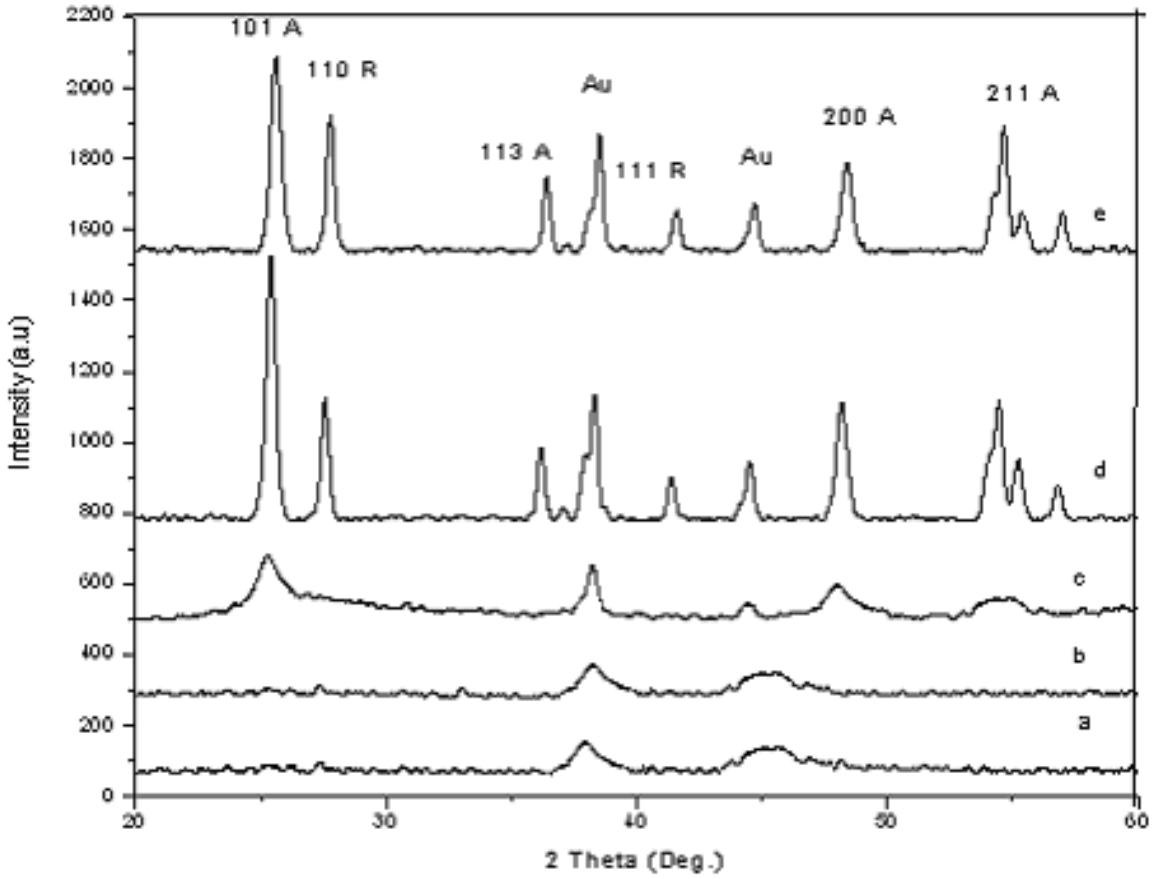

Fig. 4.5 : X-Ray diffraction patterns of the 1% Au/TiO_2 powder a) As prepared b) calcined at 100 ^0C c) calcined at 275 ^0C d) calcined at 400 ^0C and e) calcined at 600 ^0C.

Upon calcination of these samples at various temperature (100-600 ^0C) the crystallization takes place. Curve 'b' in both the figures are for samples calcined at 100 ^0C and it shows no much change in crystallinity. Curve 'c' in both the figures 4.5 and 4.6 corresponds to the samples subjected to calcination at 275 ^0C. All the peaks of these samples are broad in nature and the peaks are mostly of anatase phase of TiO_2 . This shows that the beginning of crystallization starts at or before 275 ^0C.

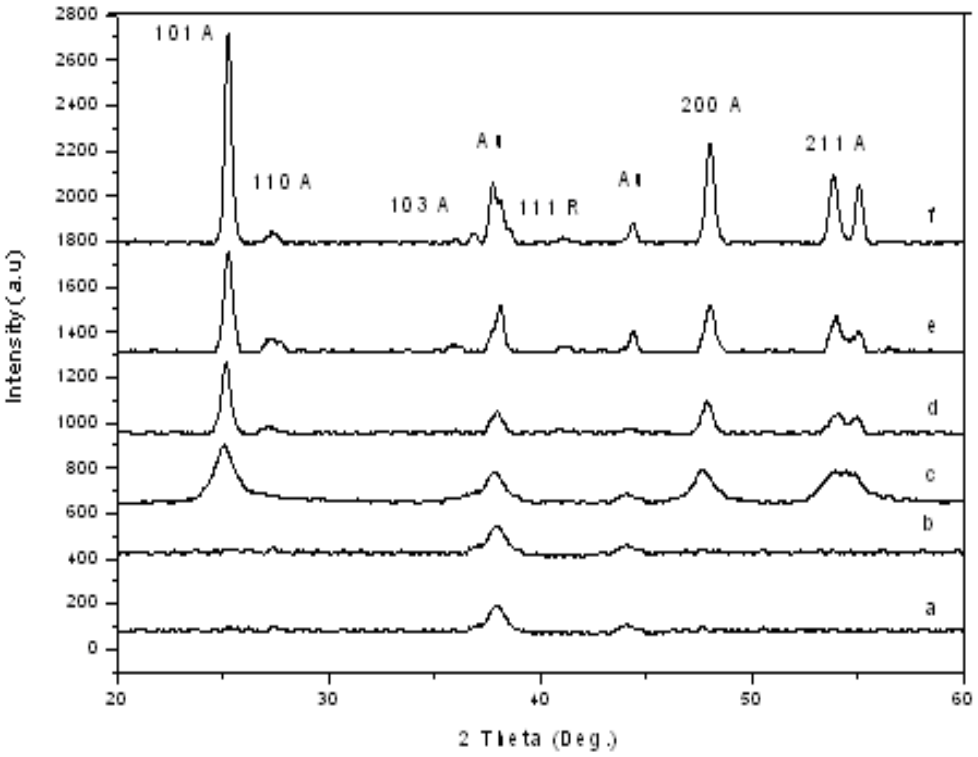

Fig. 4 .6 *:* X-Ray diffraction patterns of the 2% Au/TiO_2 powder a) As prepared b) Calcined at 100 ^{0}C c) Calcined at 275 ^{0}C d) Calcined at 400 ^{0}C e)) Calcined at 500 ^{0}C and f) Calcined at 600 ^{0}C .

The samples calcined at 400 and 500 ^{0}C (curves 'd' & 'e' in fig. 4.5 and 4.6) show a well defined peaks. Along with the peaks of anatase phase the peaks corresponding to rutile phase were also observed in curves 'd, 'e' and 'f ' of figures 4.5 and 4.6. This suggests that the anatase to rutile conversion starts at or before 400 ^{0}C. However in the undoped Ti-peroxide this anatase to rutile transformation takes place at higher temperature (600 ^{0}C). This phase transformation also depends on the amount of Au added, in 1% Au/ TiO_2 (Fig.4.6, curves c - d) the intensity of peaks corresponding to rutile phase was more than 2%Au/TiO_2. This may be attributed to the inhibition of growth of the TiO_2 crystals by surrounding Au atoms. In this system, Au particles are

adsorbed on TiO_2 crystals which restricts the contact of one TiO_2 nanocrystal with other or Au is adsorbed on active faces of rutile phase which ultimately prevents the growth of crystals. Such decrease in rutile phase with increasing concentration of Ag in TiO_2 has been reported by Li et.al.[40]

4.3.4 Thermo-gravimetric analysis

Fig.4.7 shows the TG/DTA curve of 2% Au doped Ti-peroxide (2%Au/TiO_2) gel dried in air at room temperature.

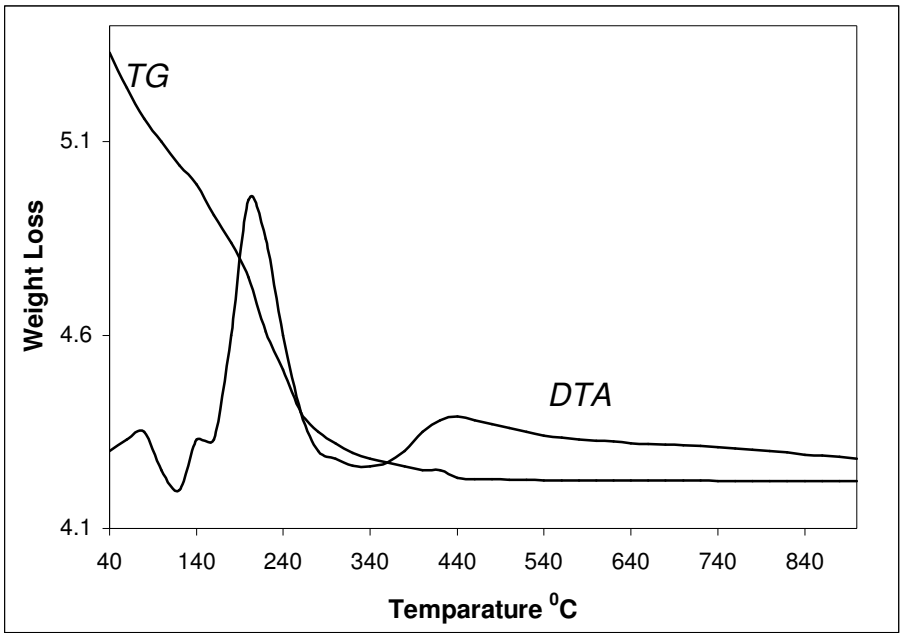

Fig. 4.7: TG/DTA curve of the 2% Au/Ti-peroxide gel dried at room temperature.

In TG curve, at around 100 ^{0}C to 400 ^{0}C a considerable weight loss(28%) is observed which is attributed to the loss of water and transformation of Ti- peroxide to TiO_2. The thermogram (TG/DTA) of 2%Au/Ti-peroxide shows the broad endothermic peak at 100

^{0}C and exothermic peaks at around 200 ^{0}C and 410 ^{0}C. The endothermic peak at 100 ^{0}C is due to the loss of water and other solvents, peak at 200 ^{0}C is due to transformation of Ti-peroxide to crystalline anatase Au/TiO_2 and the peak at 410 ^{0}C is due to the transformation of anatase to rutile phase. In both these results it can be easily pointed out that, the undoped Ti- peroxide shows transformation from peroxide to anatase TiO_2 at 400 ^{0}C whereas the same transformation occurs at 200 ^{0}C in Au/TiO_2. As compared to pure titanium peroxide the crystallization temperature of anatase and rutile phase has been lower in 2%Au/TiO_2. The crystallization of gold starts at 100 ^{0}C and the gold available in the titanium peroxide starts to crystallize at this temperature. The gold crystals may act as seeds for crystallization of TiO_2. This ultimately results in the lowering of crystallization temperature of anatase.

4.3.5 Surface morphology of Au/TiO_2

The particle size, morphology and distribution of Au in TiO_2 films were studied by observing the samples under Transmission Electron Microscope (TEM).

The images of 1%Au/TiO_2, 2%Au/TiO_2 thin films and 1%Au/TiO_2 gel calcined at 275 ^{0}C are as shown in Fig.4.8 (images a, b and c). In the TEM image of 1%Au/TiO_2 (Fig.4.8a) some dark spheroidal particles were observed and the population of these particles increases in 2%Au/ TiO_2 (Fig4.8 b). These dark particles are nothing but the gold particles. It can be seen that, the Au particles are slightly elliptical in shape such elliptical appearance of the Au colloid is typical for particles in metal sols which generally exhibit some polydispersity in both metal colloid particle size and shape.[41,42]

Measurement of several Au particles in the film by TEM indicates that, an average particle size of Au particles in these films is within 15-20 nm range.

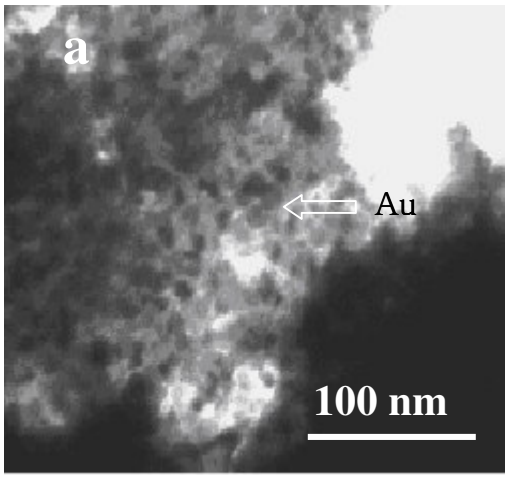

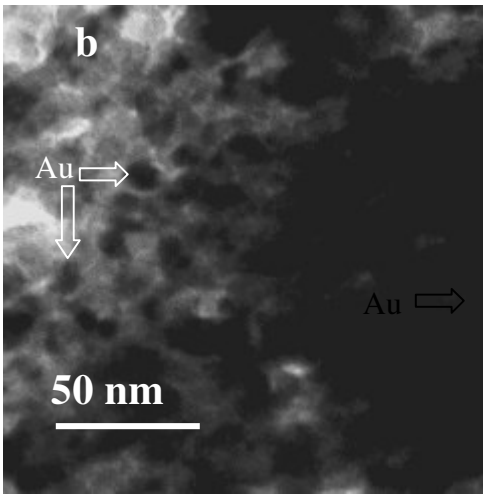

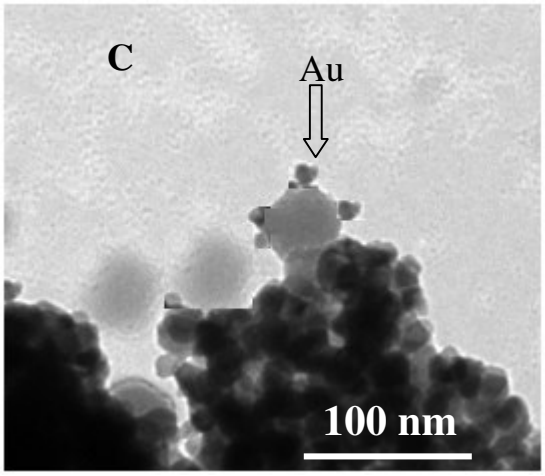

Fig. 4.8 : TEM Images of a) 1%Au/TiO_2 thin film b) 2%Au/TiO_2 thin film prepared using the gel aged for 2 hrs c) 1%Au/TiO_2 gel calcined at 275^0C.

The dark colored small Au nanoparticles on the surface of TiO_2 particle can be seen in sample of 1%Au/TiO_2 gel calcined at 275 ^{0}C. (image 'c') The increase in concentration of Au into the sol increases the particle density of Au as well as small increase in particle size. These particles on the surface of TiO_2 restricts contact of one particle with other and stabilizes the anatase phase in sample containing 2 percent Au. The actual photograph of the films is as shown below. The photograph suggests that, as the concentration of Au in TiO_2 increases there is increase in color of the film.

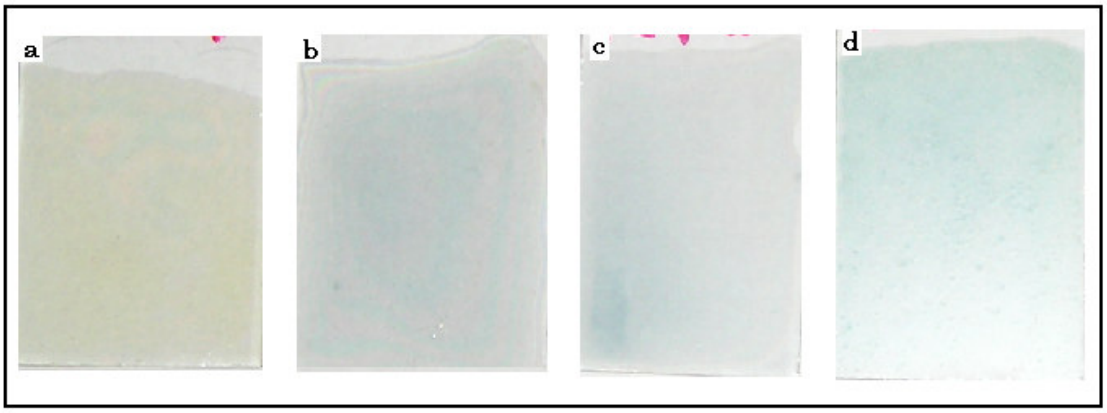

Photograph : Typical photograph of the films prepared on glass plates using sol a) Titanium peroxide, b) 0.5%Au/TiO_2, c) 1%Au/TiO_2 and d) 2%Au/TiO_2.

4.3.6 Photo-catalytic reactions using Au/TiO_2 thin films

The photo-catalytic activity of samples of TiO_2 , 1%Au/TiO_2 and 2%Au/TiO_2 was tested using the quartz reactor as described in chaper.3**.** All the experiment were performed under identical conditions.

In recent investigations the attempt were made to increase the photo-response and photo-catalytic activity of TiO_2 by doping metal ions such as Pt, Au, Ag, Fe, Cu etc in TiO_2 matrix[43-48]. However, the increase in photo-catalytic activity reported was very less. Kamat and co-workers[27] reported that TiO_2 electrode modified by deposition of Au on it using electrophoretic deposition method shows only 10-15% increase in photo-catalytic efficiency. This may be attributed to the improper distribution of Au in the TiO_2 matrix and the interaction of Au with TiO_2. Because in this and most of the other

studies reported, TiO_2 film was prepared first and Au was deposited on the surface of TiO_2 film. So the distribution of Au in TiO_2 as well as the contact between Au particles and TiO_2 may be restricted on the surface of the film. Because of this, the interfacial charge transfer process may not be so efficient which ultimately affects the photo-catalytic activity, as a result no appreciable increase in photo-catalytic activity was observed. To confirm the effect of Au on photo-activity of TiO_2 prepared by titanium peroxide based sol-gel method, we have prepared and used the films of 1%Au/ TiO_2 and 2%Au/ TiO_2 deposited on silica substrates for photo-catalytic decomposition of salicylic acid, methylene blue, methyl orange and phenol.

In the degradation of all these compounds the reaction products were analyzed before and after irradiation using UV-visible spectrophotometer. The residual % concentration of salicylic acid with time of irradiation for sample kept in darkness as well as for 1%Au/TiO_2, and 2%Au/TiO_2 catalysts are shown in fig. 4.9 (Curve a-c). The curve a represents the sample kept in darkness which shows about 12% decrease in concentration in 4 hr it may be due to the physical adsorption of salicylic acid on the surface of catalyst. The b and c suggests that, within 4 hrs there is 95% and 97% degradation of salicylic acid using 1%Au/TiO_2, and 2%Au/TiO_2 catalyst respectively.

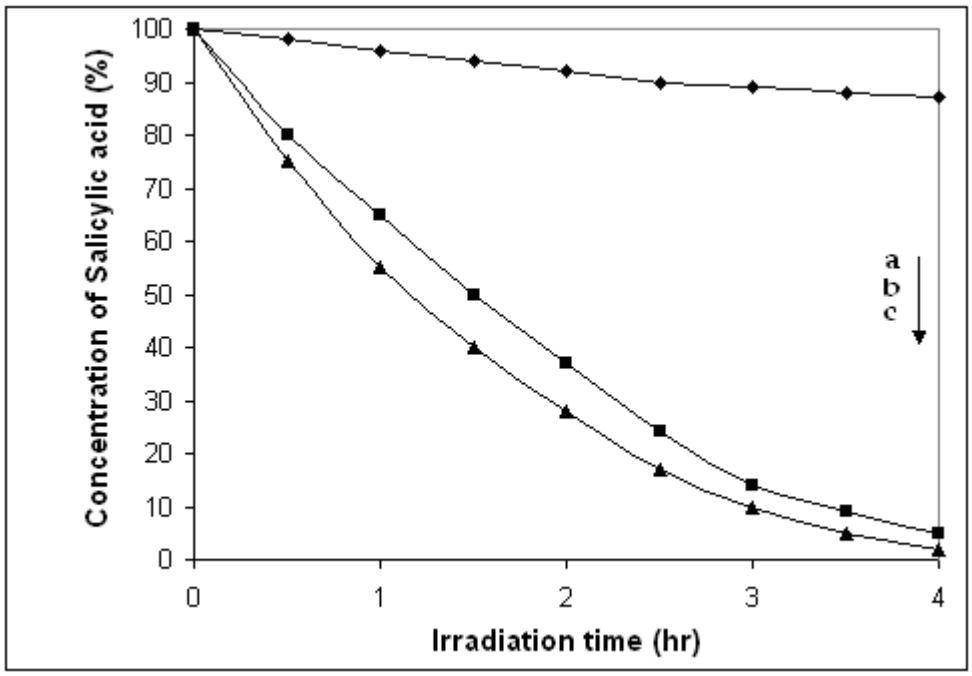

Fig. 4.9 : Change in concentration of salicylic acid using a) 1%Au/TiO_2 in darkness b) 1%Au/TiO_2 and c) 2%Au/TiO_2 thin films.

Similarly photo-catalytic degradation of methylene blue and methyl orange was also studied using these catalysts and the plot of change in concentration with time is shown in fig. 4.10 and 4.11 respectively. The curves b and c of fig.4.10 suggests that, within 4 hrs there is 92% and 96% degradation of methylene blue using 1%u/TiO_2 and 2%Au/TiO_2 catalyst respectively. In the case of methyl orange degradation, the fig.4.11 suggests that there is 92% and 93% degradation of methyl orange within 4 hrs.

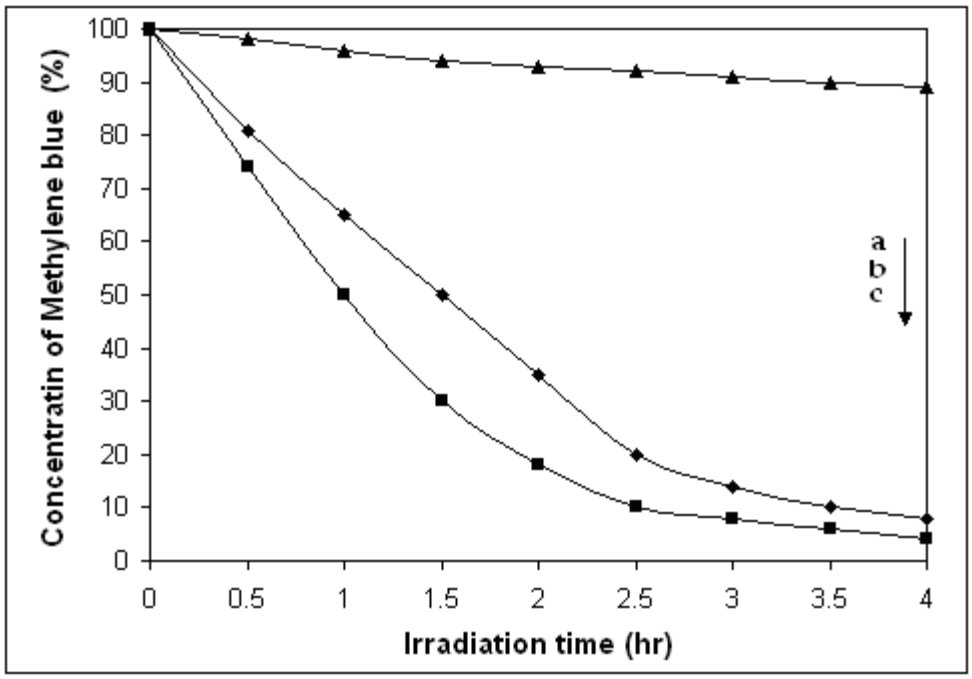

Fig. 4.10 : Change in concentration of methylene blue using a) 1%Au/TiO_2 in darkness, b) 1%Au/TiO_2 and c) 2%Au/TiO_2 thin films. .

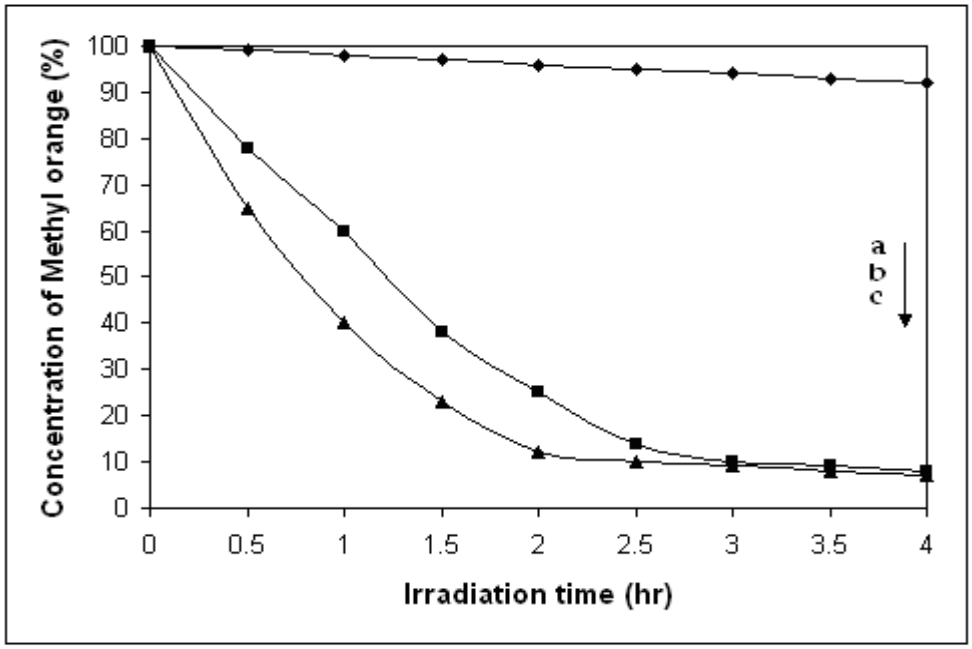

Fig. 4.11 : Change in concentration of methyl orange using a) 1%Au/TiO_2 in darkness, b) 1%Au/TiO_2 and c) 2%Au/TiO_2 thin films.

In the photo-catalytic reaction of phenol, the typical UV-visible spectra of the reaction products of the sample of phenol irradiated for 0, 2 and 4 hrs. is as shown in fig.4.12. The change in concentration of phenol with time using 1%Au/TiO_2 and 2%Au/TiO_2 catalyst has been plotted and is as shown in fig.4.13. The concentration of phenol gradually decreases with time of irradiation and after 4 hr it reaches to very low level.

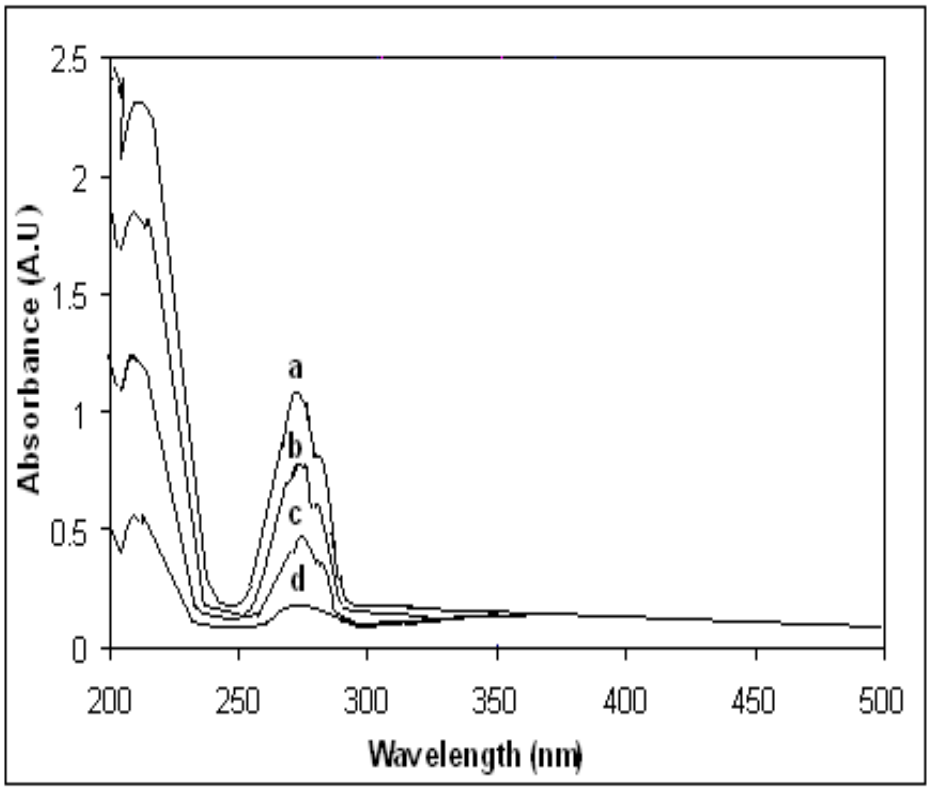

Fig. 4.12 : UV-visible spectra of reaction product of phenol (6.0×10^{-5} M) solution photo-catalyzed by thin films of 2%Au/TiO_2 on glass helix, after irradiation of sample for a) 0, b) 1, c) 2 and c) 4 hr.

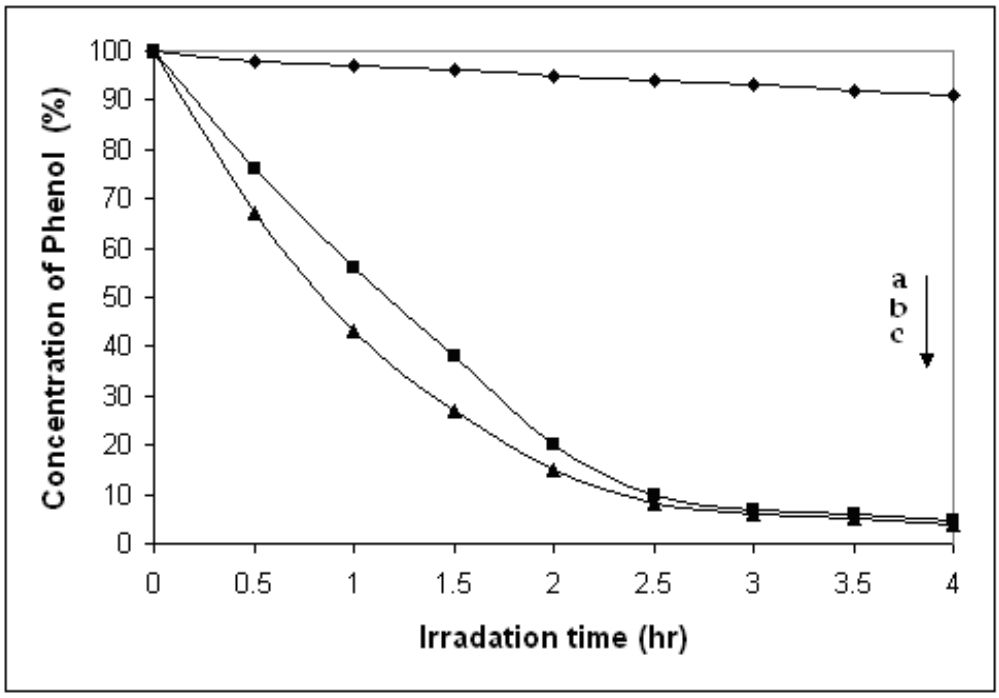

Fig. 4.13 : Change in concentration of phenol using a) 1%Au/TiO_2 in darkness, b) 1%Au/TiO_2 and c) 2%Au/TiO_2 thin films calcined at 275 ^{0}C.

It is well known that photo-catalysis experiments follow the Langmuir-Hinshelwood kinetics[49-50], where rate of reaction (R) is directly proportional to the surface coverage(θ)

$$R = -dc/dt = k_r \theta = k_r KC / (1 + KC) \qquad (4.1)$$

Where, k_r is the rate constant, K is the adsorption coefficient of the reactant and C is the reactant concentration. In the case of very low concentration of reactant in solution the product of K and C (KC) is negligible with respect to unity, so the Eq. 3.09 shows first order kinetics. The integration of Eq. 3.09 with limit condition that at the start of irradiation, t = 0, the concentration is the initial one, $C = C_0$, gives equation,

$- \ln (C / C_0) = k't$ (4.2)

where, k' is the apparent first order rate constant. The rate constant can be obtained by linear regression.

The rate of reaction in photocatalytic degradation of salicylic acid, methylene blue, methyl orange and phenol over 1%Au/TiO_2 and 2%Au/TiO_2 are plotted in fig.4.14, 4.15, 4.16 and 4.17 respectively. In the table 4.01 and 4.02, the kinetic parameters for the respective reactions are summarized

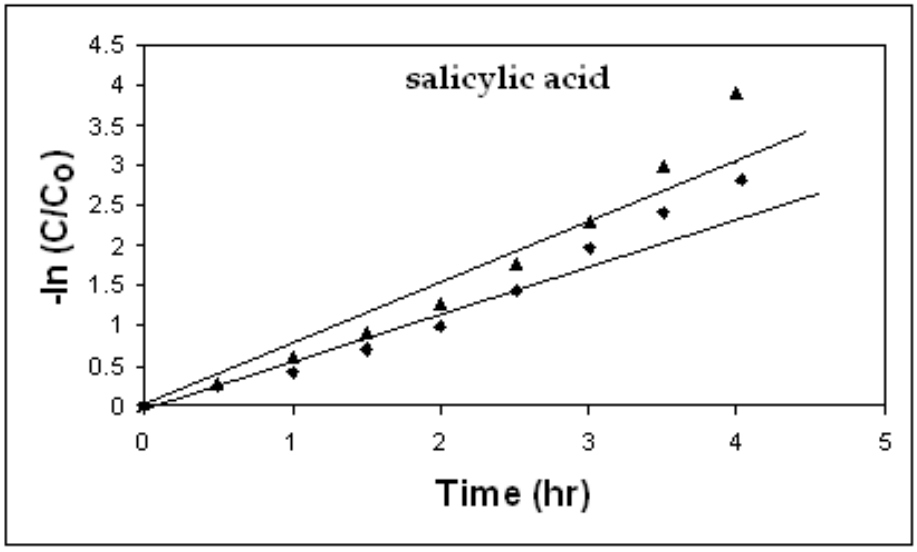

Fig. 4.14 : The first order kinetics of salicylic acid (SA) degradation using thin films A) 1%Au/TiO_2 and B) 2%Au/TiO_2 calcined at 275 ^{0}C.

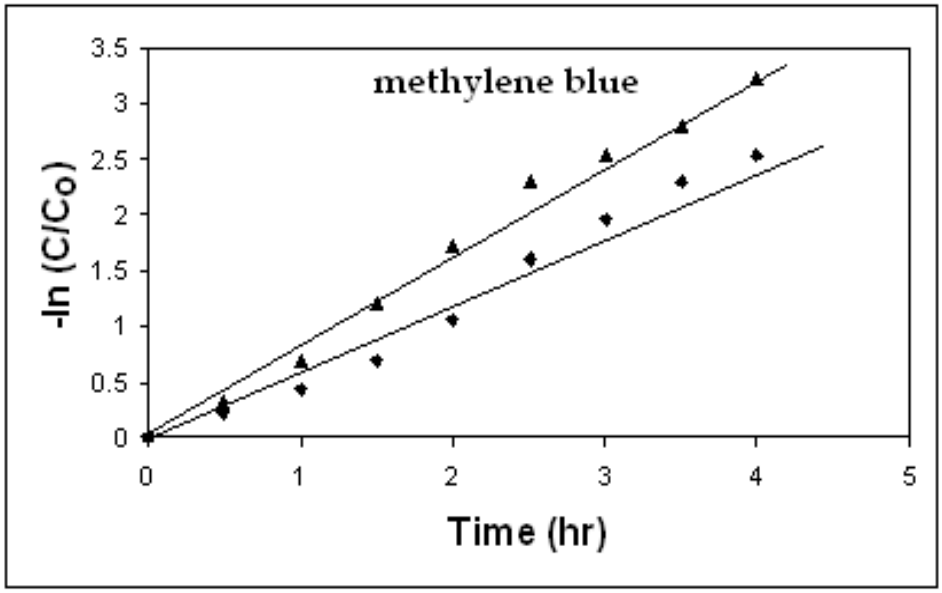

Fig. 4.15 : The first order kinetics of methylene blue (MB) degradation using thin films A) 1%Au/TiO_2 and B) 2%Au/TiO_2 calcined at 275 ^{0}C.

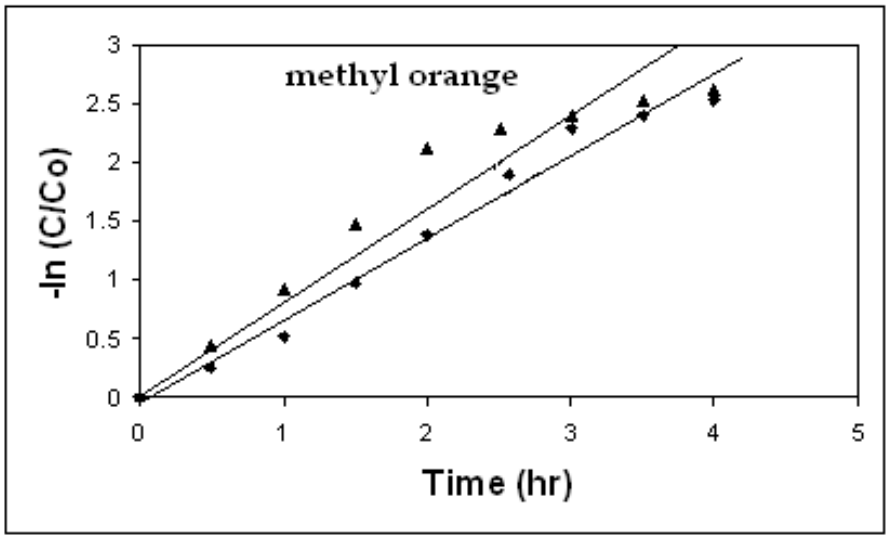

Fig. 4.16 : The first order kinetics of methyl orange (MO) degradation using thin films a) 1%Au/TiO_2 and b) 2%Au/TiO_2 calcined at 275 ^{0}C.

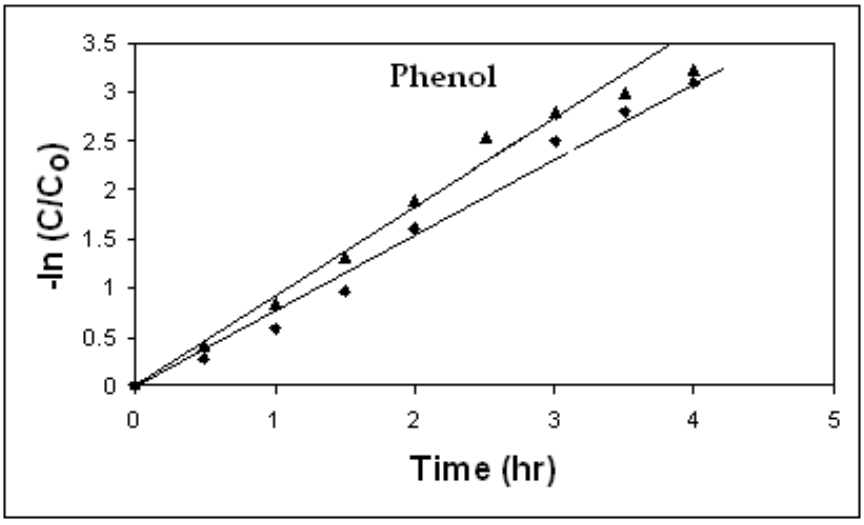

Fig. 4.17 : The first order kinetics of phenol (Ph) degradation using thin films a) 1%Au/TiO_2 and b) 2%Au/TiO_2 calcined at 275 ^{0}C.

The results of our study show that there is appreciable increase in photo-catalytic activity of Au/TiO_2 (1.3-3 times). This is because, in our process Au is doped in TiO_2 sol and then films were deposited by using this sol, so the distribution of Au into TiO_2 in sol, films and powder obtained after drying the gel is uniform and the interfacial interaction as well as charge transfer between Au and TiO_2 will be better as compared to films prepared by method reported earlier. This results positively on increasing the photo-catalytic activity. From the kinetic study, the parameters such as percentage mineralization after 1 hour of irradiation, rate constant and time required for complete mineralization were obtained (Table.4.1 and 4.2).

Table.4.1

Kinetic parameters and photocatalytic efficiency of films towards the degradation of SA, MB, MO and Ph in sun light using 1%Au/TiO_2 catalyst.

	SA	MB	MO	Ph
% degradation in 1 hr	35	33	40	44
Time required for mineralization(90%) (hr)	3.5	3.5	3.0	2.5
Rate constant (min^{-1})	0.01003	0.0082	0.012	0.01243

Table.4.2

Kinetic parameters and photocatalytic efficiency of films towards the degradation of SA, MB, MO and Ph in sun light using 2%Au/TiO_2 catalyst.

	SA	MB	MO	Ph
% pollutant remain after 1 hr	45	50	60	57
Time required for complete (90%) mineralization (hr)	3	2.5	2.5	2.25
Rate constant (min^{-1})	0.01279	0.0090	0.01307	0.01527

From the above results it is observed that, there is an enhancement in photocatalytic degradation rate by addition of 1-2% of Au in TiO_2. In degradation of SA, the rate constant observed for pure TiO_2 films, 1%Au/TiO_2 and 2%Au/TiO_2 were 0.00423 min^{-1}, 0.01003 min^{-1} and 0.01279 min^{-1} respectively. So as compared to pure TiO_2 thin film

photocatalyst, an enhancement in activity of 2.4 and 3 times respectively for 1%Au/TiO_2 and 2%Au/TiO_2 was observed. For degradation reactions of MB the rate constants obtained were 0.0063 min^{-1}, 0.0082 min^{-1} and 0.0090 min^{-1} for TiO_2 films, 1%Au/TiO_2 and 2%Au/TiO_2 respectively. The observed enhancement of 1.3 and 1.5 in rate of reaction for 1%Au/TiO_2 and 2%Au/TiO_2 than undoped TiO_2 thin films. The kinetic study of the degradation of MO gives rate constant values 0.0048 min^{-1} 0.012 min^{-1} and 0.01307 min^{-1} for TiO_2 films, 1%Au/TiO_2 and 2%Au/TiO_2 respectively whereas Ph degradation reaction gives rate constant values of 0.0060 min^{-1}, 0.01243 min^{-1} and 0.01527 min^{-1} for reactions using TiO_2 films, 1%Au/TiO_2 and 2%Au/TiO_2 catalyst respectively. In the rate of MO degradation an enhancement of 2.5 and 2.7 times was observed whereas for Ph degradation it was 2.07 and 2.5 times. This suggests that reaction rate has been enhanced by doping Au into the TiO_2 matrix. The rate constant obtained by linear regression method gives an idea regarding the increase in rate of reaction.

For the photo-catalytic reactions using Au/TiO_2 photocatalyst the following mechanism has been proposed

$$Au/TiO_2 \xrightarrow{h\nu} TiO_2\,(e^- + h^+)\,Au \qquad (4.5)$$

$$h^+ + OH^-_{ad} \longrightarrow \bullet OH_{ad} \qquad (4.6)$$

$$h^+ + H_2O_{ad} \longrightarrow \bullet OH_{ad} + H^+ \qquad (4.7)$$

$$e^- + O_2 \longrightarrow \bullet O_2^- \qquad (4.8)$$

The photo-generated holes at the valence band migrates to the surface and combines with OH^- adsorbed on TiO_2 surface (as per equation 4.5) and results in the formation of OH radicals. The electrons in conduction band, combines with O_2 (as per equation. 4.8) and forms O_2^- radical. Both these radicals are strong oxidants which oxidize the organic molecules landed on the surface of TiO_2 resulting the formation of intermediate organic species and subsequently complete oxidation of these species to CO_2, SO_2 NO_2 and H_2O as per the following scheme of phenol degradation and schemes proposed for other compounds in chapter II & III .

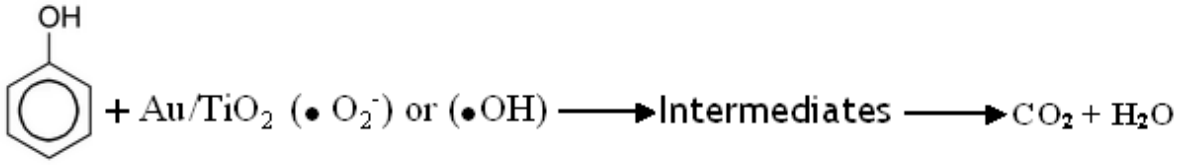

The increase in photo-activity may be attributed to the effect of Au in following ways; increased absorption in visible region by intercalation of Au in titania matrix and the electron scavenging by Au(III) ions and the decrease in fermi level to more negative side subsequently improving in interfacial charge transfer process at the TiO_2 interface by Au^0 particles. It is also proposed that, electron in conduction band migrates to the Au on the surface of photo-catalyst and improves the charge separation process. Further regarding electron transfer process at the interface of TiO_2 and the interfacial contact between Au on TiO_2, it is assumed that, the contact is not a ohmic type but a schottky barrier type so the electron after excitation migrates to metal through conduction band driven by an electric field, as a result the charge separation becomes easier[51] which

ultimately minimizes the electron hole recombination and helps in improving the photo-catalytic efficiency of the catalyst. Therefore it is the combined effect of all these processes at the surface of semiconductor films which results in overall increase in photo-activity of TiO_2. However, it is also reported that, the doping at certain concentration level is beneficial for improving photo-activity as well as efficiency of catalyst and if the Au concentration is increased further decrease in photo-activity is observed. [52,53] We have prepared Au/TiO_2 samples containing 1% and 2% Au/TiO_2 used it for photo-catalytic study but in our samples no such effect has been observed for these samples. In Ti-peroxide doping of Au more than 2% (by weight) changes the sol-gel behavior and perfect transparent gel could not be obtained, hence it was not possible for us to study the effect of Au loading at higher level.

The effect of calcination temperature on the catalytic behavior of the doped catalyst was studied by using the catalyst powder calcined at various temperatures.

Table.4.3

Effect of calcination temperature on the catalytic activity of 2% Au/TiO_2 photo-catalyst

	As prepared 2%Au/TiO_2	2%Au/TiO_2 Calcined at 275 ^{0}C	400 ^{0}C	500 ^{0}C
% Phenol degradation after 1 hr (Approx.)	9-12	50-57	43-47	38-40
Time required for complete Mineralization (hr)	-----	2.5	3.0	3.5

From the catalytic study (Table.4.3) it was observed that, among the Au/TiO_2 catalyst samples, the catalyst calcined at 275^0C shows highest catalytic activity as compared to samples calcined at higher temperatures. This may be attributed to the formation of photo-catalytically most active pure anatase phase at this temperature and the particle size. At lower temperature the particle growth will be limited so ultimately the surface area as well as number of active sites will be more hence the photo-catalytic activity obtained is more than as prepared Au/TiO_2 and catalyst calcined at higher temperatures.

In most studies, the aim of doping the transition metal or noble metal ions was to improve the photo-activity as well as efficiency of photo-catalyst. However it is suspected that the deactivation of catalyst surface in metal ion doped TiO_2 may be faster than undoped. Because the generation of electron-hole pair at the TiO_2 surface and subsequently formation of hydroxyl radicals and $\bullet O_2^-$ radicals during the photo-catalytic reaction may oxidize the metal(Au) nanoparticles[27,53] since both are very strong oxidants. As a result the surface of Au/TiO_2 may get deactivated faster as compared to undoped TiO_2. This will adversely affect the life of the catalyst so the increase in activity of the TiO_2 will be for short span and the catalyst can not be used for long term. This restricts the applicability of doped catalyst, such type of the decrease in photo-catalytic activity was reported earlier.[52] We have conducted several experiments on the decomposition of phenol in sunlight using the same catalyst in order to test the stability of the catalyst.

Table. 4.4

Stability of 2%Au/TiO_2 photo-catalyst for degradation of Phenol (50 mg/l) in sunlight.

Number of cycle	% Phenol degradation after 1 hr	Time required for complete degradation
1	31.5	4.5
2	31	4.5
3	30.7	4.55
4	30.1	4.6
5	29.4	4.6

After each degradation reaction the catalyst was separated, dried at 100 ^{0}C and used again. Results of this study are as shown in Table.4.4. The results suggests that after repeated use of the catalyst for five consecutive experiments, no such appreciable decrease in catalytic activity was observed. So the deactivation of our catalysts is very slow and it can be used for many times in catalytic reactions

4.4 Conclusions

A simple method for deposition of thin films of Au/TiO_2 on various substrates such as soda lime glass plates, glass helix and silica rashig rings by sol-gel dip coating has been developed. The films were modified by addition of colloidal Au solution in titanium peroxide sol to increase the photoresponse as well as photocatalytic activity of TiO_2 in visible light. By addition of 1-2 percent Au the absorption wavelength of TiO_2 was shifted from 340 nm in UV to 450 nm in visible region. The thermal and structural

characterization shows that crystallization temperature of anatase and rutile phases of TiO_2 has been decreased due to addition of Au. The Au/TiO_2 thin films with uniform distribution of Au in TiO_2 can be prepared using this technique. The increase in photoresponse was tested by photocatalytic decomposition of aqueous solutions of salicylic acid, methylene blue, methyl orange and phenol in sunlight. Doping 1-2 percent Au in TiO_2 improves the photocatalytic activity by 1.3-3.0 times compared to undoped TiO_2 catalyst. The stability of Au/TiO_2 was tested by using this catalyst for five consecutive experiments and shows no much change in activity. The photocatalytic activity of Au/TiO_2 thin film catalyst calcined at various temperatures shows that films calcined at 275 ^{0}C were found to more active towards the degradation of organic compounds than that of calcined at higher temperatures.

References

1. B.Kraeutler, A. J. Bard, *J. Am. Chem. Soc.* **1978**, *100*, 4317.
2. Y. Nosaka, K. Norimatsu, H. Miyama, *Chem. Phys. Lett.* **1984**, *106*, 12.
3. R. Baba, S. Nakabayashi, A. Fujishima, K. Honda, *J. Phys. Chem.* **1985**, *89*, 1902.
4. A. Heller, *Nato Asi Ser., Ser. C* **1986**, *15*.
5. K. Kalyanasundaram, M. Graetzel, E. Pelizzetti, *Coord. Chem. Re*V. **1986**,*69*, 57.
6. A. Henglein, *Chem. Re*V. **1989**, *89*, 1861.
7. P. V. Kamat, *Pure Appl. Chem.* **2002**, *74*, 1693.
8. P. V. Kamat, *J. Phys. Chem. B* **2002**, *106*, 7729.
9. P. V Kamat, M. Flumiani, A. Dawson, *Colloids Surf., A* **2002**, *202*, 269.

10. P. V. Kamat, D. Meisel, *Curr. Opin. Colloid Interface Sci.* **2002**, *7*, 282.

11. J. Z. Zhang, *Acc. Chem. Res.* **1997**, *30*, 423.

12. K.George Thomas, P. V. Kamat, *Acc. Chem. Res.* **2003**, *36*, 888.

13. P.Mulvaney, F. Grieser, D. Meisel, *Langmuir* **1990**, *6*, 567.

14. I. Pastoriza-Santos, D. S. Koktysh, A. A. Mamedov, M. Giersig, N. A. Kotov, L. M. Liz-Marzan, *Langmuir* **2000**, *16*, 2731.

15. J. Zhang, N. Coombs, E. Kumacheva, Y. Lin, E. H. Sargent, *Ad*V. *Mater.* **2003**, *15*, 1756.

16. I. Willner, B. Willner, *Pure Appl. Chem.* **2001**, *73*, 535.

17. M. ayats, A. B. Kharitonov, S. P. Pogorelova, O. Lioubashevski, E. Katz, I. Willner *J. Am. Chem. Soc.* **2003**, *125*, Web release.

18. P. V.; Kamat, D. *C. R.* Meisel, *Chimie* **2003**, *6*, 999.

19 Y. Nosaka, Y. Ishizuka, H. Miyama, *Ber. Bunsen-Ges. Phys. Chem.* **1986**, *90*, 1199.

20. A. Henglein, *Ber. Bunsen-Ges. Phys. Chem.* **1995**, *99*, 903.

21. S. Ikeda, N. Sugiyama, B. Pal, G. Marci, L. Palmisano, H. Noguchi, K. Uosaki, B. Ohtani, *Phys. Chem. Chem. Phys.* **2001**, *3*, 267.

22. A. Dawson, P. V. Kamat, *J. Phys. Chem. B* **2001**, *105*, 960.

23. E. Szabo-Bardos, H. Czili, A. Horvath, *J. Photochem. Photobiol., A* **2003**, *154*, 195.

24. Y. Nakato, M. Shioji, H. Tsubomura, *Chem. Phys. Lett.* **1982**, *90*, 453.

25. Y. Nakato, K. Ueda, H. Yano, H. Tsubomura, *J. Phys. Chem.* **1988**, *92*, 2316.

26. N. Chandrasekharan, P. V. Kamat, *J. Phys. Chem. B* **2000**, *104*, 10851.

27. V. Subramanian, E. Wolf, P. V. Kamat, *J. Phys. Chem. B* **2001**, *105*, 11439.

28. A. J. Bard, M. A. Fox, *Acc. Chem. Res.* **1995**, *28*, 141.

29. G. C. Bond, P. A. Sermon, J.C.S. Chem Comm. 1973, 444.

30. G. C. Bond, P. A. Sermon, Gold Bull. 1973, 6, 102.

31. D. Y. Cha, G. Parravano, J. Catal. 1970, 18, 200.

32. S. Galvano, G. Parravano, J. Catal. 1978, 55, 178.

33. V. Subrmaniam, E. Wolf, P. V. Kamat J. Am. Chem. Soc. 2004, 126, 4943.

34. U. Kriebig, M. Vollmer, Optical Properties of Metal Clusters, Springer, Berlin, 1995.

35. M. M. Alvarez, J. T. Khoury, T. G. Schaaff, M. N. Shafigullin, I. Vezmar, R. L. Whetten, J. Phys. Chem. B 101 (1997) 3706.

36. U. Kriebig, M. Gartz, A. Hilger, H. Hovel, in E. Pelizzetti (Ed), Fine Particles Science and Technology, Kluwer, Dordrecht, 1996, pp 499-515.

37. H. Zang, J. Banfield, J. Mater. Chem. 8(9), (1998) 2073.

38. Khlebtsov N. G, Bogatyrev V.A, Dykman L. A, Mel'nikov A. G Opt. Spectrosc. 80 (1996) 128.

39. M. J. Bloemer, J. W. Haus, P. R. Ashley, J. Opt.. Soc. Am. B 1990, 7 790.

40. S. Rengaraj, X. Z. Li, J. Mol. Catal. A : Chemical 2006, 243, 60.

41. Khlebtsov N. G, Bogatyrev V.A, Dykman L. A, Mel'nikov A. G Opt. Spectrosc. 80 (1996) 128.

42. M. J. Bloemer, J. W. Haus, P. R .Ashley, J. Opt. Soc. Am. B 7 (1990) 790.

43. H.I. Tseng, W.C Chang, J.C.S. Wu. Appl. Catal. B: Environ 2003, 37,37.

44. H.I. Tseng, J.C.S. Wu , H.Y. Chou, J. Catal. 2004, 221,432.

45. T. Lopez, R . Gomez, G. Pecci, P. Reyles, X. Bokhimi, O. Navaro, Mater. Lett. 1999, 40, 59.

46. M. Stir, T. Traykova, R. Nicula, E. Burkel, C. Baethtz, M. Knapp, Nucl. Instrum. Meth. Phys.Res. B 2003, 199, 59.

47. F.B Li, X.Z. Li. Appl. Catal. A: Gen 2002, 228,15.

48. R. Phani, S. Santucci, Mater. Lett. 2001,50, 240.

49. J. Peral, D.F. Ollis J. Catal. 1992,136,554.

50. A.V. Vorontsov, E.N. Kurkin, E.N. Savinon. J. Catal. 1999, 186, 318.

51. Y. Nosaka, K. Norimatsu, H. Miyama, Chem. Phys. Lett. 106 (1984) 128.

52. I. M. Arabatzis, T. Stergiopoulos, D. Andreeva, S. Kotova, S. G. Neophytides, P. Falaras, J. Cat. 220 (2003) 127.

53. V. Subramanian, E. Wolf, P. V. Kamat, Langmuir 19 (2003) 960.

CHAPTER-V

SUMMARY AND CONCLUSIONS

SUMMARY

Growing social concern about the impact of different chemicals on the environment has focused attention on finding ways for more effective pollution abatement methods. Following this one of more promising techniques is to use a photo-catalytic route to oxidize such chemicals. Considerable work on the TiO_2 mediated heterogeneous photo-catalysis has been reported but so far no other substance superior than TiO_2 has been found as a photo-catalyst. TiO_2 is superior than other substances, because of its high photo-catalytic activity and chemical stability in aqueous solution under UV light irradiation. For the purpose of solving the environmental problems, the highly dispersed fine particles have been mostly used in various types of photo-reactors. But the separation of suspended TiO_2 after each reaction is the main problem. This can be avoided by using the TiO_2 thin films. TiO_2 absorbs only 3-5% energy of the solar spectrum and the need of an ultraviolet (UV) excitation source, restricts its technological utility for limited applications. For widespread applications, TiO_2 photo catalyst effective in solar light or light in the visible region of the solar spectrum needs to be developed as future generation photo catalytic material. The efficiency of TiO_2 can be

increased by modification of its surface structure and increasing the photo response to visible region.

The plan of this work was to develop a method for preparation of TiO_2 and modified TiO_2 thin film photocatalyst by a novel sol-gel dip coating process using titanium peroxide as a titanium dioxide precursor. Characterization of prepared thin film photocatalyst by various analytical techniques and use of these films for photodegradation of organic impurities in water under UV light and visible light/sunlight.

The thesis consists of the preparation of modified titanium dioxide thin films for photocatalytic applications which have been tested for the degradation of various organic impurities such as salicylic acid, methylene blue , methyl orange and phenol in presence of UV and visible radiation. The films of pure titanium oxide and titanium dioxide modified with, polyethylene glycol (PEG-TiO_2), Fe (Fe/TiO_2) and Au (Au/TiO_2) were prepared by sol-gel dip coating technique using titanium peroxide as a precursor. Using this method we were able to prepare improved titanium dioxide films with good homogeneity, greater surface area and higher photocatalytic activity.

The thin films were tested for photocatalytic degradation of organic pollutants. The photodegradation reactions of salicylic acid, methylene blue, methyl orange and phenol have been studied.

The main advantage of this sol-gel process is that, it is aqueous based. Unlike in other sol-gel methods reported earlier, where organic vapors are released in atmosphere, in this sol-gel process no organic vapors are released in atmosphere during the aging

and drying process. Apart, this sol-gel dip coating process has many advantages over other thin film deposition techniques such as, sol gets easily anchored to the substrate, the method is easy in operation and cheap, the films obtained are porous in nature and this method can be utilized for coating the substrate having complex surface. The present work has been organized in the following manner.

1) The titanium peroxide based sol-gel dip coating has been studied in detail. The change in viscosity of the sol containing various concentrations of Ti has been studied. In this system the solvent is water, hence the increase in viscosity is slow which helps in the deposition of films at various viscosities The films deposited in the viscosity range of 300-6000 cps are uniform with good adhesion to the substrate and the films of thickness of 65-200 nm can be deposited. In pure titanium peroxide based sol-gel method, the film thickness of TiO_2 can be adjusted by coating a viscous sol of given viscosity in a single attempt. In the second attempt to increase the thickness the sol does not adhere to the substrate. In order to improve the adhesion for multiple coating cycles, PEG has been added into the titanium peroxide solution. The concentration of PEG has been optimized to get films with good adhesion and porosity.

The UV-visible spectroscopic characterization of the thin film shows an optical absorption in the range of 305-340 nm for films deposited using a gel aged for 8-24 hrs. The absorption edge shows red shift with aging time because of increased film thickness as well as particle size of TiO_2. The XRD analysis of the as prepared gel dried at 100 ^0C shows that titanium peroxide is amorphous whereas the dried gel powder calcined

at 200-500 ^{0}C shows characteristic peaks of anatase phase. The sample calcined at 600 ^{0}C shows few week peaks of rutile phase along with anatase suggesting the beginning of anatase to rutile transformation. FTIR spectra show that TiO_2 film has high surface hydroxyl groups and the film of PEG-TiO_2 shows higher hydroxyl content than pure TiO_2 films. The surface area analysis of the TiO_2 dried and activated gel was around 118 m^2/g which is higher than TiO_2 powder obtained by other techniques and it decreases with increase in calcination temperature.

The suitability of the films was tested by using these films for degradation of various compounds such as salicylic acid, methylene blue, methyl orange and phenol. The films calcined at 500 ^{0}C show excellent catalytic activity towards the complete degradation of these compounds. The films modified with PEG (PEG-TiO_2) shows 1.2-1.5 times enhancement in activity.

2) TiO_2 absorbs the light of wavelength less than 400 nm, restricting its catalytic activity. In order to enhance the same, the doping of TiO_2 with Fe has been studied. In this method, effect of Fe addition on sol-gel behavior, optimum concentration of Fe, and change in viscosity of Fe/TiO_2 sol with time have been studied. It was observed that, it is possible to add upto 2% Fe in TiO_2 (by weight) in this system. For preparation of Fe/TiO_2 sol containing more than 2%Fe (3-4% Fe/TiO_2), the polyethylene glycol (PEG) has been added into the sol before gel formation. The optimum concentration of PEG into Fe/TiO_2 and its effect on the sol-gel behavior has been studied and it was observed that 0.6g PEG is required for preparation of Fe/TiO_2 sol containing 4% Fe in

TiO_2. The addition of PEG not only improves the sol-gel behavior of Fe/TiO_2 sol but also improves the adhesion of film therefore this sol can be used for multiple coating cycles for increasing the film thickness. The film thickness can be increased from 65nm to 155-160 nm by coating substrate with three repeated coating cycles. Thin films of $2\%Fe/TiO_2$, PEG-$2\%Fe/TiO_2$, and PEG-$4\%Fe/TiO_2$ have been prepared using this process.

The UV-visible characterization of the PEG-Fe/TiO_2 containing 1-4% Fe shows a red shift in absorption edge. There is a shift from 340nm in UV (pure TiO_2) to 460 nm in visible (PEG-$4\%Fe/TiO_2$) range. It is believed that the shift in absorption edge is due to insertion of Fe in TiO_2 structure since the extent of shift is dependent on concentration of Fe added into TiO_2. The X-ray characterization shows that as prepared Fe/TiO_2 is amorphous and the sample need to be calcined for the crystallization of TiO_2. The sample calcined at 250 ^{0}C shows a prominent peak of 101 plane of anatase type of phase and all other characteristic peaks of anatase phase. The sample heated at 500 ^{0}C shows weak peaks corresponding 110 plane of rutile along with anatase phase. SEM characterization of the samples shows that films of pure Fe/TiO_2 are having cracks whereas films containing 0.3g and 0.6g PEG/ g of TiO_2 are porous with granular texture.

The films of pure Fe/TiO_2 and PEG-Fe/TiO_2 containing 1-4%Fe have been tested for degradation salicylic acid, methylene blue, methyl orange and phenol in sunlight. For Fe/TiO_2 and PEG-Fe/TiO_2 an enhancement of 1.2 – 2.6 times in activity of catalyst compared to pure TiO_2 thin films has been observed.

3) In continuation of our effort to increase photoresponse and photocatalytic activity, we have doped titanium peroxide sol with Au^{3+} ions as well as colloidal Au particles. The addition of Au^{3+} into titanium peroxide sol hinders the formation of transparent gel and it results in the formation of turbid precipitate. To overcome this problem, the Au metal colloidal solution has been used for doping. The addition of nanosized Au colloids at 0.5-2% (by weight) does not show much change in sol-gel behavior of titanium peroxide but at higher concentrations the precipitate of hydroxide starts to separate from the gel.

The UV-visible characterization of Au/TiO_2 shows a red shift in absorption edge. The films of pure TiO_2 shows absorption edge at 350 nm whereas the $1\%Au/TiO_2$ and $2\%Au/TiO_2$ show absorption edge at 410 and 450 nm respectively. In addition to this a peak corresponding to Au^0 (SPR) at around 540 nm is also observed in both the samples. The XRD characterization of as prepared $1\%Au/TiO_2$ and $2\%Au/TiO_2$ samples are amorphous whereas the samples calcined at 275^0C are crystalline with peaks of pure anatase phase. The samples of $1\%Au/TiO_2$ calcined at 400^0C and 600^0C shows intense peaks of both anatase and rutile phase whereas the $2\%Au/TiO_2$ calcined at same temperature shows predominantly the peaks of anatase and the peak of 110 rutile is very weak. Both the samples show that there is decrease in crystallization temperature of both the phases but increase in Au content in TiO_2 favors the formation of anatase phase.

The surface morphology using TEM analysis shows uniform distribution of spheroidal Au particles in TiO_2 matrix and particle density of Au increases with amount of addition.

The 1%Au/TiO_2 and 2%Au/TiO_2 thin films calcined at various temperatures (275, 400 and 500^{0}C) have been used for the degradation of different organic pollutants like salicylic acid, methylene blue, methyl orange and phenol. In the samples of 1%Au/TiO_2 and 2%Au/TiO_2 calcined at various temperatures, the rate of photo degradation is found to be more for sample calcined at 275^{0}C than other two hence for further study samples calcined at 275^{0}C have been employed. Among the 1%Au/TiO_2 and 2%Au/TiO_2 catalysts used for degradation experiments, rate of degradation is found to be more on later than that on the former. In the compounds studied, the enhancement in rate of degradation for phenol is found to be more and the enhancement in rate of degradation for methylene blue degradation is least. The stability of the 2%Au/TiO_2 catalyst has been studied by using this catalyst for five cycles of experiments and only 1.9-2 % decrease in activity has been observed after five experiments. This suggests that, the catalyst prepared by this technique is sufficiently stable and it could be used for many catalytic reaction cycles.

In conclusion, a simple and environment friendly method has been developed for the preparation of polyethylene glycol, iron and gold modified thin films of TiO_2 by aqueous titanium peroxide based sol-gel dip coating. Using this method films have been deposited on various substrates like glass plates, silica rashig rings and glass helix. Thin films of uniform thickness with good adhesion to the substrate can be prepared by using this method. The thin film photo-catalyst has been utilized for the photo-degradation of various organic pollutants in water. Excellent catalytic activity of pure TiO_2 has been

obtained in UV-type of reactor. The TiO_2 thin film photo-catalyst doped with Fe and Au have shown very good catalytic activity in sunlight. There is an enhancement of 1.2-3 times in catalytic activity of Fe and Au doped TiO_2 thin films than undoped TiO_2 films has been observed.

List of Publication

1. Preparation of Titanium (IV) oxide thin film Photocatalyst *via* sol-gel dip coating
   R. S. Sonawane, S. G. Hegade, M. K. Dongare, **Mater. Chem. Phys. 77 (2002) 744.**

2. Preparation and photo-catalytic activity Fe-TiO_2 thin films prepared by sol-gel dip Coating.
   R. S. Sonawane, B. B. Kale, M. K. Dongare, **Mater. Chem. Phys. 85 (2004) 52.**

3. Sol-gel synthesis of Au/TiO_2 thin films for photocatalytic degradation of phenol in sunlight
   R. S. Sonawane, M. K. Dongare, **J. Mol. Catalysis A : Chemical 243 (2006) 68.**

4. Epoxidation of styrene by anhydrous t-butyl hydroperoxide over Au/TiO_2 catalysts.
   N. S. Patil, B. S. Uphade, P. Jana, R. S. Sonawane, S. K. Bhargava, V. R. Chaudhari **Catalysis letter 94 (2004) 89.**

5. Preparation and characterization of visible light active Cr/TiO_2 thin film photocatalyst by sol-gel dip coating.
   S. P. Takle , R. S. Sonawane, B. B. Kale, M. K. Dongare **to be submitted to J. Mol. Catalysis A.**

6. Effect of Ag doping on the optical properties of TiO_2 thin films prepared by titanium
   peroxide based sol-gel method.
   S. P. Takle , R. S. Sonawane, B. B. Kale, M. K. Dongare **to be submitted to Mater. Chem. And Phys.**